

**A STUDY ON DEVELOPING SELF-CONSOLIDATING CONCRETE  
(SCC) UTILIZING INDIGENOUS NATURAL AND INDUSTRIAL  
WASTE MATERIALS**

BY

**SAHEED KOLAWOLE ADEKUNLE**

A Thesis Presented to the  
DEANSHIP OF GRADUATE STUDIES

**KING FAHD UNIVERSITY OF PETROLEUM & MINERALS**

DHAHRAN, SAUDI ARABIA

1963 ١٣٨٣

In Partial Fulfillment of the  
Requirements for the Degree of

**MASTER OF SCIENCE**

In

**CIVIL ENGINEERING**

JUNE, 2012

**KING FAHD UNIVERSITY OF PETROLEUM AND MINERALS**  
**DHAHRAN, 31261, SAUDI ARABIA**

**DEANSHIP OF GRADUATE STUDIES**

This thesis, written by **SAHEED KOLAWOLE ADEKUNLE** under the direction of his thesis advisor and approved by his thesis committee, has been presented to and accepted by the Dean of Graduate Studies, in partial fulfillment of the requirement for the degree of **MASTER OF SCIENCE IN CIVIL ENGINEERING**.

Thesis Committee

Dr. Shamsad Ahmad (Advisor)

Dr. Abul Kalam Azad (Co-advisor)

Dr. Mohammed Maslehuddin (Member)

Dr. Salah Uthman Al-Dulaijan (Member)

Dr. Ahmad Saad Al-Gahtani (Member)

170 JUL 2012

Dr. Nedal T. Ratrouf  
Departmental Chairman

Dr. Salam A. Zummo  
Dean of Graduate Studies



Date

15/7/12

*This work is dedicated to my dear  
parents, my adorable brothers, my  
lovely wife, and my blessed  
children.*

## ACKNOWLEDGEMENT

All praise is due to Allaah, SubhaanaHu wata'aala, for guiding me and granting me knowledge, courage, and health, to complete this study with success. May His peace and blessings be upon the best of mankind, Muhammad Ibn 'Abdillaah (SallaLLaahu 'alayhiwasallam), his household, his companions and those who follow his golden path of guidance till the day, on which no soul shall have power to benefit another soul, while the absolute command on that day is Allah's.

I appreciate the moral and educational guidance of my dear parents, through whom Allah had made me climb the ladder of success, the great support of my blessed wife, who maintained her tender loving care with patience in the course of my studies, and my kids, who had to endure less than two hours a day of my company throughout my MS degree. May Allah reward you all with al-Firdaws, the highest.

I'm very grateful to the custodian of the two holy Mosques, through whom Allah had given me the chance to achieve my MS degree in KFUPM, the King Fahd University of Petroleum & Minerals for supporting this research work, and the Civil Engineering department, for giving me the necessary resources to complete my program. I have to acknowledge the kind support of BASF Construction Chemicals, Saudi Arabia, for their generous supply of the superplasticizer and stabilizer used in this research. My special gratitude goes to Mr. Hisham of BASF for his smily reception each time I needed chemical admixtures.

I'm highly indebted to appreciate the kind and brotherly treatment offered by my committee chairman, Dr. Shamshad Ahmad sahab, the unquantifiable fatherly treatment and support by Dr. Mohammad Maslehuddin sahab, and the indispensable guide provided by our great Dr.

AbulKalaam Azad. Also, it's a moral responsibility on my part to acknowledge the support of Dr. Salah Al-Dulaijan and positive inspirations acquired from Dr. Ahmad Sa'ad Al-Gahtaani. I invoke Allah, the Lord of the majestic throne to continue granting your desires in this world, and increase your darajaat in Al-Firdaws, the great abode.

Furthermore, the research work would be a mess, if not for the immense support of our departmental personels: the Lab co-ordinator, Dr Mohammad Eesa; the concrete lab Engineer, Engr. Mukaram Khan sahab; the mechanics lab engineer, Engr. Umar; and the commander general of my experimental operations, Engr. Syed Imran. I owe all of you unreserved gratitude. May Allah in His infinite mercy assist you in your endeavors, both in this duniyah and in the next world.

Penultimately, I thank Dr M. H. Baluch for his big contribution to my knowledge, a rare gem responsible for 50% of my MS course work, and all that have thought me in the course of my MS degree, directly or indirectly. I pray Allah assist you with all your needs in this world and the next.

Finally, I have to thank the entire Nigerian/African community in the Eastern Province, and my friends from the Indo-Pakistan subcontinent for your company and good influences in the course of my MS degree. May Allah continue to help each and every one of you, amin.

## TABLE OF CONTENTS

LIST OF TABLES .....	xii
LIST OF FIGURES .....	xiv
THESIS ABSTRACT .....	xvii
THESIS ABSTRACT (ARABIC) .....	xviii
CHAPTER 1 .....	1
INTRODUCTION .....	1
1.1 INTRODUCTION TO SELF COMPACTING CONCRETE (SCC) .....	1
1.2 THE NEED FOR THIS RESEARCH WORK.....	3
1.3 OBJECTIVES OF THE RESEARCH.....	4
1.4 RESEARCH BLUEPRINT .....	5
CHAPTER 2.....	7
LITERATURE REVIEW .....	7
2.1 BACKGROUND ON CONCRETE TECHNOLOGY.....	7
2.2 PROBLEM SOLVED, THANKS TO THE CREATIVITY THAT MADE SCC A REALITY .....	10
2.3 PRINCIPLES AND METHODS OF SCC MIXES DESIGN .....	11
2.4 REQUIREMENTS OF SCC MIXTURES.....	14
2.5 TEST METHODS FOR EVALUATION OF THE WORKABILITY PROPERTIES OF SCC .....	15
2.5.1 The Slump Flow/Flow Table Test .....	16
2.5.2 The V-funnel Test.....	16
2.5.3 The U-box Test.....	17

2.5.4	The L-box Test .....	17
2.5.5	The GTM Screen Stability and V-funnel at $T_{5\text{ min}}$ Tests .....	18
2.6	CONSTITUENT MATERIALS USED IN SCC .....	19
2.6.1	Powders .....	19
2.6.2	Aggregates.....	23
2.6.3	Chemical Admixtures .....	23
2.7	HARDENED PROPERTIES OF SCC .....	24
2.7.1	Compressive, Tensile, and Bond Strength .....	24
2.7.2	Modulus of Elasticity of SCC .....	26
2.7.3	Shrinkage and Creep .....	27
2.7.4	Water Permeability, Water Absorption and Chloride Permeability .....	27
2.7.5	Corrosion of Rebar in SCC .....	27
2.8	ECONOMICS OF SCC.....	28
CHAPTER 3 .....		29
EXPERIMENTAL PROGRAM .....		29
3.1	INTRODUCTION.....	29
3.2	MATERIALS USED IN THE DEVELOPMENT OF SCC MIXES.....	30
3.2.1	Powders .....	30
(i)	Cement .....	30
(ii)	Silica Fume (SF) .....	31
(iii)	Fly Ash (FA) .....	31
(iv)	Natural pozzolan (NP) .....	32
(v)	Limestone Powder (LSP).....	32
(vi)	Cement Kiln Dust (CKD).....	33
(vii)	Electric Arc Furnace Dust (EAFD).....	34
(viii)	Pulverized Steel Slag (PSS) .....	35
(ix)	Calcined Clay/Metakaolin (MK).....	36
3.2.2	Coarse Aggregates .....	38
3.2.3	Fine Aggregates.....	39

3.2.4	Chemical admixtures .....	39
(i)	Superplasticizer (SP).....	39
(ii)	Stabilizer/Viscosity Modifying Admixture (VMA).....	40
3.2.5	Mixing water .....	40
3.3	SCC TRIAL MIXES .....	41
3.3.1	Mix Parameters of the Trial Mixes.....	41
3.3.2	Mix Design for the Trial Mixtures .....	42
3.3.3	Weights of Constituent materials in the Trial Mixtures .....	44
3.4	PREPARATION OF TRIAL MIXES .....	46
3.5	SELF-COMPACTABILITY TESTS ON TRIAL MIXES .....	47
3.5.1	Slump Flow Test.....	47
3.5.2	V-funnel Test.....	48
3.5.3	U-Box Test .....	49
3.5.4	Assessment of Segregation Resistance in the Trial Mixes.....	51
3.6	SELECTION OF QUALIFYING MIXESFROM THE TRIALMIXTURES.....	51
CHAPTER 4.....		53
EVALUATION OF HARDENED PROPERTIES OF THE SELECTED SCC MIXTURES .....		53
4.1	INTRODUCTION.....	53
4.2	CASTING AND CURING OF SPECIMENS.....	53
4.3	TEST SPECIMENS.....	54
4.4	TESTS FOR MECHANICAL PROPERTIES OF SCC MIXES .....	55
4.4.1	Compressive Strength .....	55
4.4.2	Splitting Tensile Strength .....	56
4.4.3	Young's Modulus .....	57
4.4.4	Bond Strength.....	59
4.5	TESTS FOR DURABILITY CHARACTERISTICS OF SCC MIXTURES .	62



4.5.1	Water Permeability .....	62
4.5.2	Chloride Permeability .....	63
4.5.3	Electrical Resistivity .....	64
4.5.4	Corrosion Resistance.....	65
CHAPTER 5 .....		69
RESULTS AND DISCUSSION .....		69
5.1	COMPRESSIVE STRENGTH.....	69
5.1.1	Mixes containing LSP.....	70
5.1.2	Mixes containing NP .....	73
5.1.3	Mixes containing MK.....	77
5.1.4	Mixes containing CKD.....	79
5.2	SPLITTING TENSILE STRENGTH.....	82
5.2.1	Mixes containing LSP.....	82
5.2.2	Mixes containing NP .....	83
5.2.3	Mixes containing MK.....	84
5.2.4	Mixes containing CKD.....	85
5.3	YOUNG’S MODULUS .....	88
5.3.1	Mixes containing LSP.....	88
5.3.2	Mixes containing NP .....	89
5.3.3	Mixes containing MK.....	89
5.3.4	Mixes containing CKD.....	90
5.4	BOND STRENGTH.....	92
5.4.1	Mixes containing LSP.....	93
5.4.2	Mixes containing NP .....	94
5.4.3	Mixes containing MK.....	96
5.4.4	Mixes containing CKD.....	97
5.5	WATER PERMEABILITY .....	100
5.5.1	Mixes containing LSP.....	100
5.5.2	Mixes containing NP .....	102

5.5.3	Mixes containing MK.....	103
5.5.4	Mixes containing CKD.....	104
5.6	CHLORIDE PERMEABILITY .....	106
5.6.1	Mixes containing LSP.....	107
5.6.2	Mixes containing NP .....	108
5.6.3	Mixes containing MK.....	109
5.6.4	Mixes containing CKD.....	109
5.7	CORROSION POTENTIALS .....	111
5.7.1	Mixes containing LSP.....	111
5.7.2	Mixes containing NP .....	112
5.7.3	Mixes containing MK.....	113
5.7.4	Mixes containing CKD.....	114
5.8	CORROSION CURRENT DENSITY.....	115
5.8.1	Mixes containing LSP.....	116
5.8.2	Mixes containing NP.....	116
5.8.3	Mixes containing MK.....	117
5.8.4	Mixes containing CKD.....	118
5.9	ELECTRICAL RESISTIVITY .....	119
5.9.1	Mixes containing LSP.....	120
5.9.2	Mixes containing NP .....	121
5.9.3	Mixes containing MK.....	121
5.9.4	Mixes containing CKD.....	122
CHAPTER SIX.....		126
CONCLUSIONS AND RECOMMENDATIONS .....		126
6.1.	CONCLUSIONS .....	126
6.1.1.	Waste Materials .....	126
6.1.2.	Mechanical Properties of SCC mixtures developed.....	127
6.1.3.	Durability Properties of SCC mixtures developed Related to Reinforcement Corrosion Resistance.....	127

6.2. RECOMMENDATIONS .....	128
6.3. RECOMMENDATIONS FOR FUTURE WORKS.....	129
REFERENCES .....	130
VITA.....	138

## LIST OF TABLES

<b>Table 2.1:</b> Test methods and acceptance criteria for the workability properties of SCC .....	15
<b>Table 3.1:</b> Chemical composition of OPC type 1.....	30
<b>Table 3.2:</b> Chemical composition of the silica fume used in the study. ....	31
<b>Table 3.3:</b> Chemical composition of the fly ash used in the study.....	31
<b>Table 3.4:</b> Chemical composition of the natural pozzolan used in the study. ....	32
<b>Table 3.5:</b> Chemical composition of LSP used in the study. ....	33
<b>Table 3.6:</b> Chemical composition of the CKD used in the study. ....	34
<b>Table 3.7:</b> Chemical composition of EAFD used in the study.....	35
<b>Table 3.8:</b> Chemical composition of the PSS used in the study.....	36
<b>Table 3.9:</b> Chemical composition of the calcined clay (MK) used in the study.....	38
<b>Table 3.10:</b> Grading of the coarse aggregate used in the study. ....	38
<b>Table 3.11:</b> Grading of the fine aggregate used in the study .....	39
<b>Table 3.12:</b> Technical data of Glenium 51 <sup>®</sup> .....	40
<b>Table 3.13:</b> Technical data of RheoMATRIX <sup>®</sup> .....	40
<b>Table 3.14:</b> Mix parameters used in the trial mixes.....	41
<b>Table 3.15:</b> Combinations and proportions of waste materials and cement proposed for each of the trial mixes.....	42
<b>Table 3.16:</b> Weights of the constituent materials for the trial mixtures.....	44
<b>Table 3.17:</b> Fixing of the SP and VMA dosages for TM2.....	46
<b>Table 3.18:</b> Segregation resistance criteria used for screening the mixtures. ....	51
<b>Table 3.19:</b> Flow results of the trial mixtures. ....	52
<b>Table 4.1:</b> Details of test specimens and test standards for the evaluation of the mechanical properties of SCC mixtures. ....	54
<b>Table 4.2:</b> Details of test specimens and test standards for the evaluation of the durability of SCC mixtures. ....	54
<b>Table 5.1:</b> Compressive strength of SCC Specimens.....	69
<b>Table 5.2:</b> Splitting tensile strength of SCC specimens. ....	87
<b>Table 5.3:</b> Chord modulus of SCC specimens .....	91

<b>Table 5.4:</b> Bond strength of SCC mixtures. ....	99
<b>Table 5.5:</b> Water penetration depth classes [98]. ....	100
<b>Table 5.6:</b> Water penetration depth of SCC specimens. ....	105
<b>Table 5.7:</b> Chloride ion penetrability based on charge passed [106]. ....	106
<b>Table 5.8:</b> Rapid chloride permeability of SCC specimens. ....	110
<b>Table 5.9:</b> Empirical resistivity thresholds for depassivated steel [109, 110]. ....	119
<b>Table 5.10:</b> Correlation parameters and electrical resistivity of SCC specimens. ....	124

## LIST OF FIGURES

<b>Figure 2.1:</b> Honeycombs in concrete elements resulting from poor compaction [19].....	8
<b>Figure 2.2:</b> Influence of water content on (a) concrete strength and permeability [20], and (b) time to initiation of corrosion [21]. .....	9
<b>Figure 2.3:</b> Basic Principles for the Production of SCC [2]. .....	12
<b>Figure 2.4:</b> Mix Design Procedure for SCC .....	13
<b>Figure 2.5:</b> SCC filling ability tests (a) Flow table/slump flow test (b) V-funnel test. ....	16
<b>Figure 2.6:</b> Passing ability test.....	18
<b>Figure 3.1:</b> Raw clay before processing. ....	37
<b>Figure 3.2:</b> (a) Crushed clay laid in furnace trays (b) Raw clay and activated clay shown side- by-side.....	37
<b>Figure 3.3:</b> Slump flow measurement equipments and accessories. ....	48
<b>Figure 3.4:</b> V-funnel testing accessories.....	49
<b>Figure 3.5:</b> U-box testing accessories.....	50
<b>Figure 4.1:</b> Matest <sup>®</sup> hydraulic type compressive strength testing machine.....	55
<b>Figure 4.2:</b> Test arrangement for splitting tensile strength. ....	56
<b>Figure 4.3:</b> (a) Tensile test samples with aligned bearing strips (b) Samples after splitting..	56
<b>Figure 4.4:</b> Test arrangement for determining Young's modulus .....	59
<b>Figure 4.5:</b> Preparation of bond test specimens (dimensions in mm).....	60
<b>Figure 4.6:</b> Test arrangement for the pull-out test. ....	61
<b>Figure 4.7:</b> Water penetration depth test set-up. ....	62
<b>Figure 4.8:</b> Rapid chloride permeability test set-up. ....	64
<b>Figure 4.9:</b> Test set-up for electrical resistivity.....	65
<b>Figure 4.11:</b> Corrosion potential measurement setup. ....	67
<b>Figure 4.12:</b> Corrosion current density measurement setup. ....	68
<b>Figure 5.1:</b> Compressive strength of SCC with LSP.....	70
<b>Figure 5.2:</b> 7, 28 and 90 days compressive strength of SCC with LSP. ....	71
<b>Figure 5.3:</b> SCC mixtures with LSP - compressive strengths as % of 28-day strength...	72
<b>Figure 5.4a:</b> Compressive strength of SCC with NP.....	73

<b>Figure 5.4b:</b> Compressive strength of SCC with NP (without M6).....	75
<b>Figure 5.5:</b> 7, 28 and 90 days compressive strength of SCC with NP.....	76
<b>Figure 5.6:</b> SCC mixtures with NP - compressive strengths as % of 28D strength. ....	76
<b>Figure 5.7:</b> Compressive strength of SCC with MK.....	77
<b>Figure 5.8:</b> 7, 28 and 90 days compressive strength of SCC with MK.....	78
<b>Figure 5.9:</b> SCC mixtures with MK - compressive strengths as % of 28D strength. ....	79
<b>Figure 5.10:</b> Compressive strength of SCC with CKD.....	80
<b>Figure 5.11:</b> 7, 28 and 90 days compressive strength of SCC with CKD. ....	81
<b>Figure 5.12:</b> SCC mixtures with CKD - compressive strengths as %of 28-day strength. ....	81
<b>Figure 5.13:</b> Splitting tensile strength of SCC mixes with LSP .....	83
<b>Figure 5.14:</b> Splitting tensile strength of SCC mixes with NP. ....	84
<b>Figure 5.15:</b> Splitting tensile strength of SCC mixes with MK. ....	85
<b>Figure 5.16:</b> Splitting tensile strength of SCC mixes with CKD. ....	86
<b>Figure 5.17:</b> Splitting tensile strength of SCC mixtures against compressive strength.....	87
<b>Figure 5.18:</b> Chord modulus of SCC mixtures with LSP.....	88
<b>Figure 5.19:</b> Chord modulus of SCC mixtures with NP.....	89
<b>Figure 5.20:</b> Chord modulus of SCC mixtures with MK.....	90
<b>Figure 5.21:</b> Chord modulus of SCC mixtures with CKD.....	91
<b>Figure 5.22:</b> Relationship between $E_c$ and $f'_c$ for SCC mixtures. ....	92
<b>Figure 5.23a:</b> Bond strength of SCC mixtures with LSP.....	93
<b>Figure 5.23b:</b> $f'_c$ and $f_{cb}$ of SCC mixtures with LSP as % of control mixture. ....	94
<b>Figure 5.24a:</b> Bond strength, $f_{cb}$ , of SCC mixtures with NP.....	95
<b>Figure 5.24b:</b> $f'_c$ and $f_{cb}$ of SCC mixtures with NP as % of control mixture. ....	96
<b>Figure 5.25a:</b> Bond strength, $f_{cb}$ , of SCC mixtures with MK.....	96
<b>Figure 5.25b:</b> $f'_c$ and $f_{cb}$ of SCC mixtures with MK as % of control mixture. ....	97
<b>Figure 5.26a:</b> Bond strength, $f_{cb}$ , of SCC mixtures with CKD. ....	98
<b>Figure 5.26b:</b> $f'_c$ and $f_{cb}$ of SCC mixtures with CKD as % of control mixture. ....	98
<b>Figure 5.27:</b> Relationship between $f_{cb}$ and $f'_c$ for SCC mixtures. ....	100
<b>Figure 5.28:</b> Water penetration depth of SCC mixtures with LSP.....	101
<b>Figure 5.29:</b> Water penetration depth of SCC mixtures with NP.....	103

<b>Figure 5.30:</b> Water penetration depth of SCC mixtures with MK. ....	104
<b>Figure 5.31:</b> Water penetration depth of SCC mixtures with CKD. ....	105
<b>Figure 5.32:</b> Rapid chloride permeability of SCC mixtures with LSP. ....	107
<b>Figure 5.33:</b> Rapid chloride permeability of SCC mixtures with NP. ....	108
<b>Figure 5.34:</b> Rapid chloride permeability of SCC mixtures with MK. ....	109
<b>Figure 5.35:</b> Rapid chloride permeability of SCC mixtures with CKD. ....	110
<b>Figure 5.36:</b> LSP mixes – variation of corrosion potential with exposure time .....	112
<b>Figure 5.37:</b> NP mixes – variation of corrosion potential with exposure time.....	113
<b>Figure 5.38:</b> MK mixes – variation of corrosion potential with exposure time.....	114
<b>Figure 5.39:</b> CKD mixes – variation of corrosion potential with exposure time. ....	115
<b>Figure 5.40:</b> LSP mixes – variation of corrosion current density with exposure time. ....	116
<b>Figure 5.41:</b> NP mixes – variation of corrosion current density with exposure time. ....	117
<b>Figure 5.42:</b> MK mixes – variation of corrosion current density with exposure time. ....	117
<b>Figure 5.43:</b> CKD mixes – variation of corrosion current density with exposure time. ....	118
<b>Figure 5.44:</b> Electrical resistivity of SCC mixtures with LSP. ....	120
<b>Figure 5.45:</b> Electrical resistivity of SCC mixtures with NP. ....	121
<b>Figure 5.46:</b> Electrical resistivity of SCC mixtures with MK. ....	122
<b>Figure 5.47:</b> Electrical resistivity of SCC mixtures with CKD.....	123
<b>Figure 5.48:</b> Electrical resistivity – moisture content curve for M5-NC-10-10. ....	125



## THESIS ABSTRACT

**Full Name**        **ADEKUNLE, SAHEED KOLAWOLE**

**Title of Study**    **A STUDY ON DEVELOPING SELF-CONSOLIDATING  
CONCRETE (SCC) UTILIZING INDIGENOUS NATURAL  
AND INDUSTRIAL WASTE MATERIALS**

**Major Field**      **CIVIL ENGINEERING (STRUCTURES)**

**Date of Degree**   **JUNE 2012**

"Self Consolidating Concrete (SCC)" is a concrete material possessing an ability to take formwork shapes without being aided mechanically, making it a 'smart concrete' material. Since its invention in the 1980's, it has enjoyed notable acceptance in many parts of the world. Saudi Arabia, on the contrary, like most Arabian Gulf countries are yet to fully tap the goodies of the novel SCC idea, probably due to the dearth of supportive evidences of its suitability with local materials and environmental conditions, and the high cost of SCC resulting from the use of the imported materials.

In this study, exploratory studies were conducted in an attempt to develop SCC mixes using locally available waste materials. Waste materials such as cement kiln dust (CKD), limestone powder (LSP), bag house dust (BHD), pulverized steel slag (PSS) and mineral admixtures like calcined clay or metakaolin (MK) – all of which are abundantly available in the Kingdom at little or no cost – were employed in the development of the SCC mixtures. The mechanical, and durability properties of these SCC were investigated, and comprehensive analysis of the experimental results was carried out.

The SCC blends produced with these waste materials were high early and ultimate (compressive, tensile and bond) strength concrete with acceptable Young's moduli in the same range as traditional concrete of equivalent compressive strength. Most of the blends had low water penetration, 'very low' chloride permeability (RCPT), high electrical resistivity and high to moderate corrosion resistance. Based on the findings in the study, it was recommended to limit the quantities of waste materials like as BHD (EAFD), PSS and NP in SCC because of their high demand for SP and VMA, and CKD because of its reduction of corrosion resistance.

**MASTER OF SCIENCE**  
**KING FAHD UNIVERSITY OF PETROLEUM AND MINERALS**  
**Dhahran, Saudi Arabia.**

## THESIS ABSTRACT (ARABIC)

### ملخص الرسالة

الاسم الكامل: سعيد كولاوولى ادى كونلى

عنوان الرسالة : دراسة تطوير خرسانة ذاتية الدمك (SCC) بالاستفادة من المواد المحلية والمخلفات الصناعية

الاختصاص: هندسة مدنية (انشاءات)

تاريخ الرسالة: يونيو 2012م

### الملخص:

إن الخرسانة ذاتية الدمك ( SCC ) تمتلك قابلية لتأخذ شكل القالب بدون المساعدة الميكانيكية , لتجعلها "خرسانة ذكية" , ومنذ اختراعها في أوائل 1980م, فقد اكتسبت قبولاً كبيراً في أجزاء كبيرة من العالم. وأما في المملكة العربية السعودية, على العكس مثل أغلب دول الخليج العربية لم تستفد بعد من ميزان هذه الخرسانة, وذلك ربما بسبب قلة الشواهد من ملائمتها للمواد المحلية والظروف المناخية, وتكلفتها العالية والنتيجة من استخدام مواد مستوردة.

في هذه الدراسة تم إجراء دراسات استكشافية وذلك لمحاولة تطوير خلطات الخرسانة ذاتية الدمك (SCC) باستخدام مخلفات المواد المتوفرة محلياً, مثل غبار الاسمنت ( CKD ), مسحوق الحجر الجيري (LSP), غبار المنازل ( BHD ), خبث الحديد المسحوق ( PSS ) والمضافات المعدنية مثل الطين أو الميتاكرولين (MK), كل هذه المواد متوفرة بكثرة في المملكة بدون تكلفة تقريباً, وقد تم استخدامها في تطوير خليط الـ ( SCC ) وقد تم فحص الخصائص الميكانيكية والديمومة لها , وإجراء تحليل شامل لنتائج الاختبارات.

وقد كان خليط الـ ( SCC ) الناتج من مخلفات المواد لديها قوة ضغط وشد وتماسك عالية في المراحل الأولى والقوى للقوة, وذلك بمعامل مرونة مقبول لنفس نطاق قوى ضغط الخرسانة التقليدية وكانت معظم الخلطات تمتلك أقل اختراق للماء, ونفاذية الكلوريد قليلة جداً ( RCPT ), ومقاومة كهربائية عالية, ومقاومة تآكل عالية إلى متوسطة, وبالاعتماد على نتائج هذه الدراسة, قد تم اقتراح حدود لاستخدام الكميات لهذه المخلفات مثل الـ BHD (EAFD) PSS , NP, في الـ SCC وذلك بسبب طلبها العالي لـ SP وVMA وCKD وذلك نظراً لتقليلهما لمقاومة التآكل.

درجة الماجستير في العلوم

جامعة الملك فهد للبترول والمعادن

الظهران 31261

المملكة العربية السعودية

# CHAPTER 1

## INTRODUCTION

### 1.1 INTRODUCTION TO SELF COMPACTING CONCRETE (SCC)

Unusual construction circumstances provoked a team of smart engineers to develop a smart concrete material in Japan in 1988. This concrete material was named "Self Consolidating Concrete (SCC)", as it possessed the ability to take form shapes without being aided mechanically. Contrary to an expectation of unacceptable performance as a result of its phenomenal fluidity, SCC easily flows through obstructions and narrow sections to fill-in the forms by its self weight without needing any form of vibration, yet free of any objectionable segregation or bleeding.

These inherent superior advantages over traditional concrete make SCC widely accepted in the construction industries, not only in Japan – its ‘birth’ place – but also across Europe, USA and other places. In contrast, Saudi Arabia, like most Arabian Gulf countries had been somewhat sceptical in fully embracing the novel SCC idea, which may due to the scarcity of convincing research evidences proving its performance in the Gulf environmental conditions and possibility of its production with local materials without having to import the popular SCC materials used in those countries where its use has been flourishing.

SCC is acceptably an important breakthrough in concrete technology in recent times. Lower than expected in-situ performance of hardened conventional vibrated concrete (CVC) due to unacceptable non-homogeneity – resulting from poor compaction or segregation – is not

uncommon. Consequently, SCC was developed to ensure adequate consolidation through self-compaction for easy concrete placement in structures having narrow sections and/or congested reinforcement. The high level of SCC fluidity in its fresh state, its filling ability and segregation resistance reduce the risk of concrete honeycombing [1].

The material components of SCC are basically the same as for CVC: cement, fine and coarse aggregates, water, mineral and chemical admixtures. The major difference lies in relative quantities of each of the component materials. Superplasticizer dosage is usually higher for the flow requirements, and this may necessitate the incorporation of viscosity modifying admixtures (VMAs) to improve cohesion and control the tendency of segregation resulting from the higher workability. Also, the amount of fines is usually higher in order to provide better lubrication for coarse aggregates to enhance deformability of the mixture. All these call for a different treatment for SCC [2]. The main task in the production of SCC is appropriate proportioning of the constituents and evaluation of the rheological properties of the mixture. Whichever of the many available methods of achieving self-compactability is employed, the ultimate aim is to obtain a concrete material possessing three basic characteristics: high deformability, good cohesion (restrained flowability) and a high segregation resistance [3].

The hardened mechanical and durability properties of SCC have been found better than that of CVC [4-12], except for the modulus of elasticity that may be slightly lower as a result of the lower coarse aggregate content [13, 14]. For the same reason, creep and shrinkage may also be higher in SCC [14]. These may be of particular concern in some applications like in the prestressed concrete members where prestress losses and long-term deflection are

important[15]. However, these problems could be solved by proper mix proportioning and incorporation of appropriate additives.

SCC offers several advantages over CVC, making it economically beneficial [16, 17]. Using SCC in construction does not only offer speed – due to the absence of restrictions on quantity of concrete to be placed in one shot for proper consolidation – it also makes placing easier than CVC. The segregation resistance of SCC and its high fluidity produces a thoroughly compacted material of uniform composition with good surface finishes. The thorough compaction definitely confers higher durability and bond strength. Also, the non-requirement of vibration eliminates some of the high construction noise characteristic of CVC.

Additionally, the self filling property of SCC offers the great benefit of site manpower reduction which enables better focus on precision rather than being preoccupied with controlling the multitude of concrete handling personnel on site. Noteworthy is the fact that the several restrictions in rebar arrangement emanates from the concern for proper consolidation of CVC through inter-rebar spaces and adequate rebar bond to concrete. Hence the SCC's higher bond strength and its high fluidity go a long way to eliminate many of these restrictions. Needless to say is the safer working environment on site since concrete handling personnel is of manageable size when using SCC in construction.

## **1.2 THE NEED FOR THIS RESEARCH WORK**

Given the SCC's excellent attributes and the trends of adoption in various parts of the world, as discussed in the previous section, it is very important to encourage local construction industry to adopt the idea. Though, a handful of construction projects in the

kingdom have employed SCC recently, it's still not fully adopted locally. Some of the key factors that might have prevented their spontaneous acceptance may be scarcity of research evidences establishing its suitability in our challenging environmental conditions and ease/possibility of production with local aggregates, and its high cost resulting from the use of large quantities of imported popular filler materials, such as fly ash and silica fume.

Therefore there is a large vacuum of information to be filled regarding suitability of SCC as a construction material in the Kingdom, with particular reference to usability of local raw materials and cost of production relative to ordinary concrete of similar strength and durability characteristics. Coupled with that is the prospect of some waste materials such as CKD, BHD, LSP, PSS and others that are available in the Kingdom, for their use in SCC production. If these materials produce fruitful results for SCC, there will be a saving in the production cost, as these materials are very cheap. Also, environmental degradation and emission of greenhouse gases will be reduced.

### **1.3 OBJECTIVES OF THE RESEARCH**

The general objective of the study was to evaluate the possibility of producing SCC utilizing locally available waste materials (natural and industrial). The specific objectives are as follows:

1. Develop optimum SCC mixtures utilizing the selected indigenous natural and industrial waste products,
2. Evaluate the mechanical properties and durability of the developed SCC,
3. Analyse the experimental data in order to model the properties of the developed SCC mixtures,

4. Provide recommendations on the use of local waste materials for SCC in Saudi Arabia based on the findings of the research work.

#### **1.4 RESEARCH BLUEPRINT**

The work was executed in six phases. The first phase involved a comprehensive and extensive literature review to acquire the state-of-the-art information on the subject.

The next phase involved formation of the research program based on the information gathered in the first phase and the research objectives.

In the third phase, the tasks entailed fabrication, preparation and calibration of testing equipments and weighing scales, preparation of test specimens moulds and experimental accessories. Also, in this phase of the work, the proposed local filler materials and imported ones to be used as control were acquired. The materials acquisition also included the fine and coarse aggregate and chemical admixtures.

The fourth phase witnessed the development of trial mixtures and evaluating the performance of rheological tests on them in a bid to select the ones meeting the currently established criteria for classification as SCC. The compliant mixtures were selected for detailed evaluation of their mechanical and durability properties.

Castings of SCC specimens for the proposed hardened tests on the selected mixes were carried out in the fifth phase. The specimens were cured in water at the laboratory ambient temperature for 28 days, after which they were sorted out for testing except those needed for 90 days curing. The testing of the specimens drew the curtain on this phase of the work.

Penultimately, experimental data were compiled, analyzed and models obtained for the relationship among various fresh and hardened mechanical and durability properties.

In the final phase, the report covering the whole process was prepared in which conclusions were drawn from the experimental results and recommendations provided.



## CHAPTER 2

### LITERATURE REVIEW

#### 2.1 BACKGROUND ON CONCRETE TECHNOLOGY

The use of concrete technology in construction in its ancient form could be traced back to the Neolithic age, and it continued through the early civilizations reaching its peak in Rome, where it was known as "opus cæmentitium". However, the modern form of reinforced concrete was brought about by the industrial revolution through the invention of cement, mass production of iron and advances in structural science [18]. Consequently, the modern cement concrete is a substance used in construction consisting of aggregates, binder (cement or its mixture with other cementitious and/or pozzolanic materials) and water, which is somewhat viscous or compactibly stiff in its freshly mixed state, but becomes hard after a while through the reaction of the binder with water (hydration reaction).

Using concrete in construction involves filling the fresh mixture in moulds or forms, which define the shapes of the structural elements after hardening. However, unlike the casting process of metals, alloys and polymers (which have high fluidity at the time of casting, hence easily take the perfect shape of formwork), conventional vibrated concrete (CVC) requires mechanical vibration or compaction to make the concrete assume the perfect shape of the formwork and achieving good internal consolidation. Mechanical vibration is further necessitated by the presence of steel bars, which are needed as concrete reinforcement but serve as obstructions to the flow of the concrete mixture in the formwork. Improper compaction of concrete mixture after placing results in porous, low strength and high

permeability rough solid, which permits easy access of aggressive species that cause the concrete and reinforcing bars to deteriorate. This defect is commonly called concrete honeycombs, as illustrated in Figure 2.1.

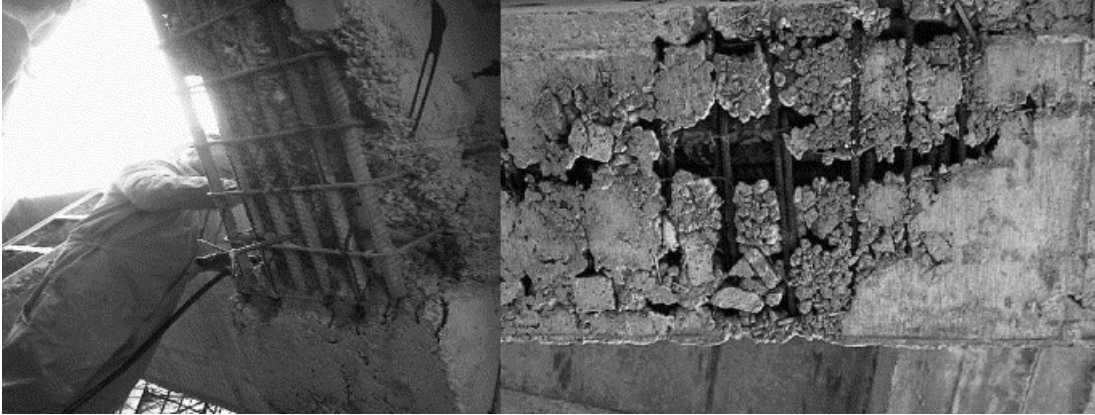


**Figure 2.1:** Honeycombs in concrete elements resulting from poor compaction [19].

Therefore, a good quality concrete has to be ‘workable’ enough to aid proper compaction or densification after placing. However, ‘too high’ workability results in segregation of the concrete, causing the aggregates to separate from the other components. This will leave behind a structure in which some parts are too weak while other parts are too strong. Obviously, the whole thing is a mess, as the old saying goes: “the strength of a chain is that of its weakest link”.

Furthermore, the first thing that comes to mind for achieving high workability of concrete is to increase the water content. However, it had been shown by several researchers that the strength and durability of concrete reduces with increasing water content. Figure 2.2(a) represents one of the several studies that established that higher water content in concrete reduces strength and permeability of concrete [20], while the time to corrosion initiation – a very important durability index – is shown to reduce with higher water content, as shown in

Figure 2.2(b) [21]. For these reasons, concrete specialists over the ages had been careful to strike a balance between adequate workability and the least possible water/cementitious materials ratio. All codes covering concrete construction have detailed specification on limits of workability – specified in terms of slump value – for each application.

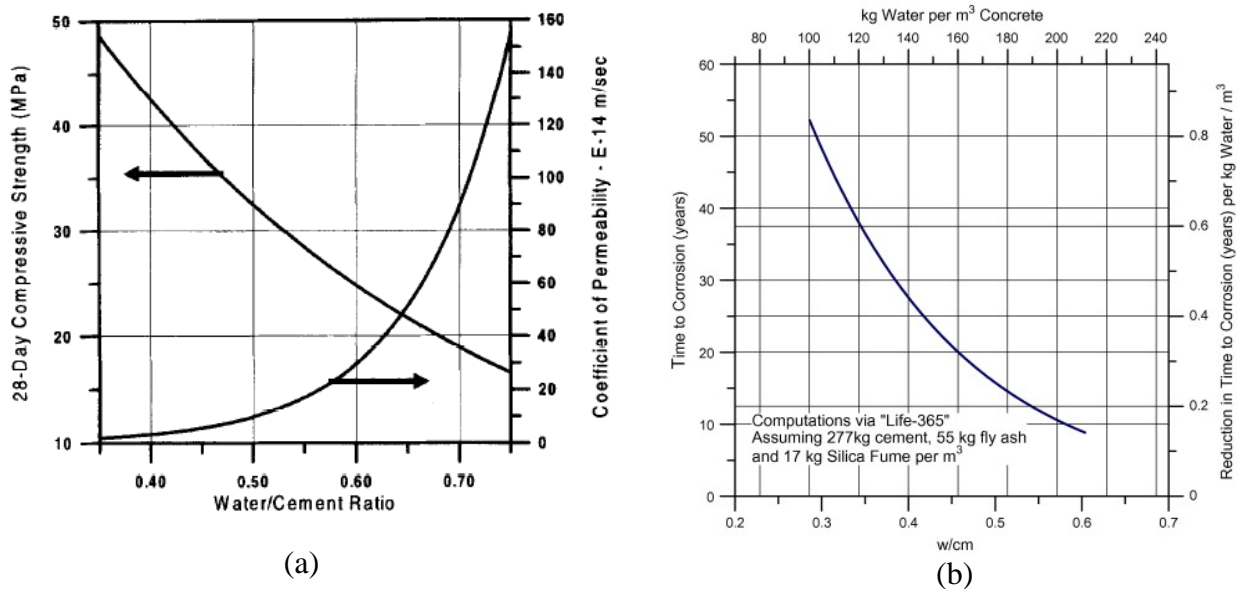


**Figure 2.2:** Influence of water content on (a) concrete strength and permeability [20], and (b) time to initiation of corrosion [21].

On top of this, even with careful and sophisticated design of the concrete constituents, the quality of workmanship in terms of supervision and knowledge is the key factor that determines the success of any concrete construction work. This is the biggest problem facing the concrete industry, as ensuring proper placement and compaction of concrete in formwork is not attained in all cases, regardless of how much the project is worth. To corroborate this, the honeycomb defect shown in Figure 2.1 is a part of the pictures taken in the evaluation and repair work of the Algiers airport building, in which over 10,000 m<sup>2</sup> of concrete honeycomb was repaired, in addition to the repair of 100 m<sup>2</sup> corrosion-damaged concrete and 500 m of cracks, all gulping over three million US dollars [19].

## 2.2 PROBLEM SOLVED, THANKS TO THE CREATIVITY THAT MADE SCC A REALITY

The problems discussed in the previous section were overcome by the invention of a smart concrete material, invented in 1986, that requires no compaction effort: it flows under its own weight. With this, it was christened 'High Performance Concrete' (HPC). Around the same time, it came to be popular to refer to a high durability concrete as an HPC. But since this new concrete material goes beyond just high durability, a more befitting name was given to it by the developers. They renamed it 'Self Compacting High Performance Concrete' (SC-HPC) [22]. Later, as it became more popular, it was simply called 'Self Compacting Concrete' (SCC) or 'Self Leveling Concrete'.

Necessity, they say, is the mother of invention. The reduction in the number of skilled construction workers in Japan for so many years from early 80's prompted special attention to the durability of concrete structures, as adequate consolidation became a popular issue. This made Professor Hajime Okamura propose the use of SCC in 1986, a concrete material that possesses an ability to fill every part of a form, only by its self weight without mechanical compaction. Further developmental studies were made by Ozawa and Maekawa, which brought about the first practical prototypes of SCC [22].

In less than a decade after starting the development and use of SCC in the early 1990's, Japan construction market had been able to consume around 400,000 m<sup>3</sup> (520,000 yard<sup>3</sup>) of SCC [23]. Also, SCC had been used successfully in Europe, since 1996, for various structural applications, such as bridges, walls and tunnel linings [23], and it keeps gaining broader use in many countries for various structural applications [24]. Another major problem the development of SCC was targeted to address is for its usefulness in highly congested

reinforced structures in seismic areas [24], and in cases where mechanical compaction of concrete is difficult or impractical, such as in underwater members, in-situ pile foundations, and other members with congested reinforcement [3].

Research efforts had recently concentrated on increasing reliability and prediction and modeling of SCC properties, improved denseness, uniformity and smooth surface finish, improved durability and high early strength for faster construction and precast application for better productivity [3, 25-27].

### **2.3 PRINCIPLES AND METHODS OF SCC MIXES DESIGN**

In terms of ingredients, SCC is made with the same material components as CVC: cement, fine and coarse aggregates, water and mineral and chemical admixtures. However, the higher quantity of superplasticizer for better flow and the higher powder content acting as “lubricant” for coarse aggregates in addition to the use of viscosity modifying admixtures (VMAs) calls for a different treatment [2]. Regarding the mix proportioning, there’s no hard rule for composing SCC. However, the specific application in which the mix is to be employed governs the choices to be made in the materials their relative quantities. All that matters is producing a concrete material having the ability to fill complex forms, flow through and bond to closely spaced reinforcements solely by its own weight, while maintaining a high resistance to segregation [23]. These basic principles governing the production of SCC were summarized pictorially by Dehn et al [2], as depicted in Figure 2.3.

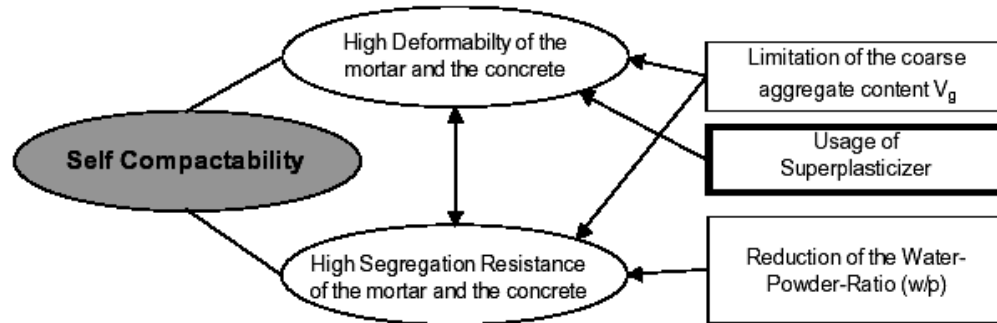


**Figure 2.3:** Basic Principles for the Production of SCC [2].

The researchers in the SCC development had employed various methods for mix design. A common design philosophy involves dividing the concrete into two parts: mortar and coarse aggregates, and by employing various mineral and chemical admixtures, the mortar rheology is adjusted to achieve SCC [22, 28, 29, 30]. Another design approach, that is gaining attention recently as it offers better understanding of the physical properties of SCC, focuses on optimization of the particle size distribution of the solid constituents – powder (binders and fillers), fine and coarse aggregates – for dense packing of the particles [30-33].

The method employed by Okamura and Ozawa [34] to achieve self-compactability of SCC involved the use of reduced aggregate content, lower water/powder ratio, and higher dosage of superplasticizer. They achieved SCC using their “simple mix proportioning system for SCC” by fixing the coarse and fine aggregate contents, and then adjusting the water/powder ratio and super plasticizer dosage [34]. Another simple method for the mix design of SCC was proposed by Su et al [1], which is easier for implementation and less time-consuming than the Japanese Ready-Mixed Concrete Association (JRMCA)’s method. In this method, the basic principle is to fill the voids of loosely piled aggregate framework with the paste of the binders [1].

Also, Sonebi [35] have explored the feasibility of using statistical methods in proportioning the constituents of medium strength SCC (MS-SCC). A segregation-controlled design methodology was introduced by Saak, et al [31]. They suggested that the yield stress, viscosity and density of the cement paste matrix control the segregation of aggregate in SCC, and a segregation free SCC with highest fluidity would be achieved at the lowest paste yield stress and viscosity of the cement paste matrix. Additionally, through rigorous theoretical analysis, they introduced the concept of a rheological self-flow zone (SFZ) in which the concrete possesses a high workability while still maintaining aggregate segregation resistance [31].

On a general note, EFNARC [17] put the design procedures for SCC in pictorial form as shown in Figure 2.4 that shows the procedure for the design of SCC mixture.

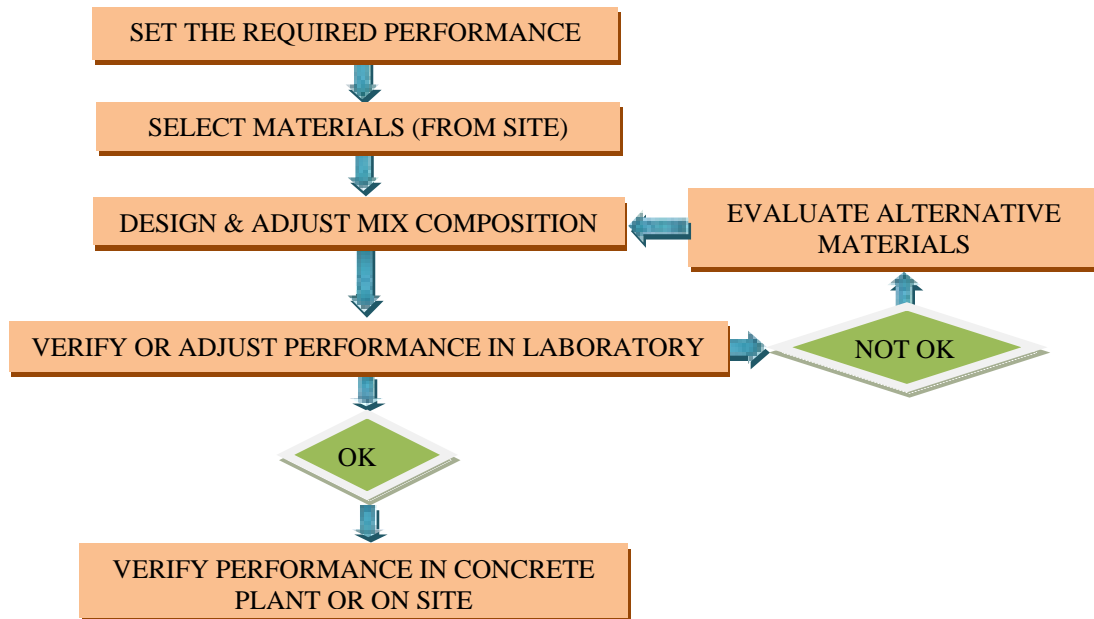


**Figure 2.4:** Mix Design Procedure for SCC [17].

## 2.4 REQUIREMENTS OF SCC MIXTURES

According to EFNARC [17], a bonafide SCC mix must meet up with three workability requirements, right at the time of placing: filling ability, passing ability and segregation resistance.

*Filling ability* refers to the ability of the SCC mix to flow into all corners of the form and establish good bond with the reinforcing bars by its own weight. Slump flow and V-funnel flow time are among the popular test methods used for determining the filling ability of SCC mixtures.

*Passing ability* has to do with the SCC mix being able to flow through tight spaces, such as those between rebars and narrow sections of formworks by its own weight, without any aid. The passing ability of an SCC mix can be determined using L-box, U-box, Fill-box, and J-ring tests.

*Segregation resistance* is the property of an SCC mix that helps to maintain both the filling and passing ability without compromising uniform mix composition throughout the transport and placing process.

These three requirements are the basic qualities a concrete mix must possess to be qualified for classification as an SCC mix. Also, there are other properties, such as workability retention, that has to do with how long from the mixing time the mix retains the three basic qualities explained above; and thixotropy, which controls the deformation characteristics of the mixture, an important feature to be considered for pumping and formwork pressure issues [36-39]. The lateral pressure exerted on forms increases with increasing degree of *thixotropy* of the mixture. This can be attributed to the reversible effect of *thixotropy* which raises the shear strength properties of material after some resting time [38].



## 2.5 TEST METHODS FOR EVALUATION OF THE WORKABILITY

### PROPERTIES OF SCC

Various types of tests have been developed for evaluation of the fresh properties/rheological behaviours of SCC. Table 2.1 [17] presents the typical criteria for SCC acceptance (up to 20 mm maximum aggregate size), and the indication of each of the workability properties. The most commonly conducted tests on fresh SCC mixes are described in detail below.

Table 2.1: Test methods and acceptance criteria for the workability properties of SCC [17].

Test Method		Indication	Typical range of values	
			Minimum	Maximum
1.	Slump flow by Abram's cone	Filling Ability	650 mm	800 mm
2.	T <sub>50cm</sub> slump flow		2 s	5 s
4.	V-funnel		6 s	12 s
10.	Orimet		0 mm	5 mm
6.	L-box (h <sub>2</sub> /h <sub>1</sub> )	Passing Ability	0.8	1.0
7.	U-box (h <sub>2</sub> /h <sub>1</sub> )		0 mm	30 mm
3.	J-ring		0 mm	10 mm
8.	Fill-box		90%	100%
5.	Time increase, V-funnel at T <sub>5 min</sub>	Segregation	0 s	3 s
9.	GTM screen stability test	Resistance	0%	15%

### 2.5.1 The Slump Flow/Flow Table Test

The slump flow test assesses the horizontal free flow of SCC mix in the absence of obstructions. This test method is based on the conventional slump test using Abram's cone. The concrete spread diameter is a measure of its filling ability (Figure 2.5(a)). It is the most common filling ability test, and it gives a good assessment of SCC's filling ability. The acceptable range for SCC spread diameter is 650 - 800 mm [17].

### 2.5.2 The V-funnel Test

This is used for determining the filling ability (flowability) of the concrete with a maximum aggregate of 20 mm. The apparatus (funnel (Figure 2.5(b))) is filled with concrete and the time taken for the concrete to flow through the funnel is measured. An acceptable flow time for SCC, is in the range of 6 to 12 s [17].

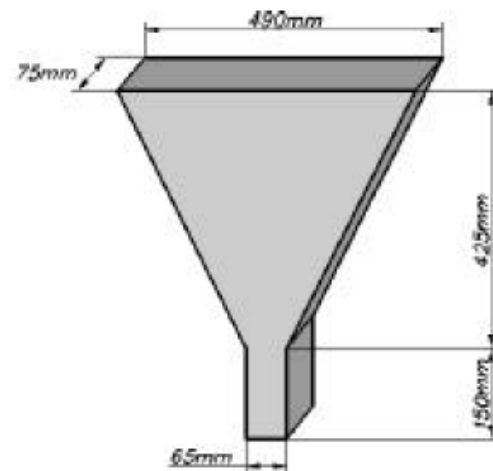


**Figure 2.5:** SCC filling ability tests (a) Flow table/slump flow test (b) V-funnel test.

### ***2.5.3 The U-box Test***

This is a popular passing ability test for SCC. The U-box apparatus (Figure Figure 2.6(a)) consists of a U-shaped vessel, with rectangular cross-section, that is divided by a middle wall into two compartments. An opening with a sliding gate, across which steel bars are placed, is made at the base of the middle wall. One compartment of the U-box is filled with concrete, and allowed to stand for 1 minute before the sliding gate is lifted. At the instance of lifting the gate, the concrete flows upwards to the other compartment through the bars crossing the opening at the base of the middle wall. As the concrete comes to rest, the height of the concrete in the filled compartment ( $H_1$ ) and that in the other compartment to which concrete flowed when the gate was lifted ( $H_2$ ) is measured, each at two places in each compartment. The mean height in each compartment is calculated, and the difference in the heights,  $H_1 - H_2$  is the 'filling height'. The maximum acceptable value of  $H_1 - H_2$  is 30mm [17].

### ***2.5.4 The L-box Test***

This is another popular passing ability test for SCC. The vertical section of the apparatus (Figure 2.6(b)) is filled with concrete and the gate is then lifted to allow the concrete to flow into the horizontal part. The ratio  $H_2/H_1$  (as shown in Figure 2.6(b) - maximum acceptable = 30mm) is a measure of the concrete *slope* at rest, indicating its passing ability [17].

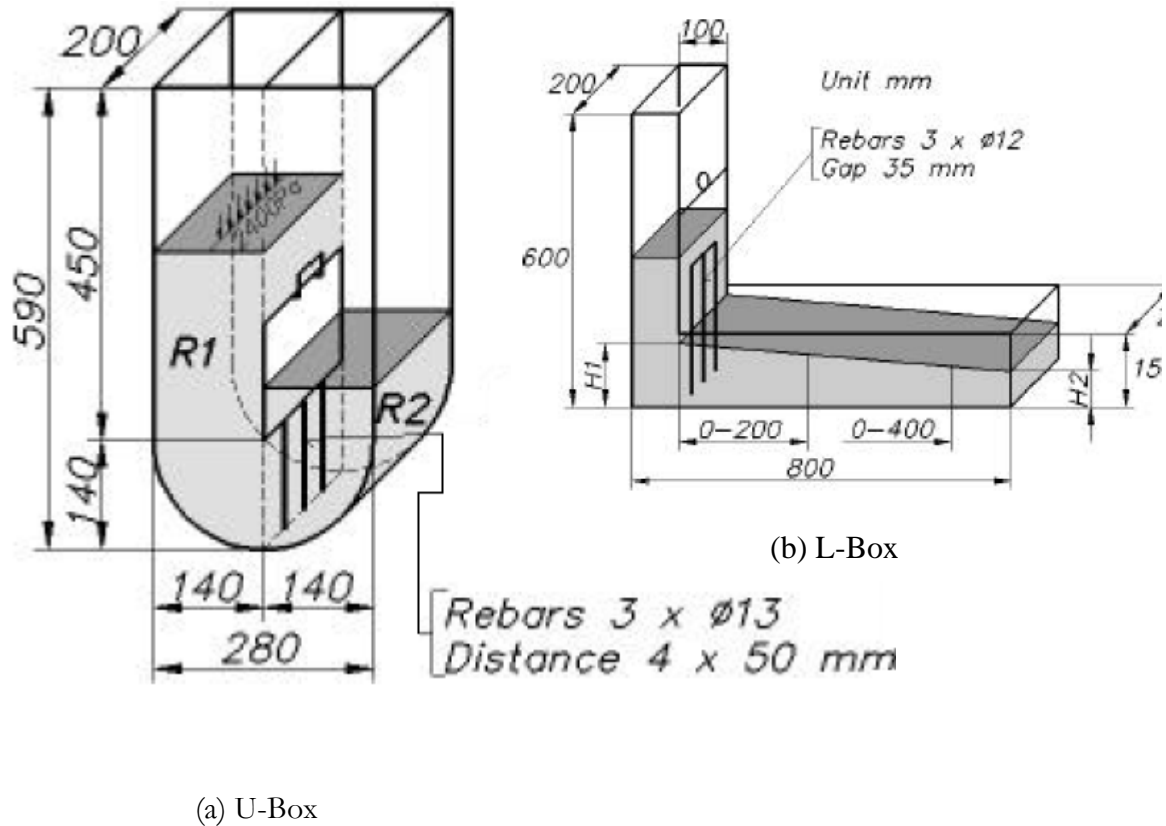


Figure 2.6: Passing ability test.

### 2.5.5 The GTM Screen Stability and V-funnel at $T_{5\min}$ Tests

The V-funnel at  $T_{5\min}$  is employed as a measure of segregation resistance of SCC. After the basic V-funnel test, without cleaning the funnel, concrete is refilled into the funnel and left to settle for 5 minutes. A significant increase in the flow time is an indication of segregation. The maximum increment of time above the basic V-funnel time should not exceed 3s [17].

In the GTM screen stability test, a 10 litre of concrete is allowed to settle so to allow any internal segregation to occur, a part of it is then poured on a 5mm sieve of 350mm diameter. After two minutes, the mortar passing through the sieve is measured. The percentage of this mortar to the original concrete should not exceed 15% [17].

Bui et al. (2002) also developed a “simple apparatus and a rapid method for testing the segregation resistance of SCC”. With this method, quick assessment of the segregation resistance of SCC can be made, both in vertical and horizontal directions. The method is also sensitive to different materials, CA/TA and water/binder ratios [40].

## **2.6 CONSTITUENT MATERIALS USED IN SCC**

The materials used to produce SCC are the same as those for conventionally vibrated concrete, though SCC contains lesser amount of aggregates and larger amount of powder (cement and fillers with particle sizes less than 0.125 mm). Other fillers, such as fly ash, silica fume, ground glass, limestone powder, etc., have also been used throughout the literature.

### ***2.6.1 Powders***

In the SCC parlance, ‘Powder’ refers to a blend of cement and fillers (particle size < 0.125 mm). The filler(s) – cementitious or otherwise – gives the higher paste volume needed for the required workability of SCC, enhancing the workability and durability of SCC, if used in appropriate quantity, without compromising the early strength [15]. The cement used for SCC should not contain C<sub>3</sub>A in excess of 10% in order to prevent problems of low workability retention [17].

Filler materials, such as fly ash, natural pozzolan, silica fume, blast furnace slag, ground glass, limestone powder (LSP), etc, are popularly used in SCC mixtures. The increased cost resulting from the use of higher dosage of superplasticizer can be offset by the reduced labor

costs. Owing to its very low cost, using LSP as a filler material in SCC increases its fluidity without an increase in its cost [35].

**Silica Fume (SF):** Silica fume, sometimes referred to as microsilica or silica dust, is a byproduct generated from the carbothermic reduction of quartz and quartzite in electric arc furnaces in the production of silicon and ferrosilicon alloys [41]. An estimate of the global generation of silicafume is put at more than 1,000,000 tons [42]. It is a siliceous material, containing 85–95%  $\text{SiO}_2$  with very fine vitreous particles [41], which improves the strength and durability properties of concrete to the extent that most modern high-performance concrete mixtures incorporate silicafume as an indispensable admixture [43]. Its extreme fineness (in the order of 10 times finer than that of cement) creates a higher demand for water [41, 43]. Several studies on the fresh and mechanical properties of SCC incorporating silica fume or microsilica have been reported in the literature [31, 37, 44, 45].

**Fly Ash (FA):** Fly ash is a by-product resulting from the incineration of coal in coal fired power plants, municipal solid wastes, rice husks, sugar cane bagasse, and so on [43, 46, 47]. Coal fired power plants generate most of the flyash available worldwide, with a low proportion being reused, primarily in construction and landfills, while some are also used in agriculture and other areas [46, 48].

The cementitious components of power station flyash are: silica ( $\text{SiO}_2$ ), alumina ( $\text{Al}_2\text{O}_3$ ) and iron oxides ( $\text{Fe}_2\text{O}_3$ ), and varying quantities of carbon and calcium (as lime or gypsum) [46, 47]. This makes it a good pozzolanic material for use in cement products. Though fly ash is known for a long time for its cementitious properties [49], its widespread use in concrete was not common until it became available in large quantities as a result of power plants being

forced by the clean air regulations to install scrubbers and electrostatic precipitators for trapping the fine particles, instead of allowing it to escape into the environment[43].

With respect to SCC, Khatib [50] studied the influence of including FA on the fresh and selected hardened properties of SCC with 0-80% partial replacement of FA in OPC at a w/b ratio of 0.36. The study showed that durable, high strength and low shrinkage SCC can be produced economically with high volume of FA [50]. The outcomes of this study were in agreement with the findings of Bouzoubaâ and Lachemi [24] in their study of SCC incorporating high volumes of class F fly ash. Several other studies on SCC incorporating FA have also been reported in the literature [8, 32, 37, 44, 45, 51-60].

***Limestone Powder (LSP):*** This is a by-product of the quarrying process of carbonate rocks. In other words, it's a type of quarry dust where the rock being quarried is a carbonate type, thus its main component is calcium carbonate,  $\text{CaCO}_3$ . The use of LSP in concrete offers many technical benefits, among which are increase in early strength and bleeding control [61, 62]. Addition of LSP of limestone powder in concrete improves the dispersion of cement particles, thus increasing the concrete workability [61-63].

Shuhua and Peiyu (2010) established that LSP does not possess pozzolanic property, as confirmed by the total amount still remaining constant even after 28 days of hydration in concrete using XRD and SEM analyses. However they showed that its filling effect in concrete microstructure (by making the ITZ denser) is so enormous that the porosity of LSP containing concretes is lower than that of traditional concrete, as confirmed by MIP analysis[64]. Similar results have been shown by other researches indicating that though LSP may not be pozzolanic, its excellent filling effect improves not only concrete early strength,

but also that of 28 days [62], in addition to the high deformability of concrete it offers in the fresh state [61-63].

The results obtained by Bonavetti et al (2003) showed that the reduction in the 28 days compressive strength of concrete containing up to 18% LSP filler was not more than 12% [61], while its low cost and durability improvement it offers makes it an important concrete ingredient. LSP was shown to exhibit a different behavior in concrete under high temperature curing in a research by Liu et al (2011), in which an ultra high performance concrete incorporating limestone powder was investigated. The results of their study showed a compressive strength higher than 120MPa under the condition of high temperature in which LSP accelerates the hydration activity while it also hydrates to form calcium monocaboaluminate [65].

In their study on the effect of fly ash and limestone powder on the fresh and hardened properties of SCC produced with two different types of aggregates (limestone and basalt aggregates), Türkel and Kandemir (2010) showed that the effect of mineral admixtures on fresh properties was more dominant than that of aggregate type. Also limestone powder and limestone aggregate combinations showed better fresh and mechanical properties as compared to basalt mixtures [59]. Generally evidences from the literature shows that LSP improves the deformability and viscosity of SCC.

Also, Valcuende et al (2012) conducted an experimental work to study the evolution of shrinkage with age in SCC made with different limestone filler and VMA contents. Their results showed that limestone fillers speed up hydration reactions and provide a finer porous structure. They also established that drying shrinkage is greater in SCC than in CVC. However the shrinkage reduces with higher content of LSP fines, a fact attributable to the



finer porous structure and larger amount of absorbed water from the aggregate serving to compensate for the auto-desiccation of the concrete [66].

### ***2.6.2 Aggregates***

The particular application determines the maximum size of the coarse aggregates. The maximum size of coarse aggregate in SCC is usually limited to 20 mm for general use, while for mass concrete, it may be as large as 50 mm [23], and its content is kept equal to or less than that of the fine aggregate. Bui et al [40] developed a rheological model for relating SCC rheology to the average spacing and diameter of aggregate. According to them, a lower flow and higher viscosity of the paste is required by a higher aggregate spacing in order to achieve satisfactory flow and segregation resistance of SCC [40]. They also established that using the same spacing but smaller aggregate size yielded better results.

### ***2.6.3 Chemical Admixtures***

Superplasticizer (SP) is essential in SCC for achieving the required workability. An appropriate SP should have a high and lasting (minimum two hours) dispersing effect for a low water/powder ratio, and also less sensitive to changes in temperature [4, 67]. Stabilizers (if needed to achieve stability) are also indispensable to produce a good SCC mix. The stabilizer is otherwise called viscosity modifying admixture (VMA), which is usually a chemical substance added to SCC mixtures to ensure a stable mix. Other admixtures, such as thixotropy-enhancing agent (TEA), air-entraining admixture (AEA), retarders, etc., may also be used.

As a result of the high cost of SCC conventional chemical admixtures, studies are going on regarding the use of cheaper mineral and chemical admixtures to achieve the stability and other SCC fresh properties, hence lowering the SCC cost. A successful use of rice husk ash (RHA) as a viscosity modifying agent for SCC had been reported in the literature [68]. Also, in a bid to exploring cheaper alternatives to expensive stabilizing agents, Rols et al conducted a study on the effect of three different types of viscosity modifying agents – starch, precipitated silica and a by-product from the starch industry – on fresh and hardened properties of SCC. Their study showed that precipitated silica and starch could be used as alternative viscosity modifying agents for SCC [69].

## **2.7 HARDENED PROPERTIES OF SCC**

### ***2.7.1 Compressive, Tensile, and Bond Strength***

Various compressive strength values have been reported for SCC ranging from low to very high strengths. A representative case of low to medium strength SCC was that research by Melo and Carneiro [30], who reported 56-days compressive strengths in the range of 21 – 38 MPa, employing metakaolin of various finesses at 5 and 35% replacement of cement and w/p ratio in the range of 0.5 – 0.7. Also, Bouzoubaâ and Lachemi [24] reported 28-day compressive strengths ranging from 26 to 48 MPa using 40 – 60 % replacement of cement (total cm = 400 kg/m<sup>3</sup>), and the w/cm ratios in the range of 0.35 – 0.45. Türkel and Kandemir [59] reported 28-day compressive strength of 17 – 47 MPa with a cement content of 350 kg/m<sup>3</sup> and w/p ratio of 0.31 – 0.34. High strength SCC having compressive strengths of up to 80 MPa has been reported by Xie et al [60]. A recent research was carried out on very high strength SCC by Liu et al [65] in which they reported that the compressive

strengths of SCC mixtures were above 120 MPa using limestone powder and high temperature curing.

Cylinder splitting strengths of about 2 – 6 MPa have been reported in the literature, corresponding to compressive strengths of about 20 – 80 MPa [70]. In a study by Brouwers and Radix [32], splitting strengths of 4.1 – 4.7 MPa were reported, corresponding to 28-day compressive strengths of 51 – 54 MPa. They further established that the tensile strength of SCC is somewhat higher than that of CVC of equivalent compressive strengths.

The concrete-steel bond is an important parameter to consider in any design. Since the assumption of strain compatibility between steel and concrete forms an integral part of the foundation upon which the design of R-C structures are based. Hence it is an important parameter to be given due attention in the development of any concrete material. Defects in concrete-steel bond may also expose the steel to corrosion [70]. SCC has better bond behavior than that of conventional vibrated concrete [2], which can be attributed to the good interlocking of aggregates and higher volume of paste [5]. Bond behavior of SCC has been reported by Khayat et al [71], Soylev and François [72], Hossain and Lachemi [73] and Valcuende and Parra [74].

The so-called ‘top-bar effect’, which is the reduction in bond strength of bar(s) at higher levels in deep members, is lower in SCC than in CVC [73]. The bond strength reduction results from the formation of voids under horizontal bars which could be caused by settlement of concrete below the bars and rising bleed water from the concrete body below the bars which is trapped below and around the bars. Therefore, the more the concrete depth below a bar, the worse is the ‘top-bar effect’ on it, and so the lower the bond

efficiency. For example, Valcuende and Parra obtained the bond strength reduction between the upper and lower zones of the tested columns as 40% – 61% for SCC, while the corresponding CVC lost 79% – 86% [74]. A well formulated SCC will be so stable that the amount of bleeding will be very minimal [70], and because of its self compactability, plastic settlement under the bars will be lower. This explains the lower observed top-bar factors in SCC.

### ***2.7.2 Modulus of Elasticity of SCC***

The modulus of elasticity of concrete increases with an increase in the quantity of aggregate of high rigidity, while it decreases with increasing cement paste content and porosity [13]. The elastic modulus of SCC is almost identical to that of a conventional vibrated concrete, made from the same raw materials. In spite of higher paste volume in SCC, the elasticity remains almost unchanged as a result of the denser packing of the SCC particles [75]. Several other researchers reported lower modulus of elasticity for SCC than CVC of similar compressive strength. The lower stiffness of SCC mixes can be attributed to its lower coarse aggregate content [70].

As compared to conventional vibrated concrete of identical compressive strength and made from the same aggregates, the elasticity modulus of SCC is lower by 20% [13], while Leemann and Hoffmann [14] reported a 16% lower value. The average 28-days modulus of elasticity of SCC was reported as 30 GPa corresponding to a cube strength of 55.41 MPa [2]. Generally in the literature, the modulus of elasticity of SCC mixes, on an average, were about 40% lower than those of the CVC mixes in the low strength ranges, while at high strength levels, reduction was less than 5% [70].

### ***2.7.3 Shrinkage and Creep***

The shrinkage and creep rates of SCC have been reported to be around 30% higher than that of conventional vibrated concrete of identical compressive strength. This is attributable to the higher paste volume in SCC [14]. Corinaldesi and Moriconi [76] suggested the addition of fiber for counteracting SCC drying shrinkage. Even for plain SCC without fibers, recent studies reported lower percentages of shrinkage and creep above CVC of similar grades. For example, Valcuende et al [66] reported less than 10% higher shrinkage in SCC than CVC. This observed improvement in SCC shrinkage properties over the years can be explained by the fact that earlier developers relied on very high paste volume to achieve high flow and stability. However recent advancements in SP and VMA and the use of optimized particle packing for achieving stability in SCC have lead to these improvements.

### ***2.7.4 Water Permeability, Water Absorption and Chloride Permeability***

The water absorption and initial surface absorption of 1% and 0.01 ml/m<sup>2</sup>/sec were reported by Kapoor et al [5] for SCC as against 2% and 0.02 ml/m<sup>2</sup>/sec for CVC of the same grade respectively. Similar trend was also reported by Zhu and Bartos [6].

A rapid chloride permeability value of 620 Coulombs was reported by Kapoor et al [5] for SCC as against 1970 Coulombs for conventional CVC of the same grade. Similar trends were observed by Patel et al [8] and Nehdi et al [9].

### ***2.7.5 Corrosion of Rebar in SCC***

Although good number of studies on durability properties of SCC were reported by various researchers [4-12], few studies on reinforcement corrosion in SCC have been reported [77].

Hassan, et al [78] investigated the corrosion resistance of SCC in full-scale reinforced beams. On the basis of the overall performance of the large-scale tested beams, they found that SCC offers better corrosion resistance than CVC of similar grade, while for small-scale cylindrical specimens, the difference was insignificant.

Yu et al [77] investigated the probabilistic nature of the time to corrosion initiation ( $T_i$ ) of rebars in SCC, the corresponding threshold values of chloride ion concentration ( $C_{th}$ ) at rebar levels, and the distribution of air voids at the rebar-concrete in concrete slabs. They reported that the rebar corrosion initiation depends upon both the alkalinity of cement and the superplasticizer type. Rebars embedded in SCC mixtures produced with cements of high alkalinity showed higher and more stable corrosion resistance than those in CVC.

## **2.8 ECONOMICS OF SCC**

Although SCC requires high content of chemical admixtures (SP, VMA, etc), which tends to raise its cost, the increased cost would be offset by savings in labor costs and savings in maintenance cost of concrete structures as a result of its high durability. Also, the use of locally available waste materials as fillers will further help in achieving more economy. These filler materials also enhance the rheology of SCC and as a result of the reduced heat of hydration, the risk of thermal cracking is lower, thus improving the durability of concrete structure [55]. In the experimental trial by Akram et al [79] reported that the cost of ingredients of SCC mixtures were around 36% less than that of CVC.

## **CHAPTER3**

### **EXPERIMENTAL PROGRAM**

#### **3.1 INTRODUCTION**

In this chapter, the materials used in the experimental program are stated along with their characteristics and sources. In accordance with the theme of this research, most of the materials employed in the research program were procured from local sources within the Kingdom. Also the experimental procedures followed in the investigation are clearly laid out. Six different waste materials that are available locally in addition to two other imported materials were employed as filler materials for developing the SCC mixtures.

The research work was executed in three major stages. The first stage involved selection and acquisition of the waste materials, aggregates and chemical admixtures, and designing the trial mixtures for selected ternary combinations of the materials. In the second stage, the task included fixing the optimal dosages of SP and VMA required for obtaining flowable SCC. This was done by running several trials and measuring the flow parameters (slump flow, V-funnel flow time and U-Box) until the values were within the acceptable limits. Twelve mixes, including the control, were tried, out of which only 10 were selected for detailed studies of their hardened properties. The study of the hardened mechanical and durability properties was conducted in the third stage.

The following sections of the Chapter serve to explain the experimental program covering the three main stages explained in the preceding discussion.

## 3.2 MATERIALS USED IN THE DEVELOPMENT OF SCC MIXES

### 3.2.1 Powders

#### (i) Cement

The cement type used was ASTM C 150 Type I, having a specific gravity of 3.15. This is the most commonly used cement type in the Kingdom. Its chemical composition is shown in Table 3.1.

**Table 3.1:** Chemical composition of OPC type 1.

Component	Weight %
CaO	64.35
SiO <sub>2</sub>	22.00
Al <sub>2</sub> O <sub>3</sub>	5.64
Fe <sub>2</sub> O <sub>3</sub>	3.80
K <sub>2</sub> O	0.36
MgO	2.11
Na <sub>2</sub> O	0.19
Equivalent alkalis	0.33
SO <sub>3</sub>	2.10
Loss on ignition	0.70
C <sub>3</sub> S	55.00
C <sub>2</sub> S	19.00
C <sub>3</sub> A	10.00
C <sub>4</sub> AF	7.00



*(ii) Silica Fume (SF)*

The SF employed in this study was sourced from a local ready mixed company. The chemical properties are shown in Table 3.2.

**Table 3.2:** Chemical composition of the silica fume used in the study.

Constituent	Weight %
SiO <sub>2</sub>	92.5
Al <sub>2</sub> O <sub>3</sub>	0.72
Fe <sub>2</sub> O <sub>3</sub>	0.96
CaO	0.48
MgO	1.78
SO <sub>3</sub>	-
K <sub>2</sub> O	0.84
Na <sub>2</sub> O	0.5
Loss on ignition	1.55

*(iii) Fly Ash (FA)*

The FA employed in this study was also sourced from the local ready mixed company. The chemical properties are shown in Table 3.3.

**Table 3.3:** Chemical composition of the fly ash used in the study.

Constituent	Weight %
SiO <sub>2</sub>	45.3
Al <sub>2</sub> O <sub>3</sub>	34.4
Fe <sub>2</sub> O <sub>3</sub>	2.37
CaO	8.38
MgO	1.86
SO <sub>3</sub>	0.46
K <sub>2</sub> O	0.57
Na <sub>2</sub> O	0.4
L.O.I	3.5

(iv) *Natural pozzolan (NP)*

The natural pozzolan used this study was obtained locally from volcanic rocks in Western Province of Saudi Arabia. Its specific gravity is 3.00, and its chemical composition is shown in Table 3.4.

**Table 3.4:** Chemical composition of the natural pozzolan used in the study.

Component	Weight %
SiO <sub>2</sub>	42.13
Al <sub>2</sub> O <sub>3</sub>	15.33
Fe <sub>2</sub> O <sub>3</sub>	12.21
MgO	8.50
CaO	8.06
K <sub>2</sub> O	0.84
Na <sub>2</sub> O	2.99
Na <sub>2</sub> O+(0.658K <sub>2</sub> O)	3.54
Loss on Ignition	-
Moisture	0.17

(v) *Limestone Powder (LSP)*

The LSP used in the research was sourced from a limestone quarry in Abu Hadriyah, Eastern Province of Saudi Arabia. It has a specific gravity of 2.60 and its chemical composition is shown in Table 3.5.

**Table 3.5:** Chemical composition of LSP used in the study.

Component	Weight %
SiO <sub>2</sub>	11.79
CaO	45.7
Al <sub>2</sub> O <sub>3</sub>	2.17
Fe <sub>2</sub> O <sub>3</sub>	0.68
MgO	1.8
K <sub>2</sub> O	0.84
Na <sub>2</sub> O	1.72
Na <sub>2</sub> O+(0.658K <sub>2</sub> O)	2.27
Loss on Ignition	35.1
Moisture	0.2

*(vi) Cement Kiln Dust (CKD)*

Sourced from a cement company in Jeddah, Western province of Saudi Arabia, the CKD used in the research has a specific gravity of 2.79, and its chemical composition is shown in Table 3.6.

**Table 3.6:** Chemical composition of the CKD used in the study.

Component	Weight %
CaO	49.300
SiO <sub>2</sub>	17.100
Al <sub>2</sub> O <sub>3</sub>	4.240
Fe <sub>2</sub> O <sub>3</sub>	2.890
K <sub>2</sub> O	2.180
MgO	1.140
Na <sub>2</sub> O	3.840
P <sub>2</sub> O <sub>5</sub>	0.120
ZrO <sub>2</sub>	0.011
Cr <sub>2</sub> O <sub>3</sub>	0.011
CuO	0.029
NiO	0.012
TiO <sub>2</sub>	0.340
V <sub>2</sub> O <sub>5</sub>	0.013
Equivalent alkalis (Na <sub>2</sub> O + 0.658K <sub>2</sub> O)	5.270
(SO <sub>3</sub> ) <sup>2-</sup>	3.560
Cl <sup>-</sup>	6.900
Loss on ignition	15.800
BaO (µg/g (ppm))	78.200
ZnO (µg/g (ppm))	65.800

*(vii) Electric Arc Furnace Dust (EAFD)*

The EAFD used in this study was obtained from a local steel manufacturing company in the Kingdom. In order to overcome the associated retarded setting time, the raw EAFD was thermally treated at 900°C in a furnace before use. Its specific gravity was 2.08, and its chemical composition is shown in Table 3.7.

**Table 3.7:** Chemical composition of EAFD used in the study.

<b>Component</b>	<b>Weight %</b>
Aluminium	0.70
Calcium	9.39
Cadmium	0.0004
Copper	0.06
Iron	33.60
Potassium	1.70
Magnesium	2.30
Manganese	1.80
Sodium	2.60
Nickel	0.01
Lead	1.31
Phosphorous	0.13
Silicon	2.38
Tin	0.03
Sulphur	0.57
Titanium	0.09
Zinc	10.00

*(viii) Pulverized Steel Slag (PSS)*

PSS was used in this study as one of the filler materials. The PSS was obtained by grinding steel slag lumps sourced from a local steel manufacturing company in the Kingdom. The grinding was performed with laboratory pulverizer to a fineness of passing #100 (150 $\mu$ m) sieve. The pulverized material has a specific gravity of 3.75. Its chemical composition is shown in Table3.8.

**Table 3.8:** Chemical composition of the PSS used in the study.

Constituent	Weight %
SiO <sub>2</sub>	16.47
Al <sub>2</sub> O <sub>3</sub>	6.67
Fe <sub>2</sub> O <sub>3</sub>	26.58
MgO	6.14
K <sub>2</sub> O	0.099
Na <sub>2</sub> O	0.26
Na <sub>2</sub> O+(0.658K <sub>2</sub> O)	0.26
Loss on Ignition	3.8
Moisture	0.2

*(ix) Calcined Clay/Metakaolin (MK)*

Calcined clay (MK) was also used in some of the trial mixes as a filler. The raw clay was sourced from Qatif, Eastern Province of Saudi Arabia. Figure 3.1 shows the raw clay before processing, while Figure 3.2(a) shows the clay crushed to smaller sizes and laid in furnace trays before calcination. Before use, the clay was thermally activated in a furnace at 850°C and then ground with laboratory pulverizer to a fineness of passing #100 (150µm) sieve. Figure 3.2(b) shows the raw clay and the calcined one side-by-side. Its specific gravity was obtained as 2.0. Table 3.9 shows its chemical composition.



**Figure 3.1:** Raw clay before processing.



**Figure 3.2:** (a) Crushed clay laid in furnace trays (b) Raw clay and activated clay shown side-by-side.

**Table 3.9:** Chemical composition of the calcined clay (MK) used in the study.

Constituent	Weight %
SiO <sub>2</sub>	46.37
Al <sub>2</sub> O <sub>3</sub>	15.37
Fe <sub>2</sub> O <sub>3</sub>	6.66
MgO	4.58
K <sub>2</sub> O	1.76
Na <sub>2</sub> O	0.95

### 3.2.2 Coarse Aggregates

The coarse aggregates used in this study were crushed limestone sourced from a local quarry in Abu Hadriah, Eastern Province of Saudi Arabia. The coarse aggregate has a maximum aggregate size of 20 mm, specific gravity of 2.60 and absorption of 1.4%. Table 3.10 shows the coarse aggregate grading.

**Table 3.10:** Grading of the coarse aggregate used in the study.

Sieve size (mm)	% passing
19.0	100
12.5	65
9.5	30
4.75	10
2.36	0



### 3.2.3 Fine Aggregates

Dune sand, a vastly available material in the Kingdom, was used as fine aggregate in this study. The specific gravity of fine aggregate was 2.56, and the absorption was 0.4%. Table 3.11 shows the grading of the dune sand used in the study.

**Table 3.11:** Grading of the fine aggregate used in the study.

ASTM Sieve #	Size (mm)	% passing
4	4.75 mm	100
8	2.36 mm	100
16	1.18 mm	100
30	600 $\mu\text{m}$	76
50	300 $\mu\text{m}$	10
100	150 $\mu\text{m}$	4

### 3.2.4 Chemical admixtures

#### (i) Superplasticizer (SP)

The superplasticizer employed in all the trial mixes was Glenium 51<sup>®</sup>. It's a new generation polycarboxylic-based ether hyperplasticiser. It was sourced from a local supplier in the Kingdom. Its technical data is shown in Table 3.12, as obtained from the manufacturer.

**Table 3.12:** Technical data of Glenium 51<sup>®</sup>.

Appearance	Brown liquid
Specific gravity @ 20°C	1.08±0.02 g/cm <sup>3</sup>
pH-value @ 20°C	7.0±1.0
Alkali content	≤ 5.0
Chloride content	≤ 0.1 %

*(ii) Stabilizer/Viscosity Modifying Admixture (VMA)*

RheoMATRIX<sup>®</sup>100 was used as the stabilizer in the trial mixes. It's an aqueous solution of a high-molecular weight synthetic copolymer, which consists of a water-soluble polymer that is capable of modifying the rheological properties of a flowing concrete mixture. It was sourced from the same supplier as Glenium 51<sup>®</sup>. Its technical properties are shown in Table 3.13, as obtained from the manufacturer.

**Table 3.13:** Technical data of RheoMATRIX<sup>®</sup>.

Appearance	Brown
Specific gravity @ 20°C	1.0 – 1.02 g/cm <sup>3</sup>
pH-value @ 20°C	6 – 9
Chloride ion content	< 0.1 %

**3.2.5 Mixing water**

The normal sweet water available in the laboratory tap was used throughout the trial mixing and preparation of test specimens for evaluation of hardened properties of successful mixes.

### 3.3 SCC TRIAL MIXES

Twelve (12) mixes were tried in the study. Two (2) of the mixes were binary mixtures, while the remaining ten (10) were ternary combinations of the waste materials with cement.

#### 3.3.1 *Mix Parameters of the Trial Mixes*

Table 3.14 shows the parameters used in the trial mixes. As can be seen from the Table, all design parameters were fixed for all the mixes, except the quantities of superplasticizer and stabilizer dosages required for each trial mix to achieve self compactibility. These dosages were obtained by trials on the concrete mixes until the rheological parameters attained satisfactory levels. The various combinations of waste materials proposed for each of the trial mixes are shown in Table3.15.

**Table 3.14:** Mix parameters used in the trial mixes.

Cement content	400 kg/m <sup>3</sup> (Constant)
Total mineral admixture content	100 kg/m <sup>3</sup> (Constant)
Total powder content	500 kg/m <sup>3</sup> (Constant)
w/p ratio	0.30 (Constant)
Sand/TA ratio	0.40 (Constant)
Superplasticizer (SP) dosage	Variable
Stabilizer (VMA) dosage	Variable

**Table 3.15:** Combinations and proportions of waste materials and cement proposed for each of the trial mixes.

S/N	Trial ID	Quantities of Powders (kg/m <sup>3</sup> of concrete)									
		CEMENT	SF	FA	NP	BHD	CKD	PSS	LSP	MK	Total powder
TM1	F-100	400	-	100	-	-	-	-	-	-	500
TM2	L-100	400	-	-	-	-	-	-	100	-	500
TM3	SL-50-50	400	50	-	-	-	-	-	50	-	500
TM4	LN-50-50	400	-	-	50	-	-	-	50	-	500
TM5	NC-50-50	400	-	-	50	-	50	-	-	-	500
TM6	NB-50-50	400	-	-	50	50	-	-	-	-	500
TM7	NP-50-50	400	-	-	50	-	-	50	-	-	500
TM8	LM-75-25	400	-	-	-	-	-	-	50	50	500
TM9	NM-75-25	400	-	-	50	-	-	-	-	50	500
TM10	CM-75-25	400	-	-	-	-	50	-	-	50	500
TM11	BM-75-25	400	-	-	-	50	-	-	-	50	500
TM12	PM-75-25	400	-	-	-	-	-	50	-	50	500

### 3.3.2 Mix Design for the Trial Mixtures

The mix design was done using the absolute volume method. The mass of total aggregate is solved for in the absolute volume equation, after which each of the fine and coarse aggregate can be obtained separately using the chosen FA/TA aggregate ratio. The analytical derivation of the masses of fine and coarse aggregates is shown as follows.

Consider the absolute volume equation represented by

$$V_{TA} + \sum_i V_i = 1 \quad \dots \dots \dots (1)$$

Where  $V_i$  is the volume of individual components excluding the aggregates. Those components are cement, mineral admixtures, water, SP, VMA and entrapped air. Equation (1) can be rewritten as

$$V_{TA} + \sum_i \frac{m_i}{\rho_i} = 1 \quad \dots \dots \dots (2)$$

in which  $m$  and  $r$  are the masses and densities of individual components. The admixture volumes are fixed for a mix and hence known. Also water volume is known from the w/cm and the cementing materials and filler contents. The only unknowns are the aggregate volume. Thus,

$$V_{TA} = V_{stones} + V_{sand} = 1 - \sum_i \frac{m_i}{\rho_i} \quad \dots \dots \dots (3)$$

Since we'll be measuring the aggregates by mass, we need to express the last equation in mass terms as

$$V_{TA} = \frac{m_{stones}}{\rho_{stones}} + \frac{m_{sand}}{\rho_{sand}} \quad \dots \dots \dots (4)$$

Let the sand/TA ratio be  $f$ , then

$$f = \frac{m_{sand}}{m_{sand} + m_{stones}} \quad \dots \dots \dots (5)$$

From this expression, we can obtain  $m_{stones}$  in terms of  $m_{sand}$  as

$$m_{stones} = \frac{f}{1-f} \times m_{sand} \quad \dots \dots \dots (6)$$

Substituting for  $m_{stones}$  in (4), the only unknown, mass of sand,  $m_{sand}$  can be obtained as

$$m_{sand} = \frac{V_{TA} \times \rho_{sand} \times \rho_{stones} \times f}{\rho_{stones} \times f + \rho_{sand} (1-f)} \quad \dots \dots \dots (7)$$

And finally the mass of stones can be obtained in by using (6). Then the individual components of the crushed stone can be obtained using the distribution stated later. The total water to be used in the mixing is obtained by adding the absorption percentages of each of sand and crushed stones.

### 3.3.3 Weights of Constituent materials in the Trial Mixtures

The weights of constituent materials for the trial mixtures, obtained by applying the algorithm developed in the previous section, are shown in Table 3.16. As more than one trials were made on each of the trial mixtures TM1 to TM12 in order to achieve acceptable SCC mixes, only the last working dosages of VMA and SP for each mixture were shown in the table, except for TM11 and TM12, where the dosages shown were the last dosage tried before it was concluded that those combination would not satisfy the flow criteria at those chosen values of mix parameters. A typical scenario of trials runs for fixing the dosages of SP and VMA is shown in Figure 3.17, which was for TM2. As can be seen from the table, as at the trial dosage in the last column, the flow results and stability behaviors are acceptable, so the last column (T5) became the final mix proportions for TM2, as can be seen in the third column of Table 3.16.

**Table 3.16:** Weights of the constituent materials for the trial mixtures.

MATERIALS	TM1	TM2	TM3	TM4	TM5	TM6	TM7	TM8	TM9	TM10	TM11	TM12
<b>Cement</b>	400	400	400	400	400	400	400	400	400	400	400	400
<b>FA</b>	100	-	-	-	-	-	-	-	-	-	-	-
<b>SF</b>	-	-	50	-	-	-	-	-	-	-	-	-
<b>NP</b>	-	-	-	50	50	50	50	-	75	-	-	-
<b>BHD</b>	-	-	-	-	-	50	-	-	-	-	75	-
<b>CKD</b>	-	-	-	-	50	-	-	-	-	75	-	-
<b>PSS</b>	-	-	-	-	-	-	50	75	-	-	-	75
<b>LSP</b>	-	100	50	50	-	-	-	-	-	-	-	-
<b>MK</b>	-	-	-	-	-	-	-	50	50	25	25	25
<b>Total powder</b>	500	500	500	500	500	500	500	475	500	500	500	475
<b>w/p</b>	0.3	0.3	0.3	0.3	0.3	0.3	0.3	0.3	0.3	0.3	0.3	0.3
<b>Water</b>	165	165	165	165	165	165	165	165	165	165	165	165
<b>1/2 in</b>	291	293	292	294	295	290	295	290	293	292	288	295
<b>3/8 in</b>	291	293	292	294	295	290	295	290	293	292	288	295
<b>3/16 in</b>	166	167	167	168	169	166	168	166	168	167	164	169
<b>3/32 in</b>	83	84	83	84	84	83	84	83	84	83	82	84
<b>Dune Sand</b>	832	837	833	840	844	830	842	828	838	833	822	843
<b>SP (% of</b>	<i>1.40</i>	<i>2.00</i>	<i>1.80</i>	<i>1.90</i>	<i>1.50</i>	<i>2.80</i>	<i>2.80</i>	<i>3.25</i>	<i>3.00</i>	<i>2.20</i>	<i>3.25</i>	<i>3.25</i>
<b>VMA (% of</b>	<i>1.40</i>	<i>1.25</i>	<i>1.50</i>	<i>1.50</i>	<i>1.50</i>	<i>1.25</i>	<i>1.50</i>	<i>1.00</i>	<i>0.50</i>	<i>1.50</i>	<i>0.50</i>	<i>0.50</i>
<b>SP</b>	7000	10000	9000	9500	7500	14000	14000	16250	15000	11000	16250	16250
<b>VMA</b>	7000	6250	7500	7500	7500	6250	7500	5000	2500	7500	2500	2500

**Table 3.17:** Fixing of the SP and VMA dosages for TM2.

MATERIALS	T 1	T 2	T 3	T 4	T 5
Cement (Kg/m <sup>3</sup> )	400	400	400	400	400
LSP (Kg/m <sup>3</sup> )	100	100	100	100	100
Total Cem. mat (Kg/m <sup>3</sup> )	500	500	500	500	500
w/p	0.3	0.3	0.3	0.3	0.3
Water	165	165	165	165	165
1/2 in	293	293	295	294	293
3/8 in	293	293	295	294	293
3/16 in	168	167	168	168	167
3/32 in	84	84	84	84	84
Dune Sand	838	837	842	839	837
SP (% of cem mat)	<i>1.60</i>	<i>1.80</i>	<i>1.80</i>	<i>1.80</i>	<i>2.00</i>
VMA (% of cem mat)	<i>1.50</i>	<i>1.50</i>	<i>0.75</i>	<i>1.25</i>	<i>1.25</i>
SP (g)	8000	9000	9000	9000	10000
VMA (g)	7500	7500	3750	6250	6250
RESULTS					
Flow Table (650 – 800 mm)	<i>610</i>	<i>635</i>	800	650	680
V-Funnel Time (6 – 12 s)	9.0	11.0	-	-	11.0
U-Box (0 – 30 mm)	20.0	-	-	-	-
Bleeding (Visual)	None	None	Slight	None	None
Segregation (Visual)	None	None	<b>High</b>	None	Negligible
Remarks*	NS	NS	NS	NS	S

\* NS = Not Selected, S = Selected as the final mix proportion for the trial mixture

### 3.4 PREPARATION OF TRIAL MIXES

For each of the trials conducted, appropriate weights of the dry components were measured and then added together in a laboratory electric mixer of a revolving drum type. After mixing the dry components for a minute, around 50% of the required water was added while the drum was still rolling, and the mixture blended further for a minute or two until all particles



have become wet. The remaining water was divided into two parts, and in each, measured quantities of SP and VMA were added. The SP containing part of remaining mixing water was added gradually to the mixture, keeping the mixer running until the SP water have mixed nearly homogenously with the mixture. At this stage, the VMA water was let into the mixture and the mixer continued to run. The whole mixing process, starting from the time SP was added to the mix was maintained at  $15 \pm 5$  minutes. After thorough mixing, the mixture was ready for discharge into plastic bowls, in which it was allowed to rest for 10 – 15 minutes before it became a candidate for self-compactibility tests.

### **3.5 SELF-COMPACTABILITY TESTS ON TRIAL MIXES**

Three self-compactibility tests were performed on each of the trial mixtures. These are slump flow, V-funnel and U-box. Segregation resistance was evaluated by visual judgment according to criteria to be explained later.

#### ***3.5.1 Slump Flow Test***

This test was performed for the trial mixes for accessing their filling ability, in accordance with the guides contained in EFNARC SandG for SCC [17]. The main apparatus is the conventional Abram's cone having an internal base and top diameters of 200 mm and 100 mm, and a height of 300 mm. A base plate of a stiff non absorbent material is also needed along with other accessories, like hand trowel, scoop and a measuring tape.

A well sampled quantity of fresh concrete was filled into a moistened slump cone using the scoop, while firmly holding the cone, placed centrally on a moistened baseplate kept on level stable ground. Excess materials were struck off using the trowel to the level of the cone's

top. The cone was then raised vertically and the concrete was allowed to flow out freely, flowing radially on the baseplate. The average value of diameters measured in two perpendicular directions was recorded as the flow diameter for each of the trial mixtures. Figure 3.3 shows the slump flow measurement accessories.



**Figure 3.3:** Slump flow measurement equipments and accessories.

### ***3.5.2 V-funnel Test***

This is another filling ability test performed on trial mixes for assessing their flow speeds through narrow openings in the absence of obstructions. The test was performed in accordance with the guides contained in EFNARC SandG for SCC [17]. The accessories consist of a V-funnel, a bucket, a trowel, a scoop and a stopwatch.

The V-funnel was firmly set on ground, and its internal surfaces were moistened without allowing any surplus water to remain in the funnel. With the funnel's bottom gate closed, the funnel was completely filled with normally sampled concrete, and the extra material was struck off using the trowel. Within 10 seconds after filling the funnel, the bottom gate was

opened, while the concrete discharges by gravity into a bucket placed underneath. The time taken in seconds from the instant the gate was opened to the time when the funnel could be seen through from above was recorded as flow time for each of the trial mixture. Figure 3.4 shows the V-funnel and related accessories.



**Figure 3.4:** V-funnel testing accessories.

### ***3.5.3 U-Box Test***

This is a passing ability test performed for the trial mixes for assessing their ability to flow through narrow openings in the presence of obstructions, performed in concordance with the EFNARC SandG for SCC [17]. The equipments consist of the U-box, a trowel and a scoop. The U-box apparatus consists of a U-shaped vessel, with rectangular cross-section, that is divided by a middle wall into two compartments. An opening with a sliding gate, across which steel bars are placed, is made at the base of the middle wall.

One compartment of the U-box was filled with concrete, just like the filling on the V-funnel described earlier. The exception here is that the concrete sample is allowed to stand for 1 minute before the sliding gate is lifted. At the instance of lifting the gate, the concrete flows upwards to the other compartment through the bars crossing the opening at the base of the middle wall. As the concrete came to rest, the height of the concrete in the filled compartment (H1) and that in the other compartment to which concrete flowed when the gate was lifted (H2) was measured and recorded for two places in each compartment. The mean height in each compartment was calculated, and the difference in the heights,  $H1 - H2$ , was recorded as *the filling height* for that mixture. Figure 3.5 shows the U-box testing equipment.



**Figure 3.5:** U-box testing accessories.

### 3.5.4 Assessment of Segregation Resistance in the Trial Mixes

For segregation resistance of the trial mixtures, no special test, such as screen stability test, was conducted. The assessment of the cohesion properties were made by visual judgement. According to EFNARC [17], visual observation of a flowing concrete on the flow table can offer some indication of its segregation resistance. Emphasis was laid on observing band of mortar or cement paste without coarse aggregate at the perimeter of the pool of concrete on the flow table. In line with this, a ‘mortar band width’ criteria set in this study to classify mixes with respect to mixture stability is shown in Table 3.18.

**Table 3.18:** Segregation resistance criteria used for screening the mixtures.

<b>Mortar Band width</b>	<b>Segregation Class</b>
No mortar band observed	None
Band width $\leq$ 10 mm	Negligible
10mm < Band width $\leq$ 20 mm	Low
20mm < Band width $\leq$ 50 mm	High
Large mortar band > 50 mm	Severe

### 3.6 SELECTION OF QUALIFYING MIXESFROM THE TRIALMIXTURES

The flow results of the trial mixtures are shown in Table 3.19. As can be seen from the table, TM11 and TM12 failed the V-funnel tests with 17 and 24 seconds flow times, respectively. As such, these two mixes were discarded from the set, while the remaining passing mixes were considered for studies on hardened properties.

**Table 3.19:** Flow results of the trial mixtures.

S/N	Trial ID	Flow Table (650–00mm)	V-Funnel Time (6–12s)	U-Box (0–30mm)	Bleeding (Visual)	Segreg. (Visual)
TM1	F-100	780	10.0	10	None	Neg.
TM2	L-100	680	11.0	5	None	Neg.
TM3	SL-50-50	660	7.0	6	None	None
TM4	LN-50-50	690	11.0	0	None	None
TM5	NC-50-50	650	6.5	27	None	None
TM6	NB-50-50	770	10.0	8	None	None
TM7	NP-50-50	750	7.5	2	None	Neg.
TM8	LM-75-25	760	9.0	3	None	None
TM9	NM-75-25	770	7.5	5	None	Neg.
TM10	CM-75-25	800	9.0	0	None	Neg.
TM11	BM-75-25	680	17.0	0	None	None
TM12	PM-75-25	790	24.0	5	None	Low

## **CHAPTER 4**

# **EVALUATION OF HARDENED PROPERTIES OF THE SELECTED SCC MIXTURES**

### **4.1 INTRODUCTION**

This chapter covers the details of casting, preparation and testing of the SCC specimens prepared from the qualified mixtures, for the evaluation of their hardened mechanical and durability properties. Mechanical properties tested were compressive strength, splitting tensile strength, bond (pull-out) test and static modulus of elasticity. The durability tests were: water permeability, chloride permeability, electrical resistivity and corrosion tests. In addition, to these durability tests, specimens were prepared and exposed for long time durability studies of sulfate resistance of the SCC mixes.

### **4.2 CASTING AND CURING OF SPECIMENS**

From each of the 10 qualified mixtures, test specimens were cast into various mould sizes by scooping from the mixture discharged from the mixer. The casting process was done without vibrating the mixtures, as opposed to casting of CVC mixtures in which casting is done in layers and each layer vibrated before the next. The SCC specimens were cured in sweet water for a period of 28 days at a fairly constant laboratory temperature of 25°C. The specimens for 90-day compressive strength test were left in the curing tanks until 90 days.

After curing, they were sorted out for the evaluation of their mechanical properties and durability characteristics.

#### 4.3 TEST SPECIMENS

Table 4.1 shows the test specimens prepared for evaluating the mechanical properties of the SCC mixtures, and the corresponding test standard for which they were prepared, while Table 4.2 shows those meant for the evaluation of selected durability characteristics.

**Table 4.1:** Details of test specimens and test standards for the evaluation of the mechanical properties of SCC mixtures.

PROPERTY	TEST STANDARD	SPECIMEN	TEST AGE
Compressive strength	ASTM C 39	100 mm cube	3, 7, 14, 28 & 90 days
Tensile strength (Split)	ASTM C 496	75 × 150 mm cyl	28 days
Modulus of elasticity	ASTM C 469	75 × 150 mm cyl	28 days
Bond strength	Pull out test	12 mm dia bar centrally embedded in 150 mm cube	28 days cured in water

**Table 4.2:** Details of test specimens and test standards for the evaluation of the durability of SCC mixtures.

PROPERTY	TEST STANDARD	SPECIMEN	TEST AGE
Water permeability	DIN 1048	100 mm cube	28 days
Chloride permeability	ASTM C 1202	75 × 150 mm cylinder	28 days
Electrical resistivity	2-electrode method	75 × 150 mm cylinder	28 days
Corrosion (Potentials & rate)	LPR Method	12 mm bar centralized in 75 × 150 mm cylinder	28 days cured, then exposed to 5% Cl <sup>-</sup>



## 4.4 TESTS FOR MECHANICAL PROPERTIES OF SCC MIXES

### 4.4.1 *Compressive Strength*

Compressive strength specimens were 100 mm × 100 mm × 100 mm concrete cube specimens. The compressive strength was determined according to ASTM C 39 after 7, 14, 28 and 90 days of water curing. The specimens were tested using an automatic compressive testing machine of hydraulic type, shown in Figure 4.1. Compressive loading was applied at a constant rate of 1.5 kN/s until the specimen failed. The maximum load (kN) was noted. The compressive strength was calculated by dividing the failure load by the cube cross-sectional area.



**Figure 4.1:** Matest<sup>®</sup> hydraulic type compressive strength testing machine.

#### 4.4.2 Splitting Tensile Strength

Splitting tensile strength specimens were 75 mm × 100 mm concrete cylinders. The test was conducted according to ASTM C 496 on 28-day cured specimens. The specimens were tested using an automatic compressive testing machine of hydraulic type, shown in Figure 4.1. Compressive loading was applied at a constant rate of 0.4 kN/s through narrow bearing strips, complying with the provisions of ASTM C 496, until the specimen failed by splitting. The splitting load (kN) was recorded for each of 3 samples representing each mix. Figures 4.2 and 4.3 show the test arrangement.



**Figure 4.2:** Test arrangement for splitting tensile strength.

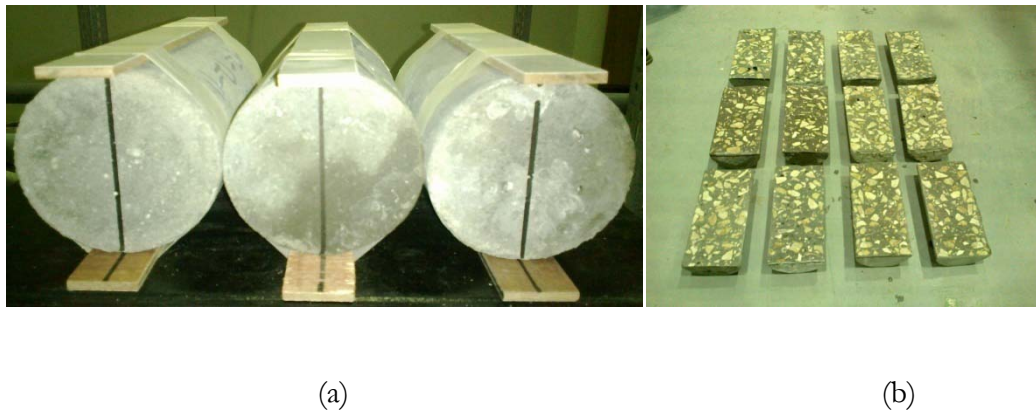


**Figure 4.3:** (a) Tensile test samples with aligned bearing strips (b) Samples after splitting.

The splitting tensile strength was determined using the formula in the Section 8.1 of ASTM C496M – 04, given by:

$$T = \frac{2P}{\pi ld}$$

*where:*

$T$  = splitting tensile strength, MPa,

$P$  = maximum applied load indicated by the testing machine, N,

$l$  = specimen length, mm, and

$d$  = specimen diameter, mm.

For each mix, the average of 3 specimens was recorded as the splitting tensile strength of that concrete mix.

#### ***4.4.3 Young's Modulus***

The Young's modulus or modulus of elasticity of a material is an important mechanical property that affects the deformation characteristics under a given state of stress. A material with a low Young's modulus shows more deformation than the one with a higher modulus, even if they have the same strength. With respect to concrete, the modulus of elasticity varies with strength, though it still depends to some extent on the properties of the constituent materials.

For the determination of Young's (chord) modulus for the SCC specimens, 75 mm x 100 mm concrete cylinder specimens were used. The test was conducted according to ASTM C

469 on 28-day cured specimens. The specimens were tested using the same automatic testing machine used in compressive and tensile strength tests. Compressive loading was applied at a constant rate of 0.5 kN/s at the ends of the specimen, via a load cell, until it failed. The failure load (kN) and the corresponding deformation (mm) were recorded for each of the three specimens representing each SCC mixture.

Figure 4.4 shows the test arrangement. The arrangement consisted of a cylindrical sample clamped in 2 circular steel frames, perfectly aligned and bearing 2 LVDTs on opposite sides, such that any compressive strain applied at the ends of the test specimen is picked up by the LVDTs. The linear deformations captured by the LVDTs and the load sensed by the load cell are recorded by a data logger. The load and linear deformation data were copied from the logger for stress-strain curves plotting and calculation of chord modulus, using the formula in the Section 7.1 of ASTM C469M – 04, given by:

$$E = \frac{S_2 - S_1}{\epsilon_2 - 0.000050}$$

where:

$E$  = Chord modulus of elasticity, MPa,

$S_2$  = Stress corresponding to 40 % of ultimate load,

$S_1$  = Stress corresponding to a longitudinal strain,  $\epsilon_1$ , of 50 millionths, MPa, and

$\epsilon_2$  = Longitudinal strain produced by stress  $S_2$ .

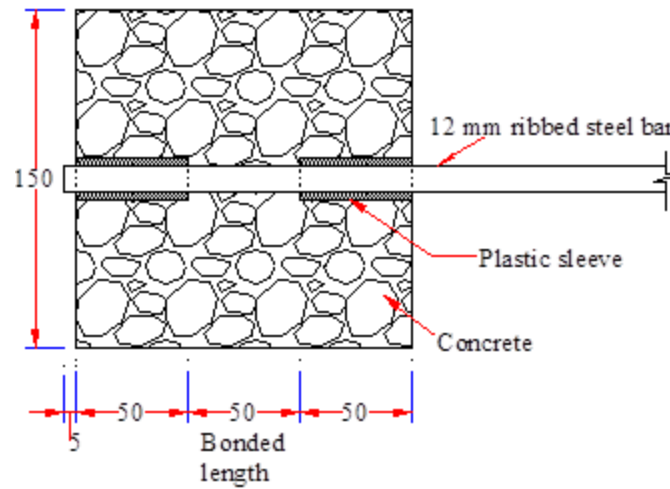


**Figure 4.4:** Test arrangement for determining Young's modulus

For each mix, the average of three specimens' modulus of elasticity was recorded as the modulus of elasticity of that concrete mixture.

#### ***4.4.4 Bond Strength***

For the determination of bond strength for the SCC specimens, 150 mm × 150 mm × 150 mm concrete cube specimens, with 12 mm rebar embedded, were prepared. The centrally embedded rebar was provided with 2 plastic sleeves, as shown in Figure 4.5, such that only the middle 50 mm of the cube is bonded to the steel, while the remaining portions of the rebar are free to move within the sleeves, which are held firmly by the surrounding concrete.



(a) Schematic diagram of bond specimen



(b) Steel bars with plastic sleeves

**Figure 4.5:** Preparation of bond test specimens (dimensions in mm).

The pull-out specimens were tested using a screw type universal testing machine. Figure 4.6 shows the test arrangement. A pullout loading was applied on the projecting steel bar from the cube, while the concrete cube itself was restrained by a holding accessory, as shown in the figure. At the bottom end of the cube, the unloaded end of the bar was flanked by an LVDT held firmly by a clamping device. The bar slip captured by the LVDT and the pull load recorded by the load cell attached to the machine were recorded by a data logger. The pullout load was applied at a constant rate of 2.0 mm/min until the steel bar started to slip. The failure load (kN) was recorded for each of three samples representing each SCC

mixture. The bond strength was determined by dividing the peak load by the bonded area of the steel bar. For each mix, the average of 3 specimens' bond strength was recorded as the bond strength of that SCC mixture.



**Figure 4.6:** Test arrangement for the pull-out test.

## 4.5 TESTS FOR DURABILITY CHARACTERISTICS OF SCC MIXTURES

### 4.5.1 *Water Permeability*

The water permeability of SCC specimens was assessed according to DIN 1048. The test entails the determination of depth of water penetration under a constant supply of water at 5 bar pressure on a cube surface perpendicular to the casting direction. 150 mm × 150 mm × 150 mm cubes were prepared for this test. The test machine is shown in Figure 4.7.

The dry samples were clamped with the clamping device on the machine against a water supply under a pressure of 5 bars, and the supply maintained for 3 days. The cube samples were then removed and split into 2 halves parallel to the water supply direction. The water profile was marked and the depth of water penetration recorded for each specimen.

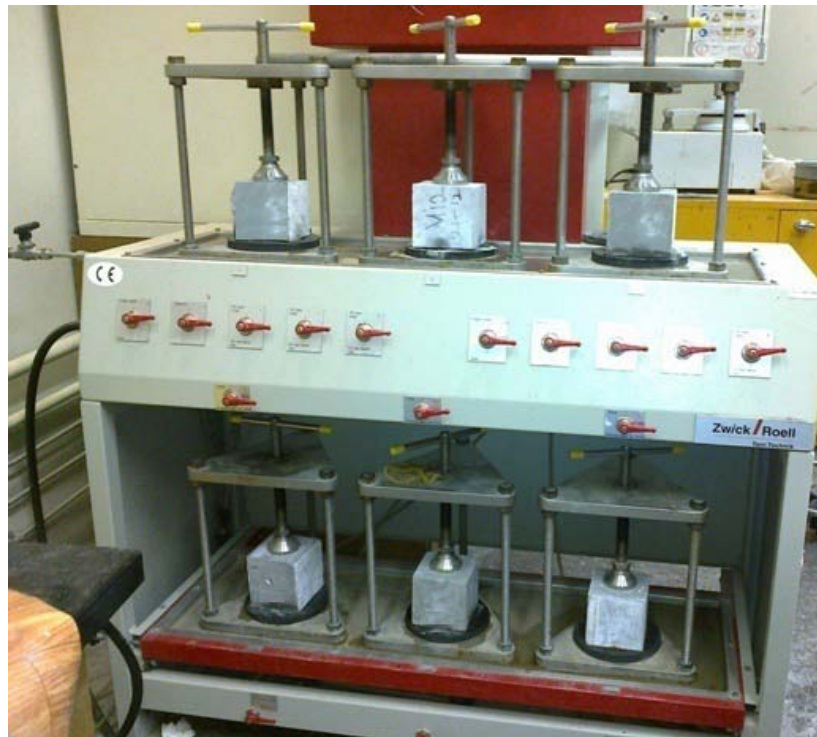


**Figure 4.7:** Water penetration depth test set-up.



#### *4.5.2 Chloride Permeability*

The chloride permeability of SCC specimens was assessed using rapid chloride permeability procedure of ASTM C1202. This method basically determines the electrical conductance of concrete in which the charge carrying species is chloride ion via the pores of the concrete.

A 50 mm thick concrete disk was cut out from the center of the 75 x 150 mm cylindrical specimen. The curved surfaces of the concrete disks were coated with epoxy, and then the disk specimens were conditioned in vacuum dessicator for 4 hrs as described in ASTM C1202. After conditioning, the disk specimens were left in water in the dessicator and kept saturated for about 18 hours.

Following the 18 hours of saturation, the disks were clamped between two half cells, one filled with 3%NaCl solution (w/w) and the other with 0.3 N NaOH solution. An automatic computerized testing machine was used for the test. A potential difference of 60 V DC was maintained across each cell holding the specimens, and the current flowing through each one was recorded at intervals by the computer, via the testing machine. The total charge passed, in coulombs is recorded over a six hour period. The test was performed at a room temperature of 25°C. The machine handles all the relevant calculations contained in ASTM C1202 including correction for disk diameter. The final adjusted amount of coulombs was read and recorded from the computer. Figure 4.8 shows the test set-up.



**Figure 4.8:** Rapid chloride permeability test set-up.

#### **4.5.3 Electrical Resistivity**

The performance of any concrete mixture in corrosion resistance is not only a function of its pore size and distribution, but also dependent upon its electrical resistivity. The electrical resistivity of an SCC specimen was assessed by measuring the resistance across the ends of a 75 x 150 mm cylindrical specimen using a multimeter with its probes connected to spongy terminals, which were kept moist in order to secure a good electrical contact of the ends of the concrete specimen. A mechanical device was used to maintain a tight contact of the wet spongy terminals with the ends of the concrete. Figure 4.9 shows the test set-up for electrical resistivity.



**Figure 4.9:** Test set-up for electrical resistivity.

#### ***4.5.4 Corrosion Resistance***

The corrosion resistance of SCC specimens was evaluated by exposing them to 5% sodium chloride solution. Reinforced SCC specimens, measuring 75 mm in diameter and 150 mm high, were prepared with a 12-mm diameter steel bar placed at the center. A cover of 25 mm was provided at the bottom. The reinforcing steel bars were coated with cement paste followed by an epoxy coating at the bottom of the bar and at the concrete-air interface to avoid crevice corrosion. Figure 4.10 shows the schematic view of the corrosion resistance specimen.

Reinforcement corrosion was monitored by measuring the corrosion potentials, according to ASTM C 876, and the corrosion current density by the linear polarization resistance method (LRPM) [63]. The corrosion measurements were conducted at regular intervals.

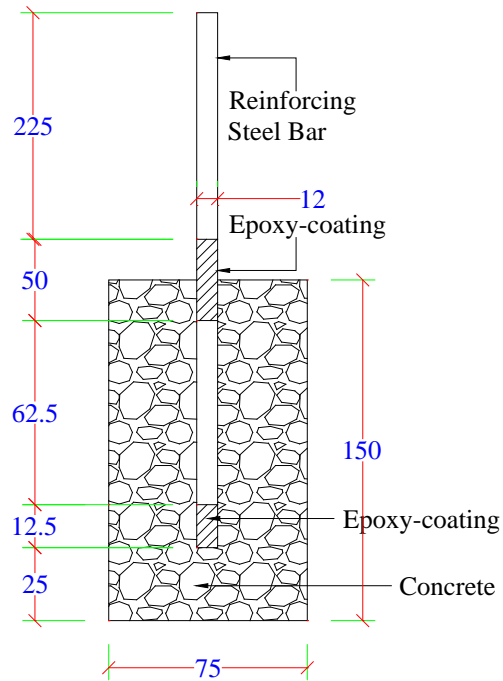


**Figure 4.10:** Schematic diagram of corrosion resistance test specimen (Dimensions in mm).

**Corrosion potentials:** The corrosion potentials were measured using a saturated calomel reference electrode (SCE). The electrical lead from the reference electrode was connected to the positive terminal of a high impedance digital voltmeter while the steel bar in the concrete specimen was connected to its negative terminal, as shown in Figure 4.11.



**Figure 4.11:** Corrosion potential measurement setup.

**Corrosion current density:** The three electrode method was utilized to measure the resistance to polarization ( $R_p$ ) using a Potentiostat/Galvanostat. The steel rod was connected to the working electrode terminal while a steel plate and a reference electrode were connected to the counter and reference electrode terminals of the Potentiostat/ Galvanostat, respectively. The setup is shown in Figure 4.12.

The steel was polarized to  $\pm 10$  mV of the corrosion potential at a rate of 3 mV/min and the resulting current between the counter and the working electrode was measured.  $R_p$  was determined as the slope of the current-potential curve. Corrosion current density ( $I_{corr}$ ) was evaluated using the following relationship [80]:

$$I_{corr} = \frac{B}{R_p}$$

where:

$I_{corr}$  = Corrosion current density,  $\mu\text{A}/\text{cm}^2$

$R_p$  = Resistance to polarization,  $\Delta E/\Delta I$ ,  $\Omega.\text{cm}^2$

$$B = \frac{\beta_a \times \beta_c}{2.3(\beta_a + \beta_c)}$$

$\beta_a$  and  $\beta_c$  are the anodic and cathodic Tafel constants, mV/decade, respectively.



**Figure 4.12:** Corrosion current density measurement setup.

The Tafel constants are normally obtained by polarizing the steel to  $\pm 250$  mV of the corrosion potential (Tafel plot). However, in the absence of sufficient data on  $\beta_a$  and  $\beta_c$ , a value of B equal to 26 mV for steel in active condition and 52 mV for steel in passive condition is often used [81]. Lambert et al [82] have reported a good correlation between corrosion rates determined using these values and the gravimetric weight loss method.

## CHAPTER 5

### RESULTS AND DISCUSSION

#### 5.1 COMPRESSIVE STRENGTH

Table 5.1 shows the summary of compressive strengths for the 10 qualified SCC mixes. The table shows the compressive strengths at ages 3, 7, 14, 28 and 90 days of curing. The reported values of compressive strength are averages of three specimens prepared from each mix. This is the naming convention adopted for the SCC mixes. F stands for FA, S for SF, and N for NP and so on. So M3-SL-10-10 stands for mix #3 with 10% SF and 10% LSP of the total powder content of 500 Kg/m<sup>3</sup>. The remaining part of powder is 80% cement in all cases.

**Table 5.1:** Compressive strength of SCC Specimens.

Mix ID	Compressive Strength (MPa)				
	3 days	7 days	14 days	28 days	90 days
M1-F-20-ctrl	40.8	52.9	58.6	71.6	74.4
M2-L-20	39.8	48.5	57.0	63.5	71.5
M3-SL-10-10	46.5	62.4	68.1	78.3	83.7
M4-LN-10-10	39.0	52.5	64.5	67.9	73.8
M5-NC-10-10	48.7	55.7	61.8	65.9	82.8
M6-NB-10-10	5.8	16.8	33.0	46.0	66.8
M7-NP-10-10	36.1	49.7	57.9	66.0	74.8
M8-LM-15-5	51.5	59.4	61.6	66.8	85.9
M9-NM-15-5	36.2	46.6	51.2	65.2	70.2
M10-CM-15-5	53.7	58.6	63.3	78.9	91.1

### 5.1.1 Mixes containing LSP

Figure 5.1 shows a graph of compressive strength evolution with curing time, plotted from values in Table 5.1 for the SCC mixes containing LSP. These mixes are M2, M3, M4 and M8. The 7, 28 and 90 days strengths are presented in Figure 5.2, while Figure 5.3 shows the same values as ratios/percentage of the 28 days strength for each mix. As can be seen from Figure 5.1, all mixes in this category have compressive strengths at all ages lower than that of the control mix, apart from M8 which not only have the highest 90 days strength gain, but also slightly exceed the control mix at 90 days.

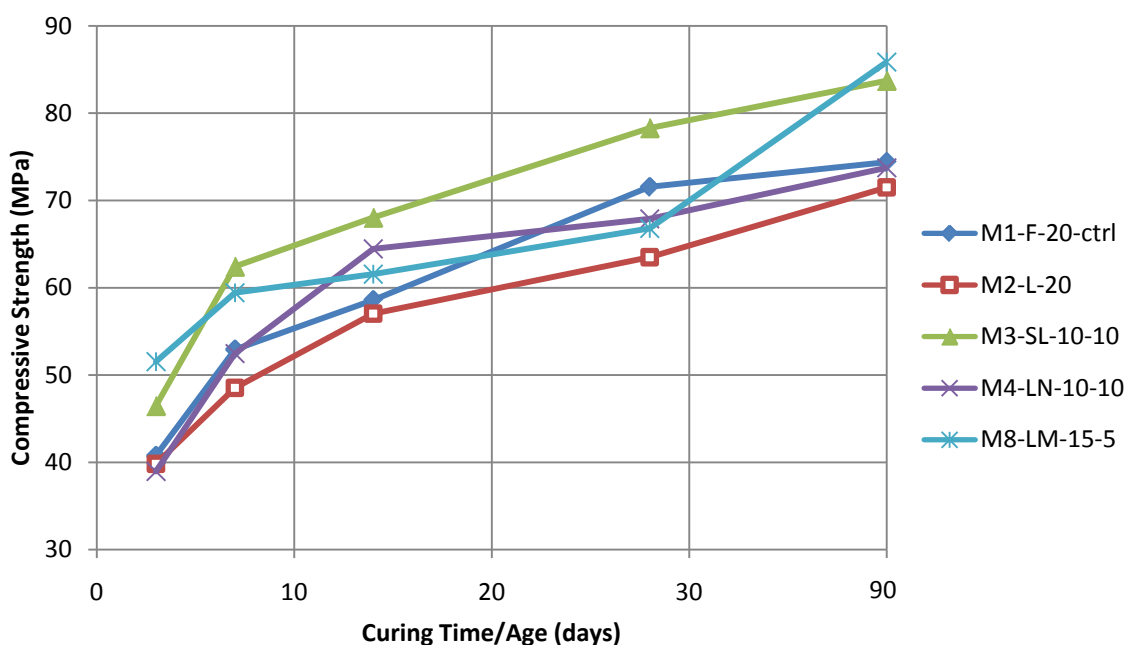


**Figure 5.1:** Compressive strength of SCC with LSP.

The mix with the highest percentage of LSP of the total powder, M2-L-20 having 20% LSP can be seen to possess the least compressive strength at all ages. This can be attributed to the fact that LSP does not possess pozzolanic property [62, 64]. However, except at 28 days, the



amount by which its strength is lower than that of the control mix is not considerable, given the fact that it's not pozzolanic, while the FA in the control mix is. It shows its use does not reduce considerably the concrete strength, and its other benefits such as bleeding control [61, 62] and improvement in concrete deformability in the fresh stage [61-63], in addition to its low cost makes it important in formulating SCC mixes. The lower observed difference in compressive strength can be attributed to its excellent filling property in the concrete microstructure, even if it's not pozzolanic [64]. This is in agreement with the findings of Bonavetti et al [61], who showed that the reduction in the 28 days compressive strength of concrete containing up to 18% LSP filler was not more than 12%.

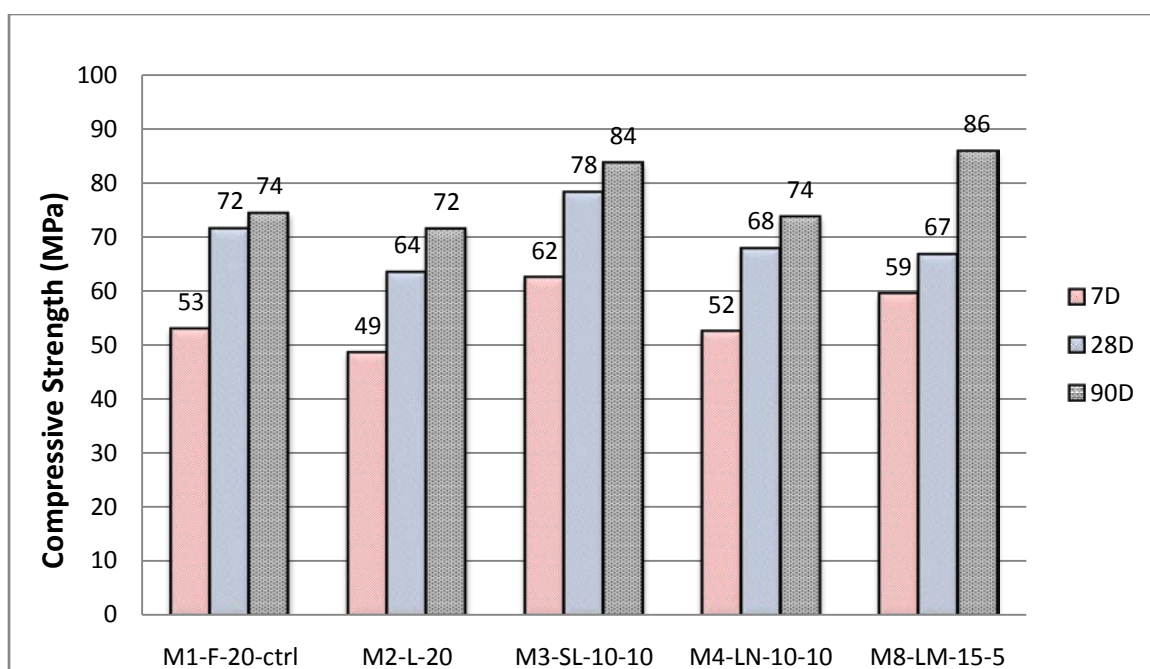


**Figure 5.2:** 7, 28 and 90 days compressive strength of SCC with LSP.

When half the quantity of LSP in M2 was replaced by other fillers, the improvement in compressive strength at all ages is obvious. This means that all these fillers have pozzolanic activities, though to varying degrees and speeds. The best performance in compressive

strength was observed with SF replacing half of LSP as in M3. This is in agreement with the established fact in the literature that silica fume is not only highly pozzolanic, but its pozzolanic reaction is fast [31, 37, 43-45].

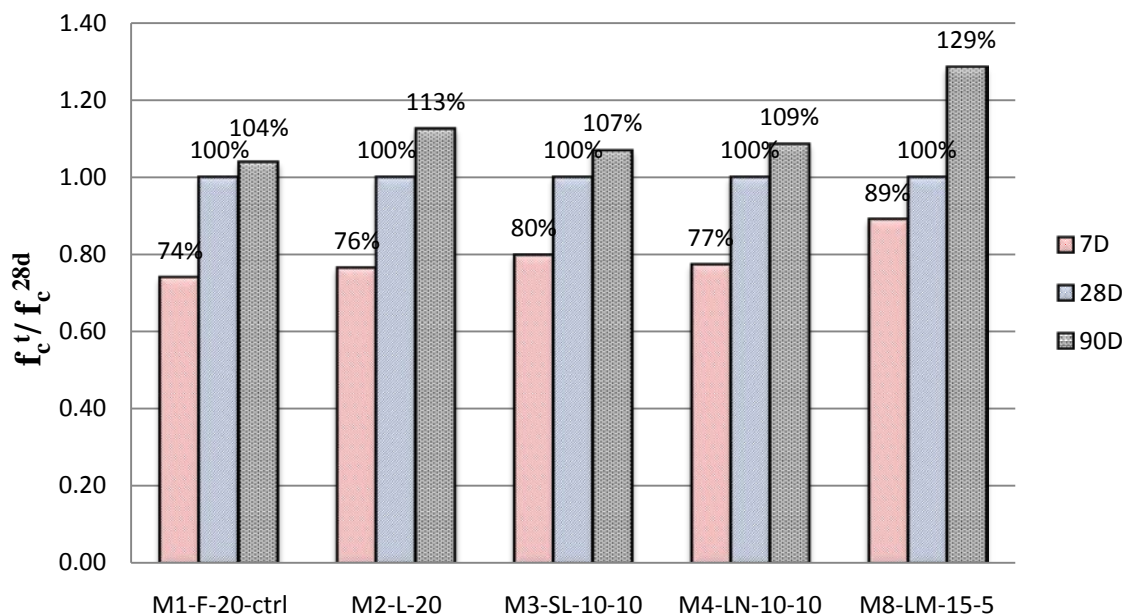


**Figure 5.3:** SCC mixtures with LSP - compressive strengths as % of 28-day strength.

The observed trend in M4 with NP shows that, though it's pozzolanic, its pozzolanic activity is slower than that of SL and MK at early ages. This is in accordance to past researchers [83, 84] that have shown that NP has a slow pozzolanic activity. M8 with MK taking the place of half of LSP can be seen to display the next high improvement in strength at early age after SF, although its activity slowed down towards 28 days making to match the strength of LSP-NP blend. However, it's still the best in this group in the long run, given its highest 90-day strength gain and the highest 90-day to 28-day strength ratio (Figure 5.3). Also from Figure 5.3, the 20% LSP mix (M2) showed the next highest 90D/28D ratio after the LSP-MK mix. This shows that LSP may improve the hydration reaction after 28 days. The high pozzolanic

activity of MK has been reported in the literature [30, 50, 85, 86]. It improves both mechanical and durability properties of concrete, though its performance is determined by the kaolinitic purity level of the source clay.

### 5.1.2 Mixes containing NP

Figure 5.4 shows a graph of compressive strength evolution with curing times, plotted from values in Table 5.1 for the mixes containing NP. These mixes are M4 – M7 and M9. The 7, 28 and 90 days strengths are presented in Figure 5.5, while Figure 5.6 shows the same values as ratios/percentage of the 28 days strength for each mix.

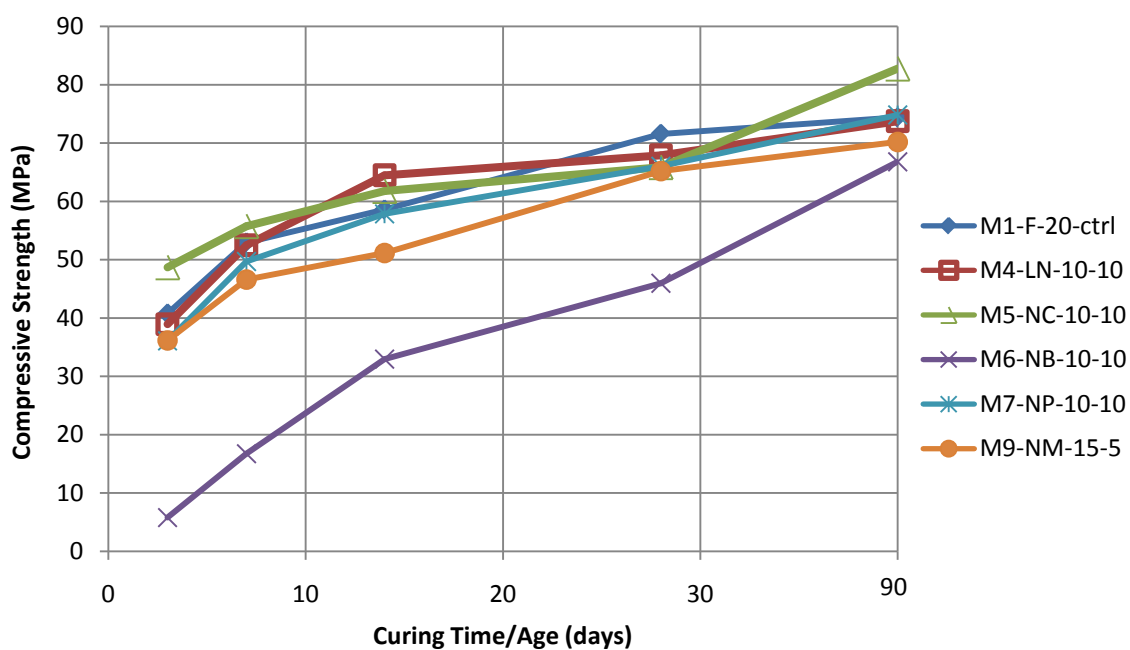


Figure 5.4a: Compressive strength of SCC with NP.

From the figures, the mixture incorporating BHD (EAFD), M6-NB-10-10, can be seen to be the worst of them. A serious delay in setting time was observed in this mix in the casting process, although a previous researcher [87] who used the same material with thermal treatment did not report any notable delay in the setting time, even at a very high dosage. The observed delay in setting in this research may be due to a strange reaction between the particular SP and VMA used which probably hinders the clinker particles from coming together for hydration.

From Figure 5.4b, it can be seen that all the mixes in this group perform closely to the control mixture at all ages. This could be explained by the fact that the slow hydration attributed to NP, as discussed the last section, could be offset by the other pozzolanic fillers present in these mixtures.

The inclusion of CKD showed the best improvement in terms of early and long-term strength enhancement, standing at 85% and 126% of 28 day strength, respectively. Not only that this blend exhibited the best early and long-term strength to 28 days strength ratio, its absolute value at these stages are the highest, though it has 28 day strength lower than that of the control mixture. These observations at first would make one think that CKD is a wonderful pozzolan. However, the assessment of its reactivity from past studies is to the contrary. For example, Al-Harthy et al [88] showed that CKD did not improve compressive strengths in their mixtures, though it had no adverse effect up to certain limits. Similar observations were reported by Maslehuddin et al [89] and Wang and Ramakrishnan [90], provided it does not exceed 5% replacement of cement. On the other hand, other researchers have reported positive performance of CKD in a blend with blast furnace slag

[91, 92]. So the observed compressive strength improvement in CKD-NP blend will need to be studied at microstructural level in future studies.

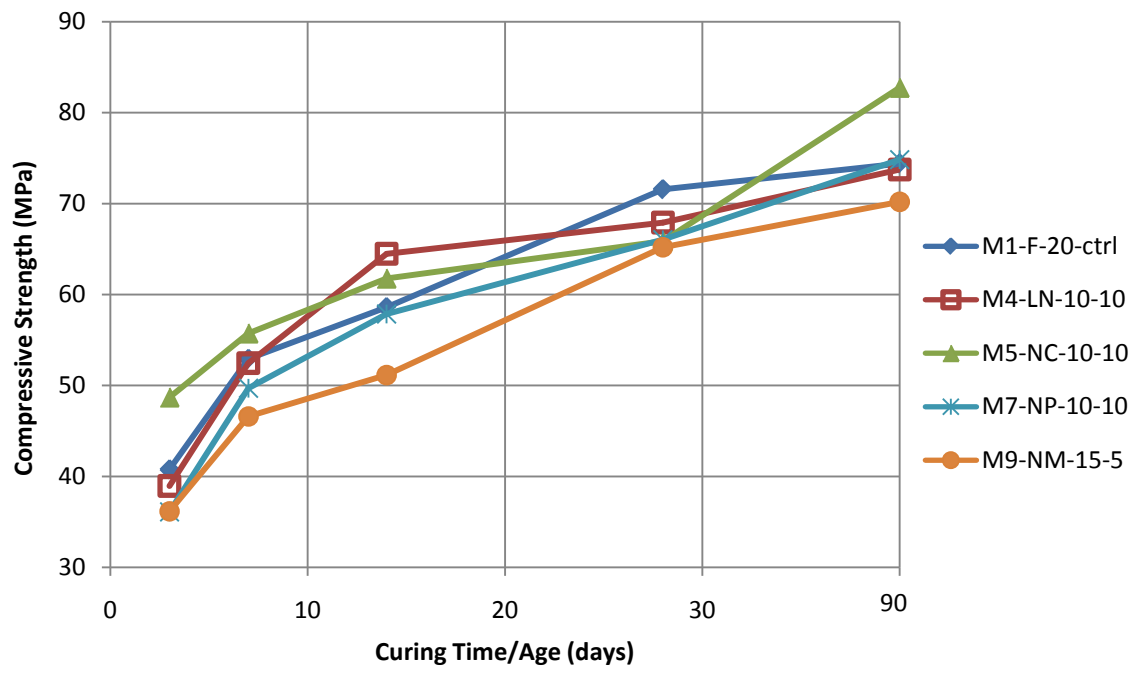


**Figure 5.4b:** Compressive strength of SCC with NP (without M6).

The data in Figure 5.4 also show that PSS also contributes well to enhancing the slow activity of NP. However, the NP-MK blend showed the least performance both in early and long-term compressive strength. This is contrary to the observed good improvement in strength shown by MK with LSP. Therefore, MK may not be a good co-filler with NP, though the 28 days strength is still in the same high strength range with other blends in this group.

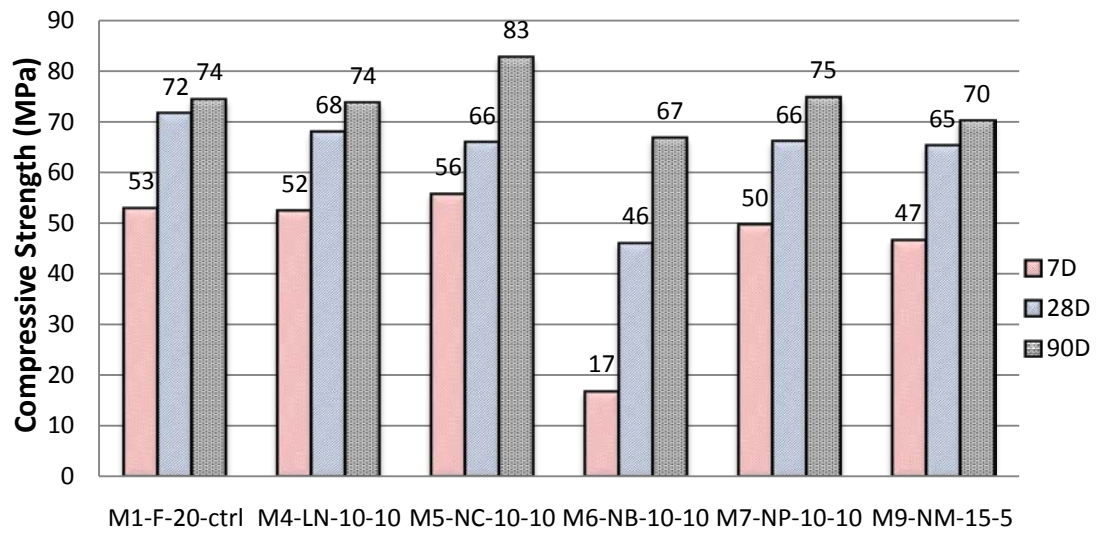


Figure 5.5: 7, 28 and 90 days compressive strength of SCC with NP.

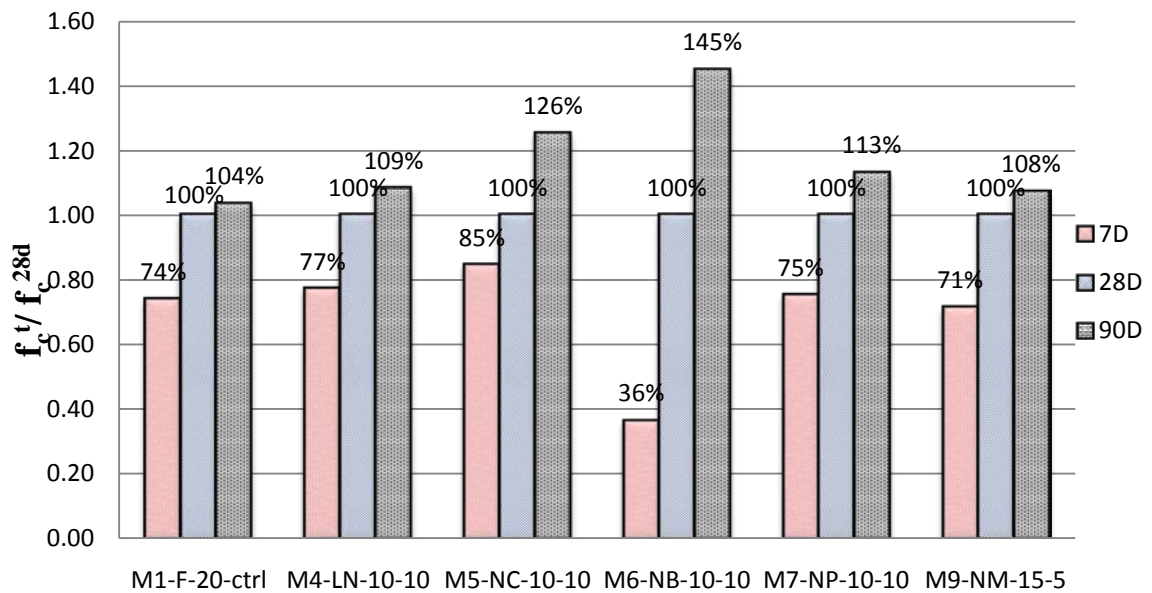
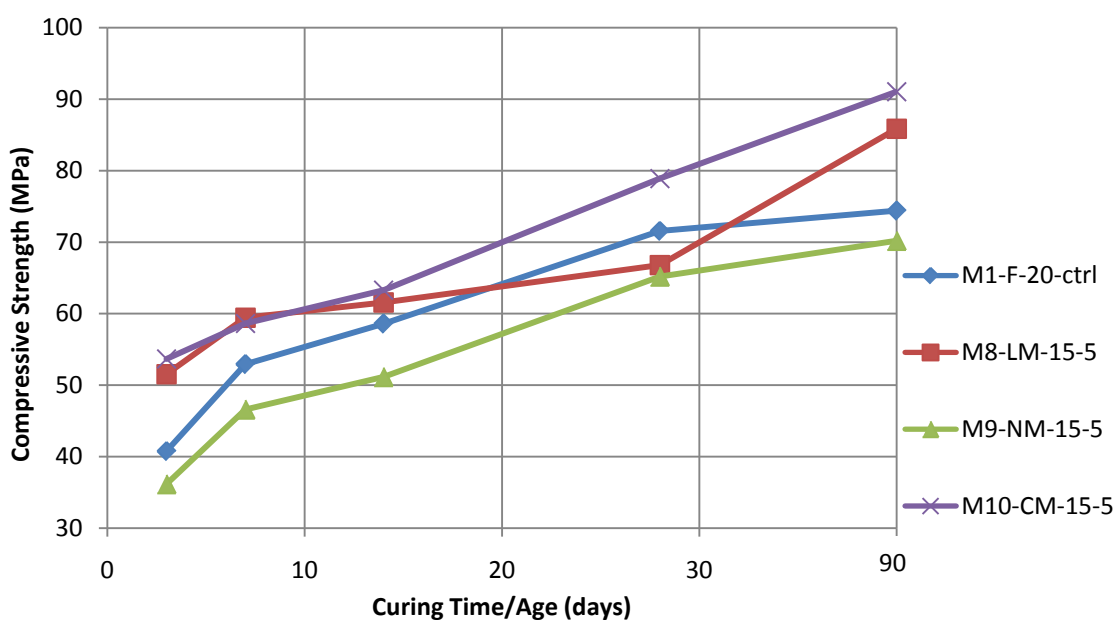


Figure 5.6: SCC mixtures with NP - compressive strengths as % of 28D strength.

### 5.1.3 Mixes containing MK

Figure 5.7 shows a graph of compressive strength evolution with curing times, plotted from values in Table 5.1 for the mixes containing MK. These mixes are M8 – M10. The 7, 28 and 90 days strengths are presented in Figure 5.8, while Figure 5.9 shows the same strength values as ratios/percentages of the 28-day strength for each mix.



**Figure 5.7:** Compressive strength of SCC with MK.

As can be seen from Figures 5.7 and 5.8, the best performing filler in co-blending with MK is CKD (M10-CM-15-5). This blend was made of 15% CKD and 5% MK in a total powder content of  $500 \text{ Kg/m}^3$ . A look at Figure 5.9 shows that this blend developed the highest early strength, and subsequently maintained the hydration pace even up to 90 days. Although the LSP blend closely matched up with the CKD blend at the early age, it

could not show as much performance at 28 days and later. CKD was seen earlier to give the best performance among all the blends with NP.

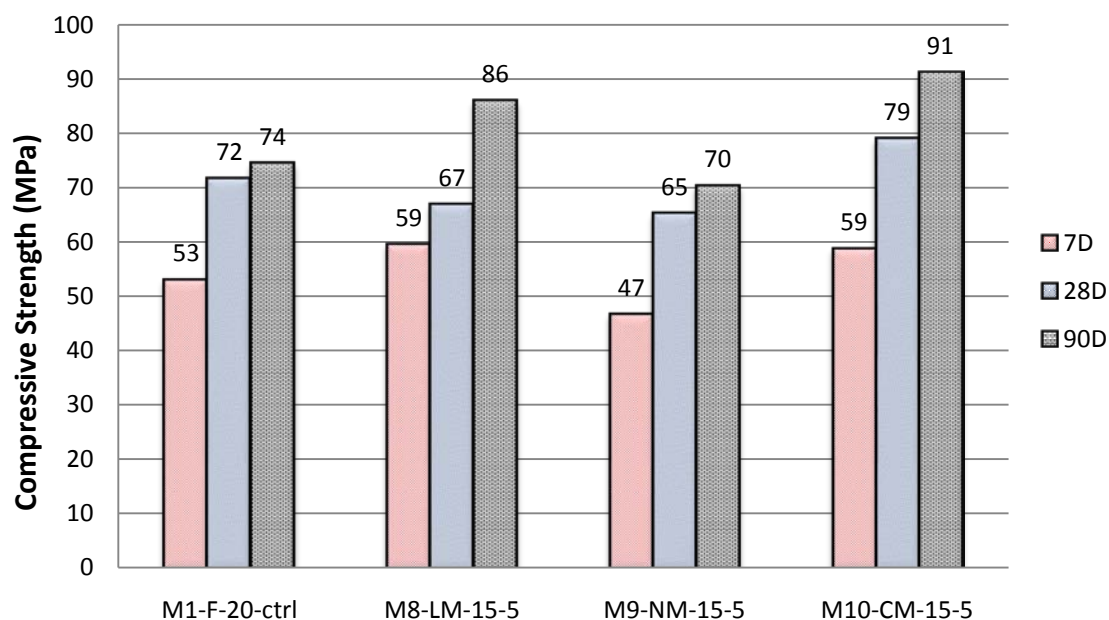


**Figure 5.8:** 7, 28 and 90 days compressive strength of SCC with MK.

With respect to the effect of curing, the LSP blend (M8-LM-15-5) stands positively out of the group. This blend exhibited the highest 7D/28D strength ratio, and it showed significant improvement with curing beyond 28 days. The NP blend could not perform as much as these two mixes due to the slower and lower strength activity as elaborated in the last section. Also, the observed better performance of LSP blend containing the same relatively higher LSP proportion as NP can also be traced to the excellent filling effect of LSP [62] at the microstructural level.



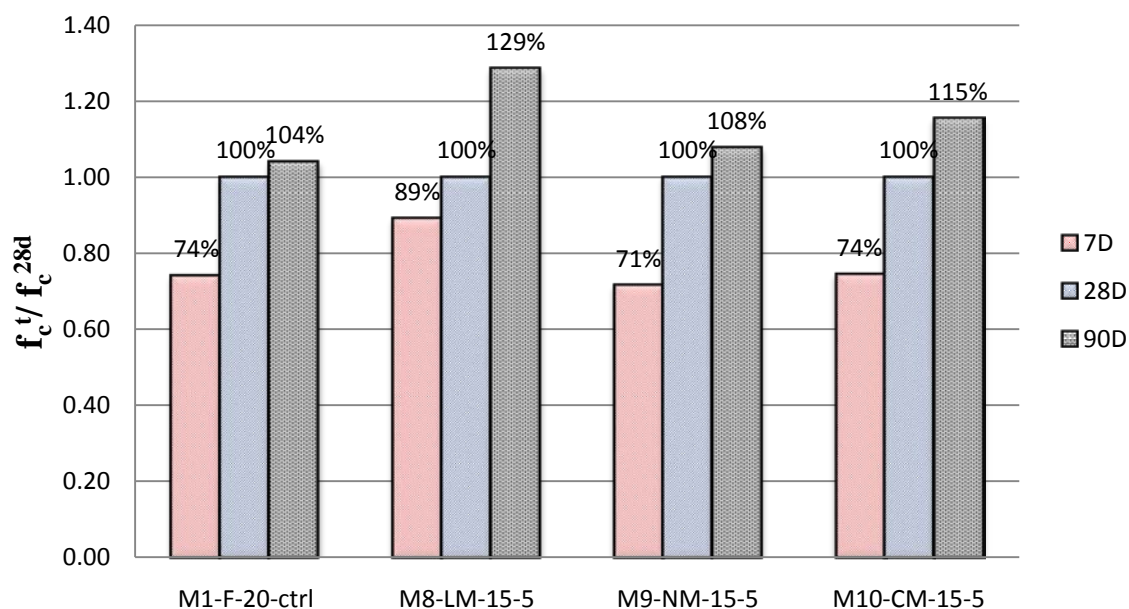


**Figure 5.9:** SCC mixtures with MK - compressive strengths as % of 28D strength.

#### 5.1.4 Mixes containing CKD

Figure 5.10 shows a graph of compressive strength evolution with curing time, plotted from values in Table 5.1 for the mixes containing CKD. These mixes are M5 and M10. The 7, 28 and 90 days strengths are presented in Figure 5.11, while Figure 5.12 shows the same values as ratios/percentage of the 28-day strength for each mix.

At this stage of the discussion, it's no more a news item that CKD had shown good compressive strength development among all the fillers used in this research. Though the reports in the literature did not favour these observations, none of those studies surveyed was done on SCC. It's therefore possible that CKD has a better strength performance in SCC than in CVC.

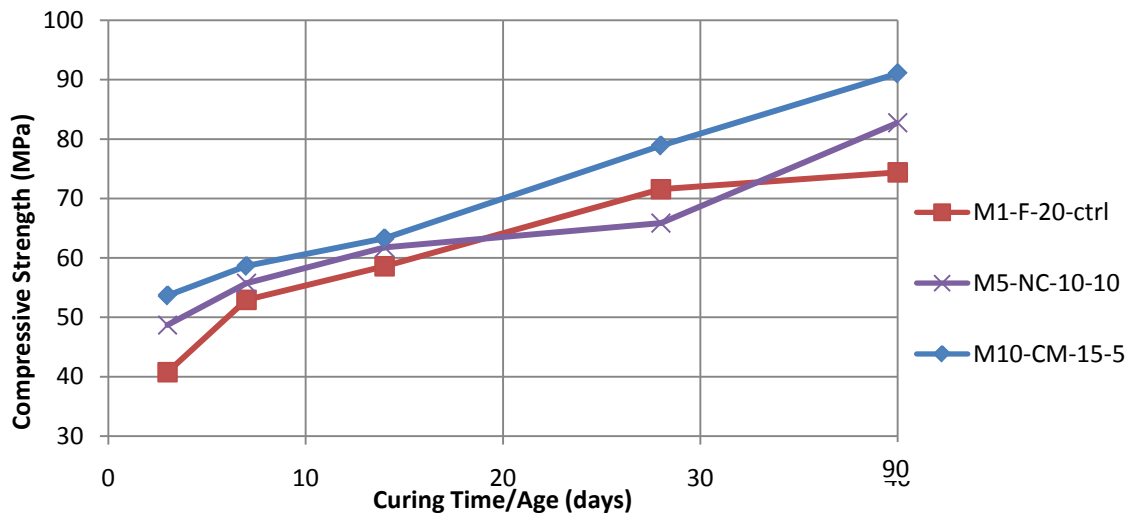


**Figure 5.10:** Compressive strength of SCC with CKD.

A look at Figure 5.10 reveals that though M5 performs better than the control mix (except at 28 days), M10 with 15% CKD outperformed M5 with 10% CKD, showing an increase in the compressive strength performance with increasing dosage of CKD. This is as expected since NP has not been showing off any dazzling performance in compressive strength behavior in the previous discussions. This may also be due to good pozzolanic activity of MK [30, 50, 85, 86]. Also, the higher 90-day/28-day compressive strength ratio shown by M5 (Figure 5.12) is a testimony to the alleged slow pozzolanic activity of NP [83, 84]. It's thus important to cure NP blends further than 28 days, if that can be accommodated.

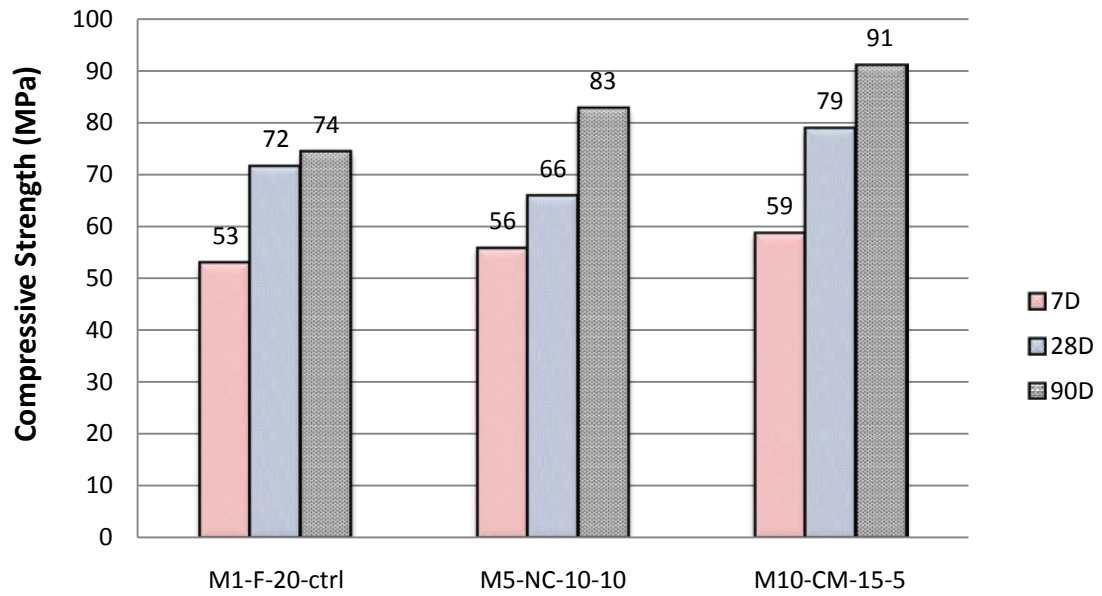


Figure 5.11: 7, 28 and 90 days compressive strength of SCC with CKD.

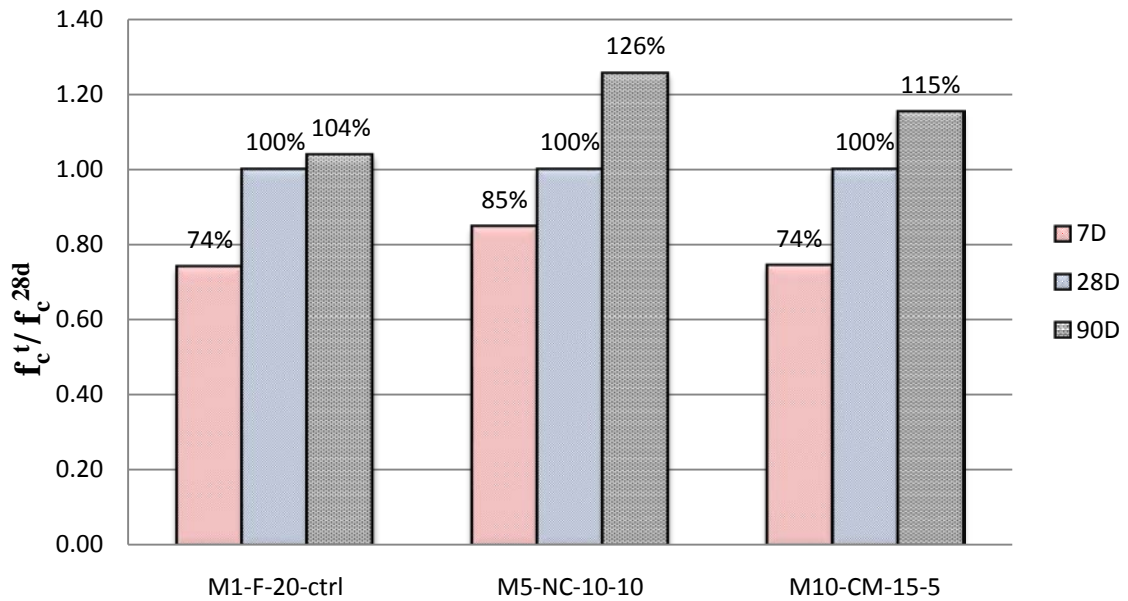


Figure 5.12: SCC mixtures with CKD - compressive strengths as % of 28-day strength.

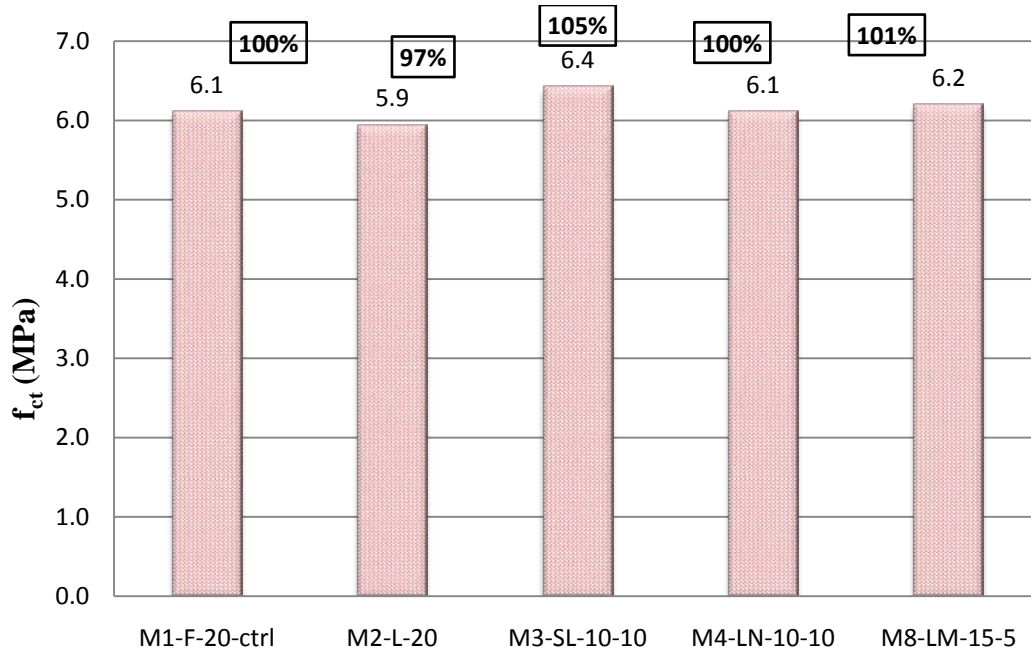
## 5.2 SPLITTING TENSILE STRENGTH

The tensile strength of concrete is an important mechanical property that greatly affects the size and extent of tension related failure behaviors such as flexural cracking in beams, inclined cracking from shear and torsion, and splitting resulting from rebar interaction with surrounding concrete [93]. The tensile strength of concrete is usually assessed by the *split-cylinder* test in accordance with ASTM C496.

### 5.2.1 Mixes containing LSP

Figure 5.13 shows the splitting tensile strengths of SCC specimens for the mixes containing LSP. The values in boxes close to the top of each bar represent the percentages of the control for each mix. From the figure, it's clear that the splitting tensile strengths of these mixtures are not too sensitive to variations in compressive strengths. This can be explained that each mixture contains unique combinations of fillers and so variations in the resulting tensile strengths may not reflect proportionately to the variations in compressive strengths.

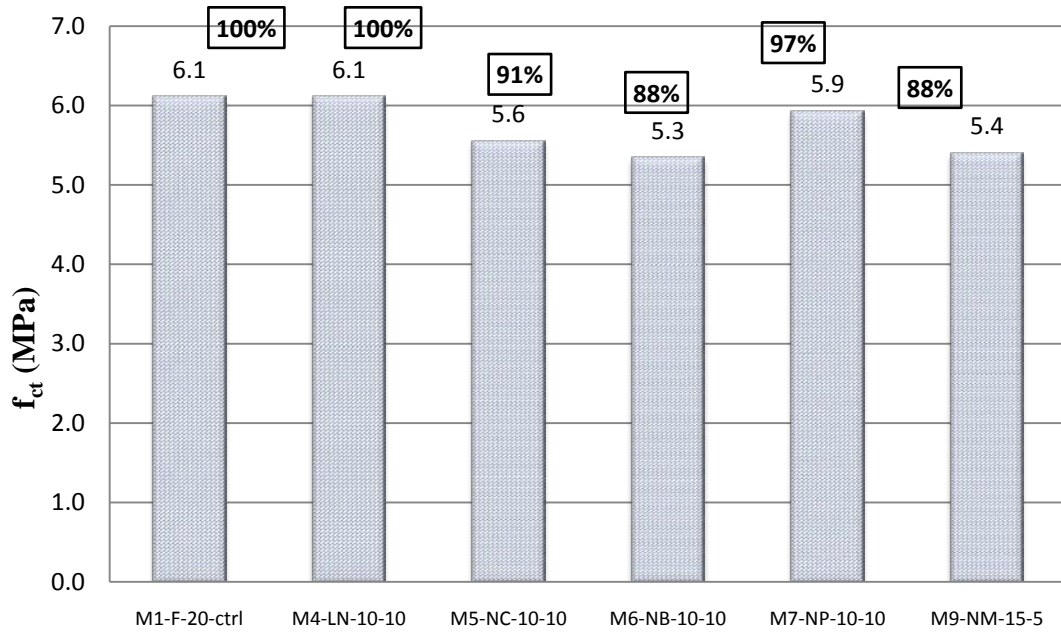
Nevertheless, the pure LSP blend shows some 3% lower value of tensile strength than the control mixture, while a 5% gain can be seen when half the LSP is replaced with SF. This could be explained by the same reasons given in Section 5.5.1 in the discussion of compressive strengths of the same group of SCC mixtures. Both NP and MK blend with LSP show similar tensile behavior to that of the control mixture with FA only.



**Figure 5.13:** Splitting tensile strength of SCC mixes with LSP.

### 5.2.2 Mixes containing NP

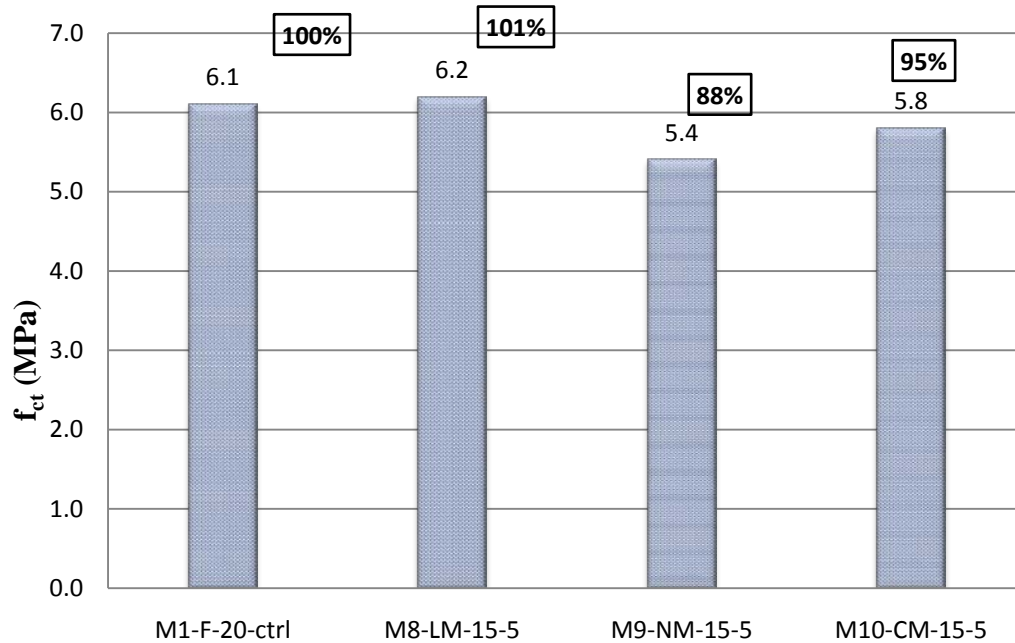
Figure 5.14 shows the splitting tensile strength of SCC specimens for the mixes containing NP. The case here is a bit different to what we had in the previous section. Both LSP and PSS blends with NP show similar tensile behavior to the control mix, though the latter is slightly lower. However, CKD, BHD and MK blends with NP exhibit lower tensile strength. The case with BHD is clear. Its strength in compression is the lowest in all the mixtures studied, as discussed in section 5.1.2 (see Table 5.1 and Figure 5.5a). Although both the CKD and MK blends with NP showed similar compressive strengths, CKD still slightly performs better in the tensile behavior.



**Figure 5.14:** Splitting tensile strength of SCC mixes with NP.

### 5.2.3 Mixes containing MK

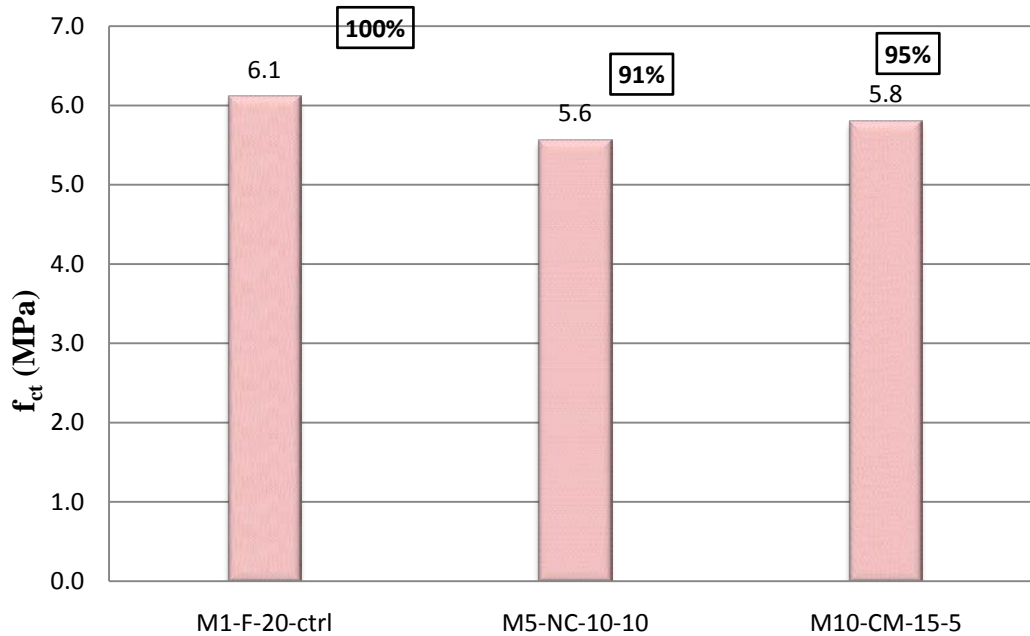
Figure 5.15 shows the splitting tensile strength of SCC specimens for the mixes containing MK. With the NP blend developing a compressive strength below that of the control, its lower tensile strength will be expected. However, the LSP blend with NP performs like the control mixture in tensile strength even with its compressive strength (67 MPa) clearly below that of the control (72 MPa), while the CKD-MK blend does the reverse. This phenomenon may be attributed to the highly variable nature of tensile strength relative to compressive strength as reported by Wang et al [93].



**Figure 5.15:** Splitting tensile strength of SCC mixes with MK.

#### 5.2.4 Mixes containing CKD

Figure 5.16 shows the splitting tensile strengths of SCC specimens for the mixes containing CKD. Again we would expect a lower tensile strength from CKD-NP blend, given its lower compressive strength than that of the control mixture. However the slightly lower tensile performance of the CKD-MK may be attributed to the highly variable nature of tensile strength [93] highlighted in the previous section.



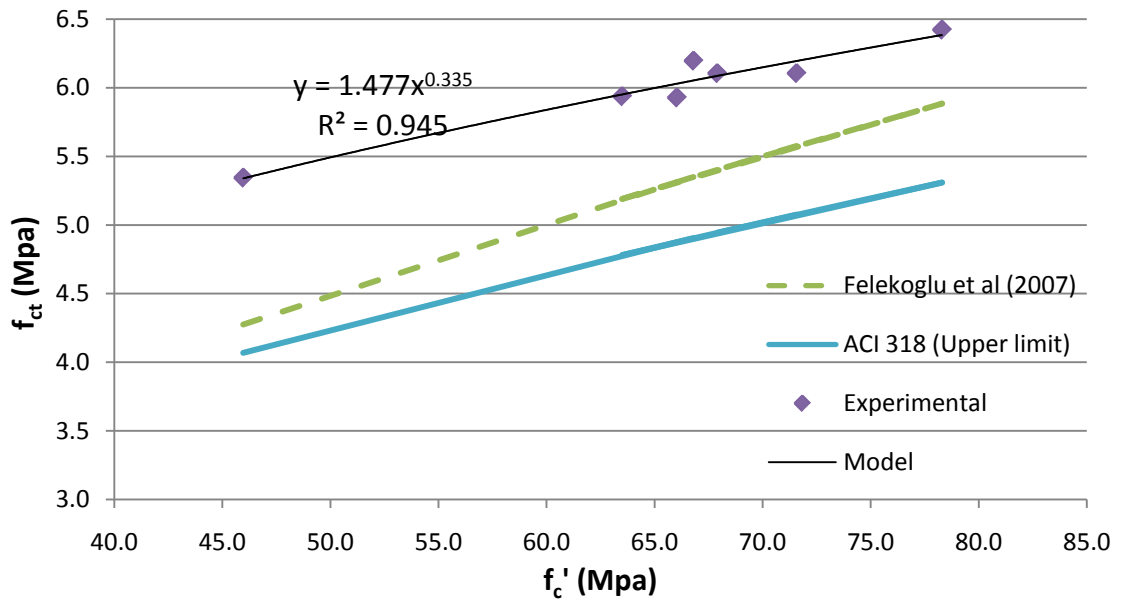
**Figure 5.16:** Splitting tensile strength of SCC mixes with CKD.

Table 5.2 shows the summary of 28-day splitting tensile strength ( $f_{ct}$ , MPa) and the corresponding 28-day strength ( $f'_c$ , MPa) for the 10 SCC mixtures. The reported values are averages of three specimens prepared from each mix. The naming convention for the SCC mixes remains the same. Figure 5.17 shows the relationship between splitting tensile strength against compressive strength for the SCC mixtures. From Table 5.2, it can be seen that the values of cylinder splitting strength range from 5.3 – 6.4 MPa, corresponding to compressive strengths of 46.0 – 78.9 MPa. These values seem to be higher than the values for CVC of similar compressive strengths, as can be visualized in Figure 5.17. However, it was established in the literature that the tensile strength of SCC is higher than that of CVC of equivalent compressive strengths [32]. SCC cylinder splitting strengths of about 2 – 6 MPa have been reported in the literature, corresponding to compressive strengths of about 20 – 80 MPa [70].



**Table 5.2:** Splitting tensile strength of SCC specimens.

MIX ID	$f_{ct}$ (MPa)	$f'_c$ (MPa)
M1-F-20-ctrl	6.1	71.6
M2-L-20	5.9	63.5
M3-SL-10-10	6.4	78.3
M4-LN-10-10	6.1	67.9
M5-NC-10-10	5.6	65.9
M6-NB-10-10	5.3	46.0
M7-NP-10-10	5.9	66.0
M8-LM-15-5	6.2	66.8
M9-NM-15-5	5.4	65.2
M10-CM-15-5	5.8	78.9



**Figure 5.17:** Splitting tensile strength of SCC mixtures against compressive strength.

### 5.3 YOUNG'S MODULUS

Because of the worries that SCC may have a lower elastic modulus [13, 14], which may constitute deflection problems and prestress losses in prestressed elements [15], it's a popular practice to assess the elastic modulus of SCC mixtures developed. This research also covered the investigation of elastic moduli of the SCC mixtures studied, in accordance with ASTM C469.

#### 5.3.1 Mixes containing LSP

Figure 5.18 shows the chord modulus of SCC for the mixes containing LSP. The values on each bar represent the chord moduli, while those in boxes are their corresponding percentages of the control mix. A look at the figure reveals that all the mixtures in this category exhibits slightly less stiffness than the control mixture, with the best of them being the LSP-MK blend.

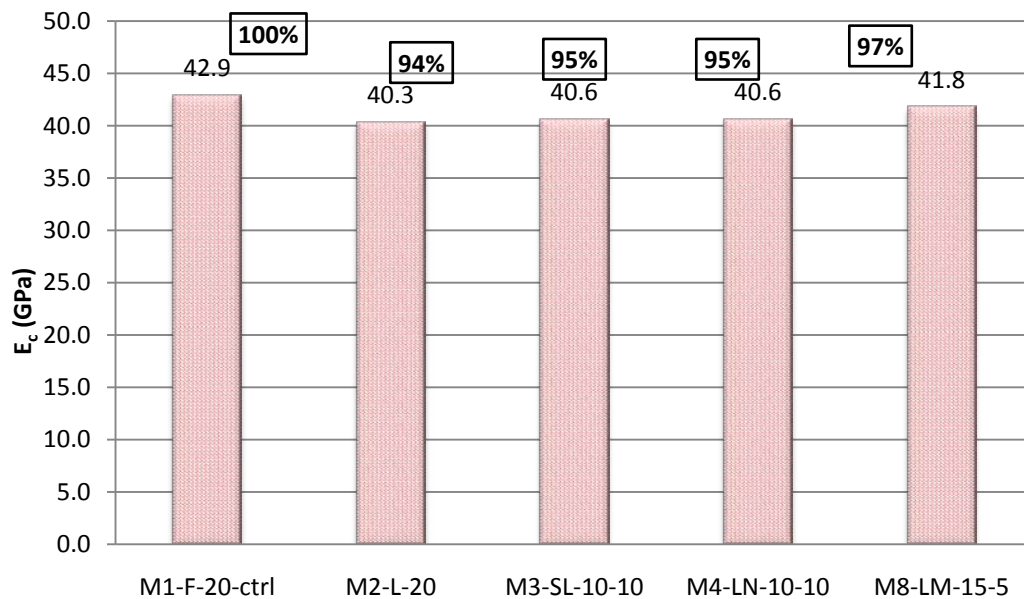


**Figure 5.18:** Chord modulus of SCC mixtures with LSP.

### 5.3.2 Mixes containing NP

Figure 5.19 shows the chord modulus of SCC specimens for the mixes containing NP. The Figure shows that all the mixtures are less stiff than the control mixture, ranging from around 10% in CKD, BHD and PSS blends to 3% less in MK-NP blend. This observation is still in line with the observed slightly lower compressive strengths of these mixtures than the control mixture.

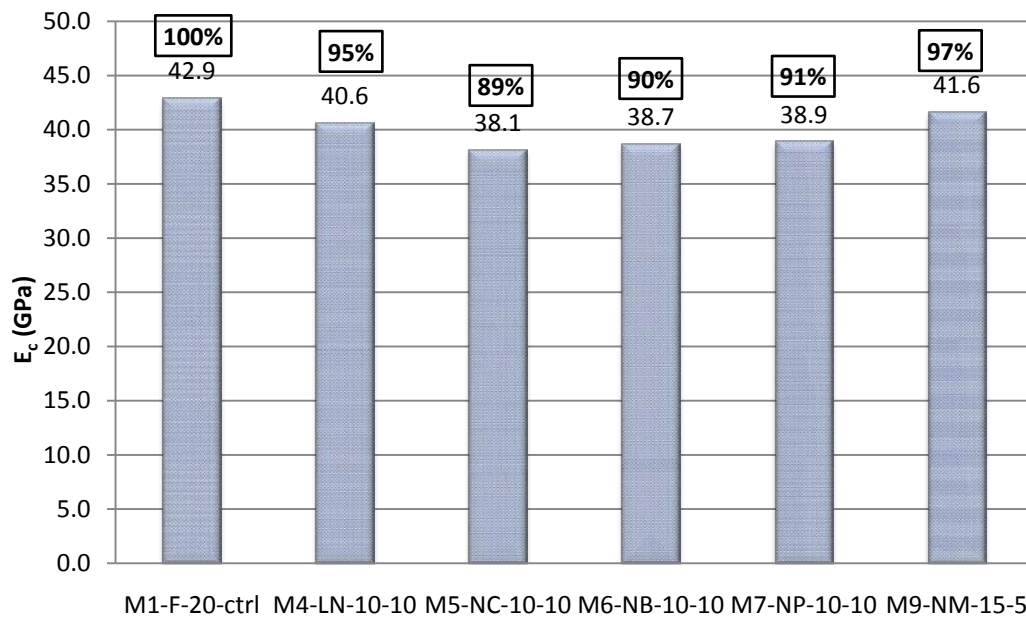
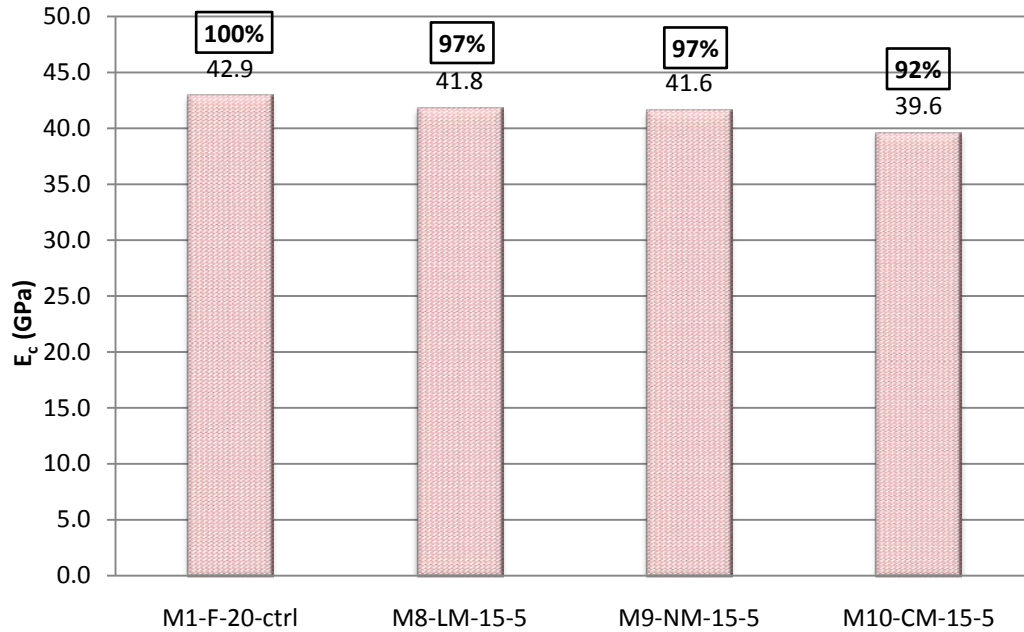


**Figure 5.19:** Chord modulus of SCC mixtures with NP.

### 5.3.3 Mixes containing MK

Figure 5.20 shows the chord modulus of SCC specimens for the mixes containing MK. Also here, the stiffness values are similar to that of the control mixture, except in the case of CKD-MK blend, which is expected to be stiffer going by its highest compressive strength in this class. This may be seen as a testimony to the claim that the elastic modulus of concrete

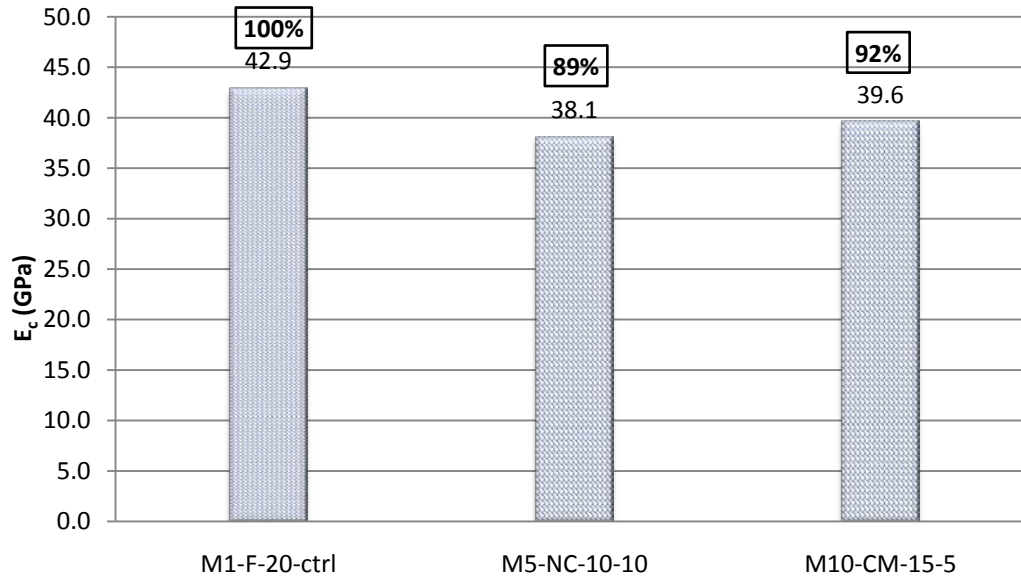
does not only depend on its compressive strength, but it's also a function of the properties of the constituent materials [93].



**Figure 5.20:** Chord modulus of SCC mixtures with MK.

#### 5.3.4 Mixes containing CKD

Figure 5.21 shows the chord modulus of SCC specimens for the mixes containing CKD. The observation here is similar to that noticed in the previous sections, and the discrepancy seen in the case of CKD-MK blend was explained in the last section as being attributable to the ‘constituent material’ effect on concrete stiffness.



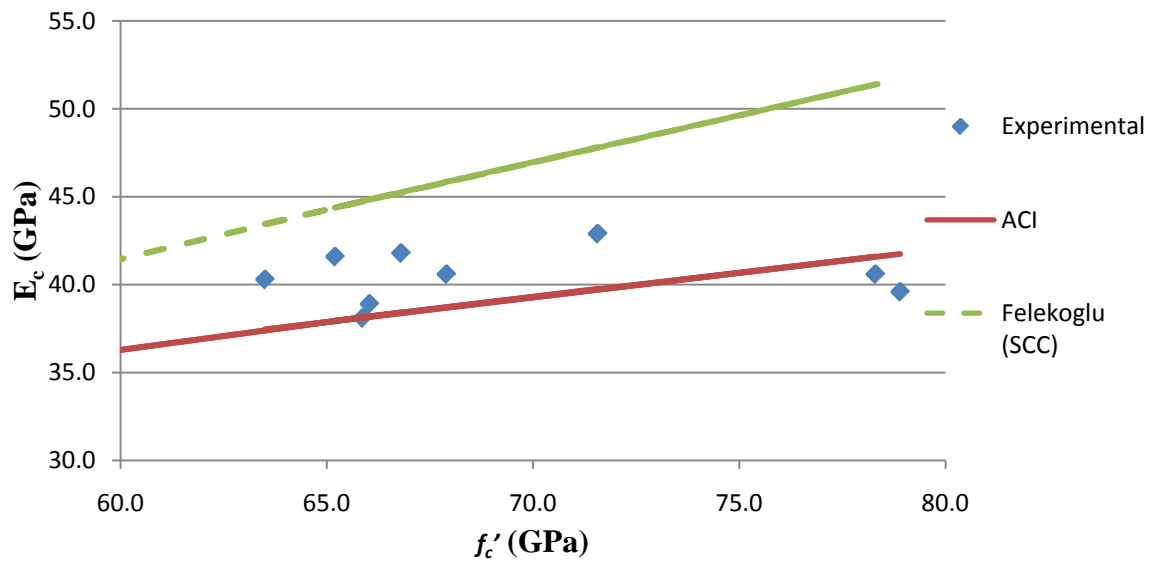
**Figure 5.21:** Chord modulus of SCC mixtures with CKD.

Table 5.3 shows the 28-day Young's/chord moduli ( $E_c$ , GPa) for the 10 SCC mixes. The reported values are average of three specimens prepared from each mixture. Figure 5.22 shows the relationship between the elastic moduli and compressive strengths for SCC mixtures.

**Table 5.3:** Chord modulus of SCC specimens

MIX ID	$E_c$ (GPa)
M1-F-20-ctrl	42.9
M2-L-20	40.3
M3-SL-10-10	40.6
M4-LN-10-10	40.6
M5-NC-10-10	38.1
M6-NB-10-10	38.7
M7-NP-10-10	38.9
M8-LM-15-5	41.8
M9-NM-15-5	41.6
M10-CM-15-5	39.6

From Figure 5.22, it can be noticed that majority of the elastic modulus values exceeded the values predicted for CVC of corresponding compressive strengths by the provisions of ACI 318-08, while some are around the same values with that of ACI. Since all the mixtures (Except M6) belong to high strength category of SCC, this observation is consistent with the findings of Domone [70] who showed that the elastic modulus of high strength SCC may be the same or higher than that of CVC of corresponding compressive strength, though it could be as low as 60% in the low strength region. Felekoğlu et al [94] got even higher values than those of CVC of similar compressive strengths.



**Figure 5.22:** Relationship between  $E_c$  and  $f'_c$  for SCC mixtures.

#### 5.4 BOND STRENGTH

The bond strength developed by a rebar embedded in concrete is greatly controlled by the quality of the concrete and its compressive and tensile strengths [74].

### 5.4.1 Mixes containing LSP

Figure 5.23 shows the bond strength of SCC specimens for the mixes containing LSP. The values on each bar represent the bond strength,  $f_{cb}$  in MPa, while those in boxes are their corresponding percentages of the control mix. From the figure, it can be seen that none of the mixtures surpassed the control in bond capacity. This would be expected for these mixtures, owing to their lower compressive strengths, except for the LSP-SF blend. It was stated earlier that the compressive and tensile strengths of concrete both play roles in controlling its bond behavior.

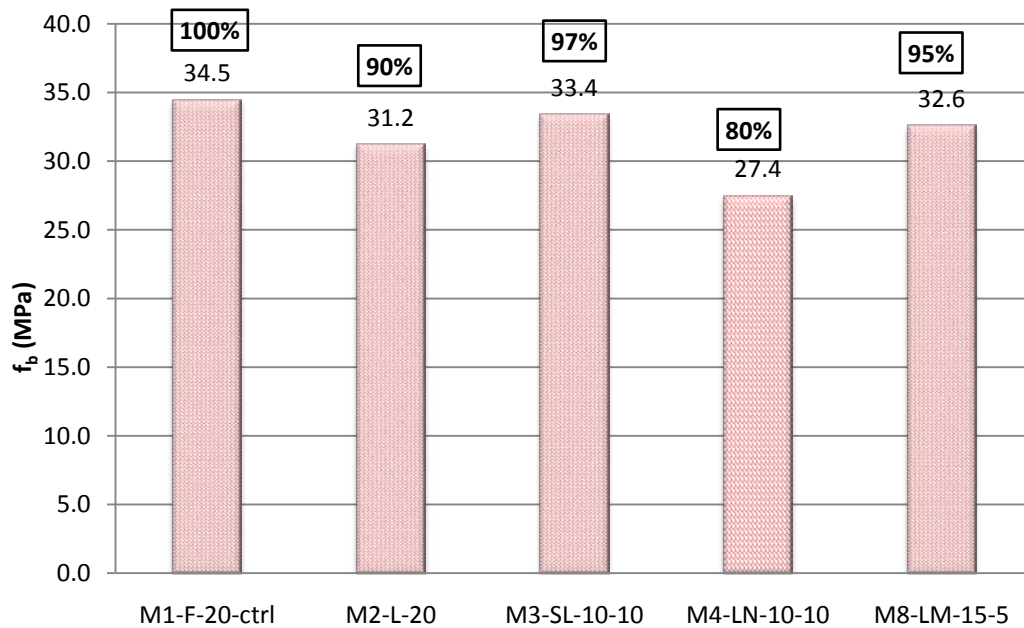


**Figure 5.23a:** Bond strength of SCC mixtures with LSP.

Looking at Figure 5.23a and b, it is easy to see why the pure LSP blend develops lower bond strength than the control, as both the tensile and compressive strengths are obviously lower. The same goes for the LSP-MK blend. But in the case of the LSP-NP blend (M4), the extent of reduction in ultimate bond capacity is not justified by the slight reduction in its

compressive strength. Hence it may be right to think in the direction of top-bar effect, since it's established earlier to be a major player in a mixture's bond behavior [26, 70, 74, 95, 96].

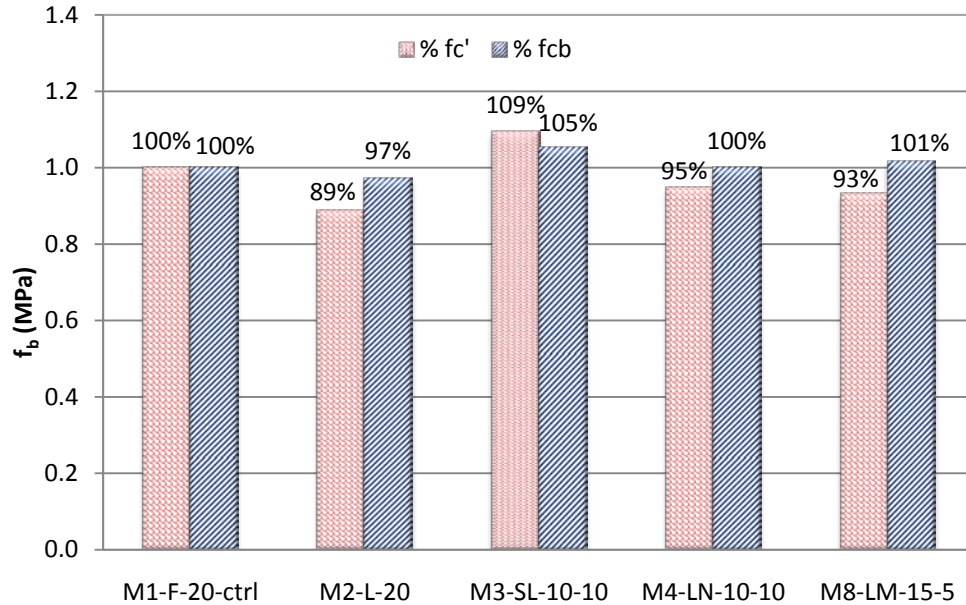


**Figure 5.23b:**  $f_c'$  and  $f_{cb}$  of SCC mixtures with LSP as % of control mixture.

A flash-back into its plastic stability reveals it to be one of the most stable mixes. Thus it may be that the short term stability observed in the fresh state was not sustained in the long run, since segregation is sometimes a time dependent phenomenon [17]. The same explanation may be offered for the LSP-SF blend (M3) which just manages to get very close to the control mixture's bond capacity value, in spite of its slightly better tensile and compressive capacities.

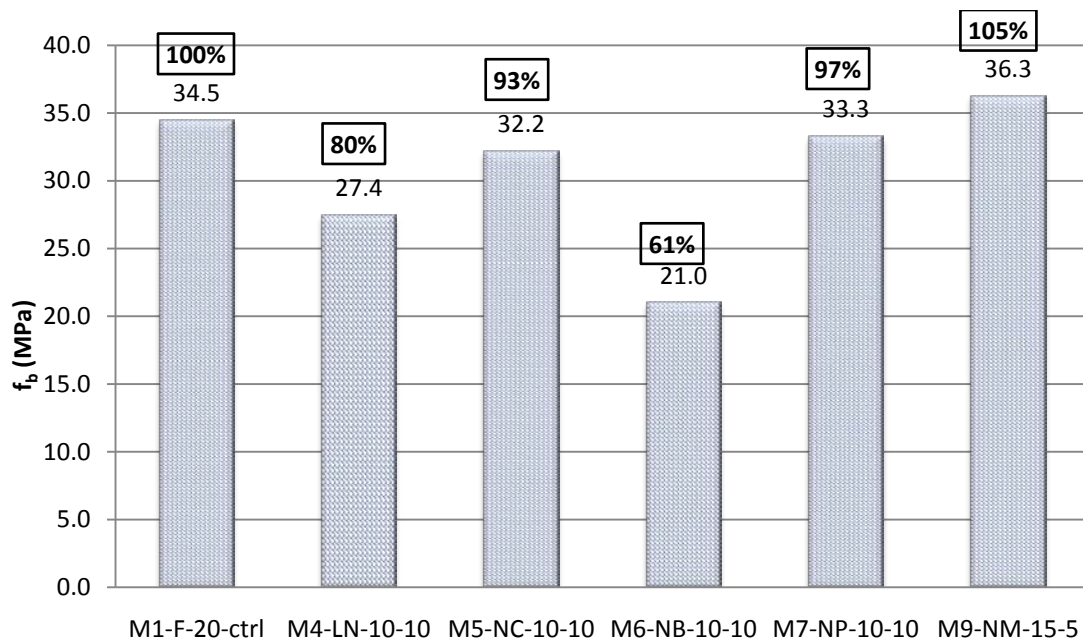
#### 5.4.2 Mixes containing NP

Figure 5.24 shows the bond strength of SCC specimens for the mixes containing NP. The values on each bar represent the bond strength values,  $f_{cb}$  in MPa, while those in boxes are



their corresponding percentages of the control mix. Looking again at Figures 5.25a and b, the lower ultimate bond capacities of M5 and M6 can easily be explained from the perspective of their lower compressive and tensile strengths. The case with M4 had been explored in the previous section. The only issue at hand now is that M9, having around 10% less tensile and compressive strengths, still exceeds the control in ultimate bond capacity.

First there's no doubt the mixture was 'super-stable' in the fresh state. Also the fact that it's a leader of all the mixtures studied in bond strength result consistency is never an overstatement, since it had a flimsy standard deviation of 0.3 MPa and a near-non-existent COV of 1%. Therefore, it may be worthwhile to think that its fresh stability surpassed those of all other mixes, making the embedded rebar to experience very little top-bar effect compared to all other mixes.



**Figure 5.24a:** Bond strength,  $f_{ib}$ , of SCC mixtures with NP.

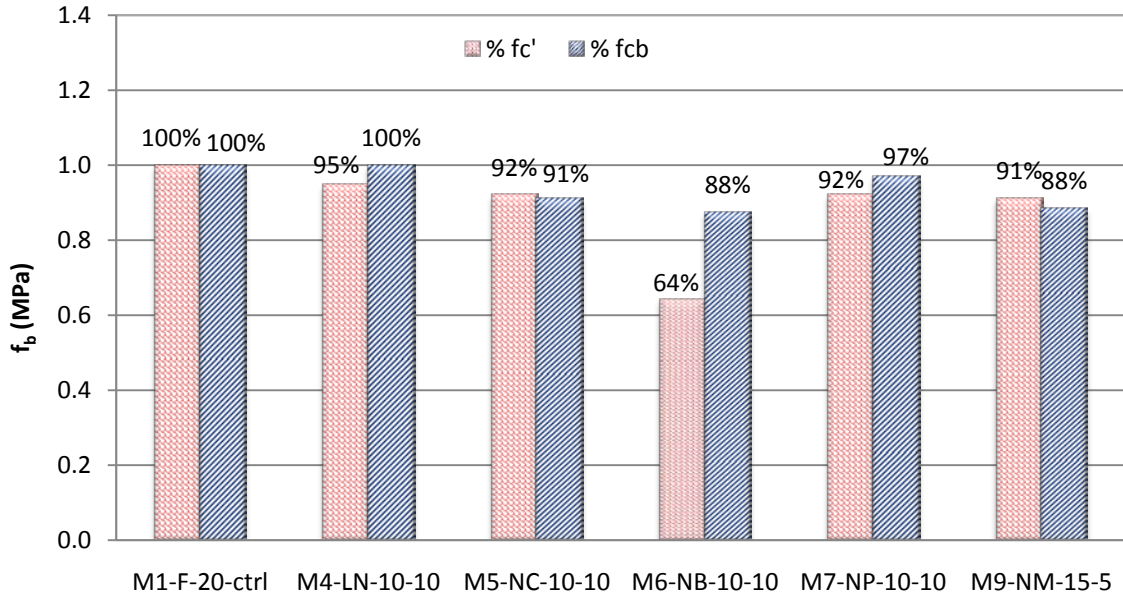


Figure 5.24b:  $f_c'$  and  $f_{cb}$  of SCC mixtures with NP as % of control mixture.

### 5.4.3 Mixes containing MK

Figure 5.25 shows the bond strength of SCC specimens for the mixtures containing MK.

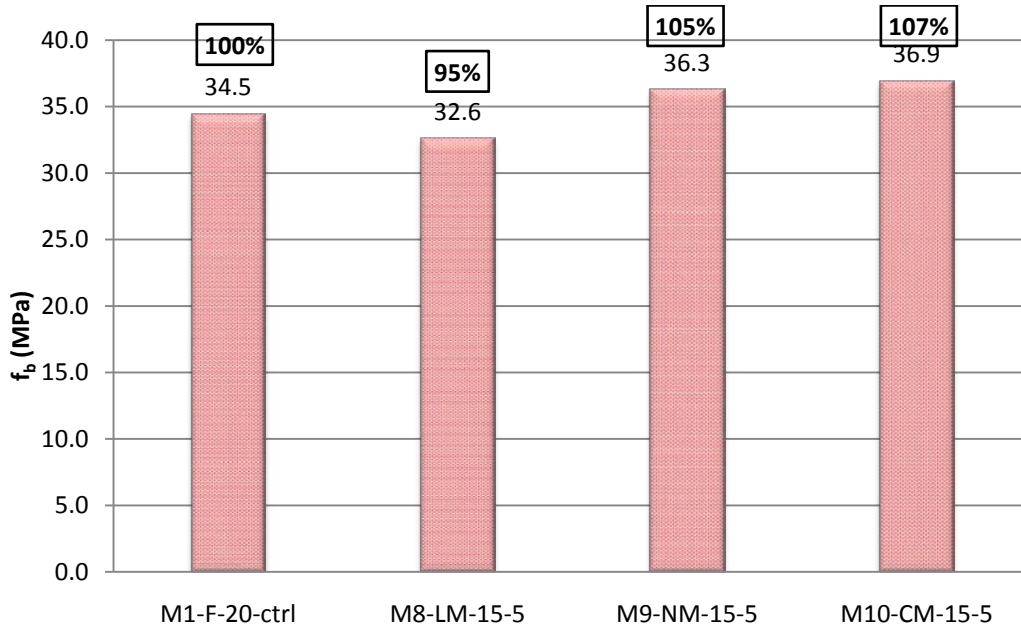
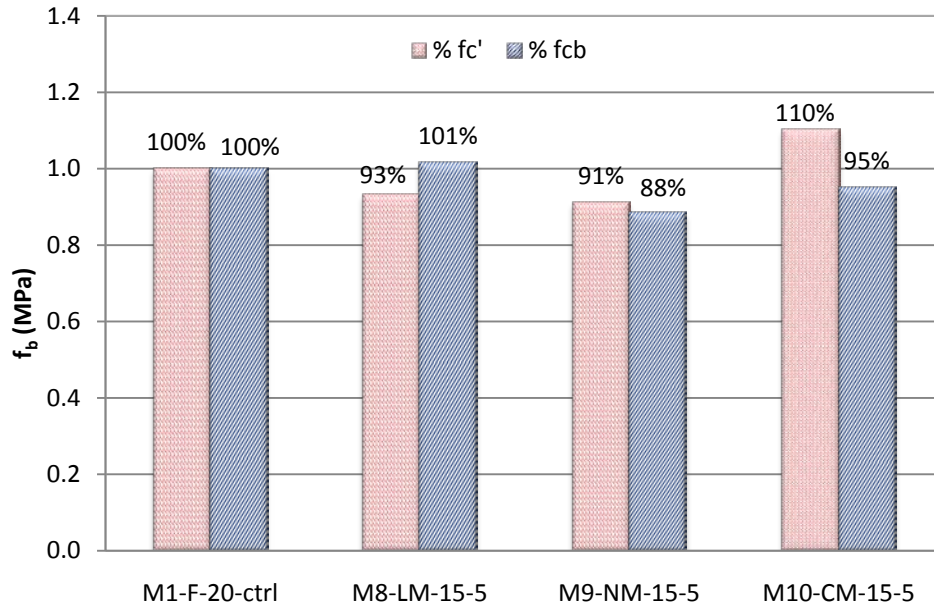


Figure 5.25a: Bond strength,  $f_{cb}$ , of SCC mixtures with MK.



**Figure 5.25b:**  $f_c'$  and  $f_{cb}$  of SCC mixtures with MK as % of control mixture.

From Figures 5.26a and b, the observed higher ultimate bond capacity of MK-CKD blend is obviously justified on account of its higher compressive strength than the control mixture. The reverse explanation to that of M10 holds for M8, as its situation is also reversed. The case of M9 had been discussed extensively in the last section.

#### 5.4.4 Mixes containing CKD

Figure 5.26 shows the bond strength of SCC specimens for the mixes containing CKD. Lending an eye on Figure 5.26a obviates the justification for the lower strength in bond of CKD-NP blend (M5) observed in the figure. Also the CKD-MK blend follows similar line of reasoning, given its relatively higher compressive strength than the control mixture.

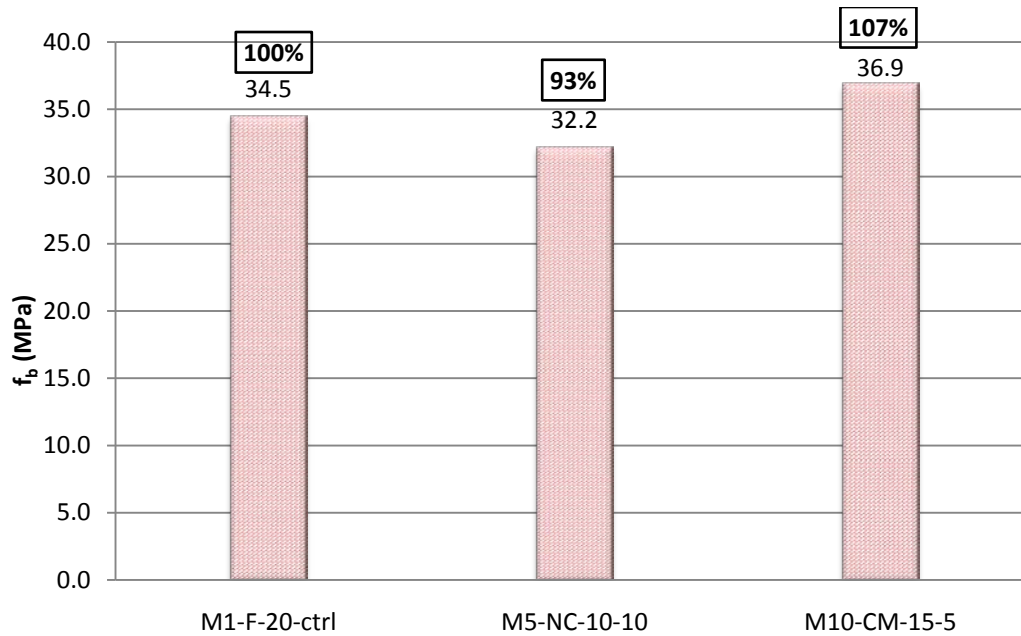


**Figure 5.26a:** Bond strength,  $f_{cb}$ , of SCC mixtures with CKD.

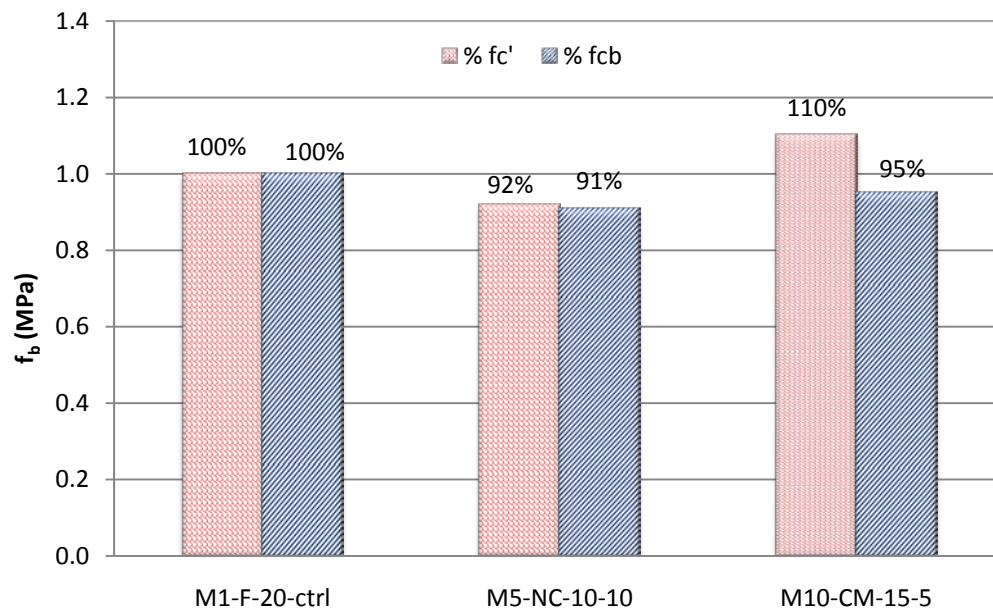


**Figure 5.26b:**  $f_c'$  and  $f_{cb}$  of SCC mixtures with CKD as % of control mixture.

Table 5.4 shows the 28-day bond strength ( $f_{cb}$ , MPa) for the 10 SCC mixes.

**Table 5.4:** Bond strength of SCC mixtures.

MIX ID	$f_{cb}$ (MPa)
M1-F-20-ctrl	34.5
M2-L-20	31.2
M3-SL-10-10	33.4
M4-LN-10-10	27.4
M5-NC-10-10	32.2
M6-NB-10-10	21.0
M7-NP-10-10	33.3
M8-LM-15-5	32.6
M9-NM-15-5	36.3
M10-CM-15-5	36.9

Figure 5.27 shows the relationship between  $f_{cb}$  and  $f'_c$  for SCC mixtures. From the figure, it can be seen that, although there seems to be no good correlation between the measured values of  $f_{cb}$  and  $f'_c$ , the bond strength values are higher for most samples than the predicted values computed using equations of Orangun et al [97] and Chapman and Shah [95]. This observation goes well with the information obtainable from the literature. SCC has been said to have better bond behavior than that of conventional vibrated concrete [2], a fact attributable to the good interlocking of aggregates and higher volume of paste [5]. Not only does SCC bond behavior surpass that of CVC, the 'top-bar effect' is also lower in SCC than in CVC [73]. It's expected that a well formulated SCC will be so stable that the amount of bleeding will be very minimal [70], and plastic settlement under the bars will be lower, owing to its self compactibility properties.

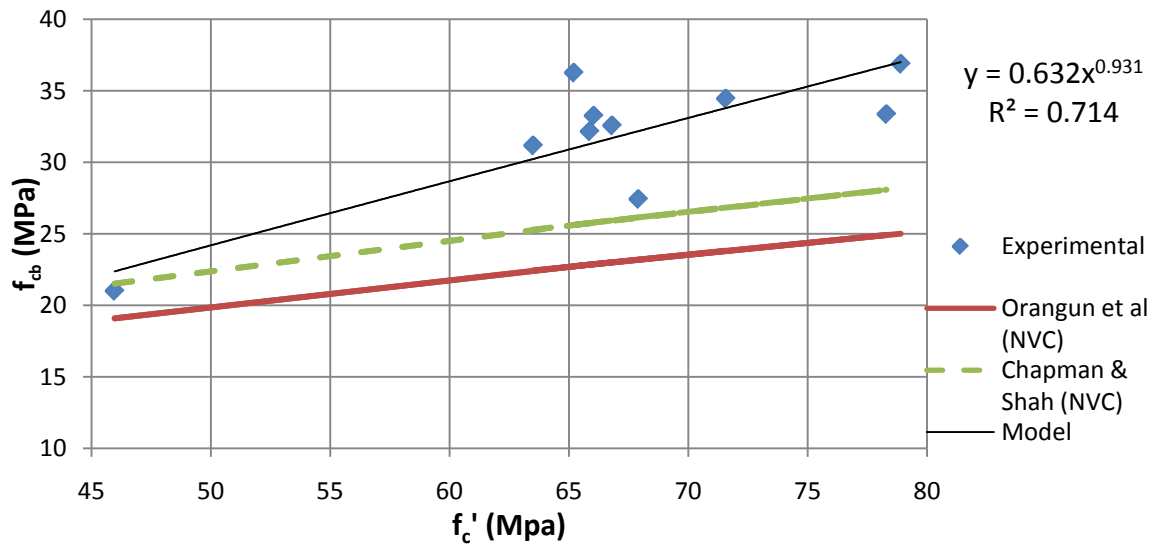


Figure 5.27: Relationship between  $f_{cb}$  and  $f'_c$  for SCC mixtures.

## 5.5 WATER PERMEABILITY

The depth of water penetration is a reliable durability assessment test [99]. The higher the water penetration depth, the lower the durability of such a concrete material. Table 5.5 shows the classes of water penetration depth [98].

Table 5.5: Water penetration depth classes [98].

Range of d	Penetration class
$d < 30$ mm	Low
$30 \text{ mm} \leq d \leq 60$ mm	Moderate
$d > 60$ mm	High

### 5.5.1 Mixes containing LSP

Figure 5.28 shows the water penetration depth of SCC specimens for mixes containing LSP.

The values on each bar represent the water penetration depth, d in mm, while those in boxes

are their corresponding percentages of the control mix. The low water penetration depth of the pure LSP and LSP-SF blends can be justified easily from their properties. LSP has an excellent filling effect in the concrete microstructure (by making the ITZ denser) [62, 64], and that's why the porosity of LSP containing concretes is lower than that of traditional concrete, as confirmed by MIP analysis [64]. Hence a lower water penetration depth is expected in LSP containing concrete [100]. SF on the other hand is a highly pozzolanic siliceous material with very fine vitreous particles, which improves strength and durability properties of concrete [41].

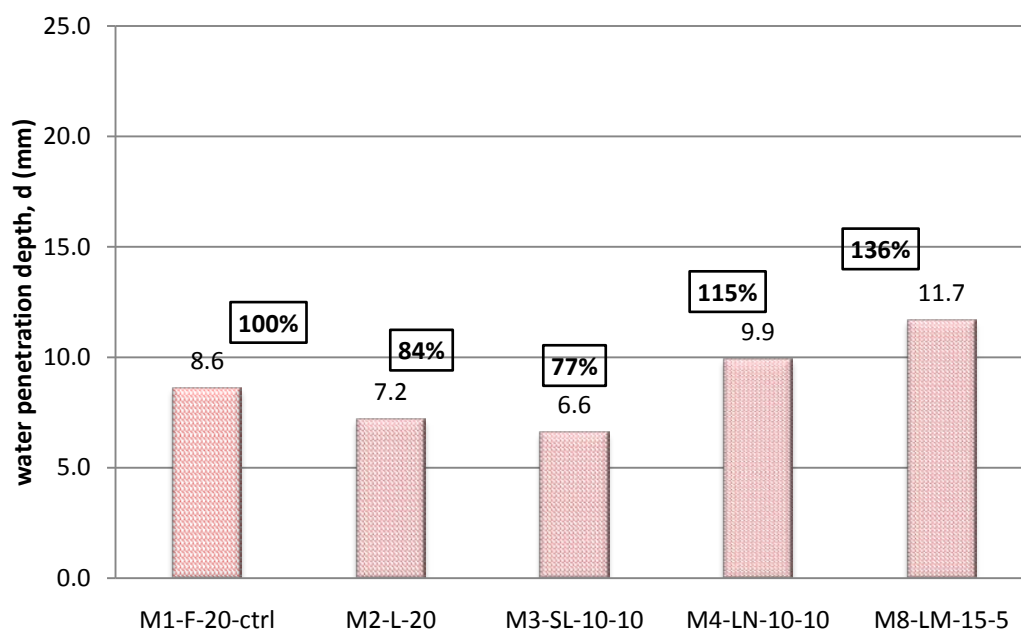


**Figure 5.28:** Water penetration depth of SCC mixtures with LSP.

Furthermore, both NP [99, 100] and MK [85, 86, 101, 102] have been found to improve the durability properties of concrete. Therefore, all these mixtures are expected to have low water penetration depth as a result of the durability improvement characteristics of their fillers. The 136% penetration obtained in M8 cannot be seen as too high if the actual value

itself is considered (11.7 mm). This value is less than half way the limit for a low penetration class of concrete (Table 5.6).

### ***5.5.2 Mixes containing NP***

Figure 5.29 shows the water penetration depth of SCC specimens for mixes containing NP. From the figure, the penetration depth of 12.2 mm seen for NP-PSS blend is an indication that PSS also improves durability property of concrete, as the water penetration depth of this mixture (M7) is less than half way the limit for a low penetration class of concrete. The LSP-NP blend was explored in the last section. But for the case of the NP-CKD, though the penetration depth (18.2 mm) is a low penetration class, the surge in the value from other NP blends shows that CKD may not be a very good filler material when it comes to durability, and may need to be limited in quantity. This in line with the findings of Maslehuddin et al [89], who reported reduction in durability properties of concrete with increasing quantity of CKD. In the same line of argument, Al-Harthy et al [88] also found that the water absorption of the mortar increased with increasing CKD contents. A limit of 5% replacement of cement was said to be optimum in order to avoid reduction in durability of concrete [89].



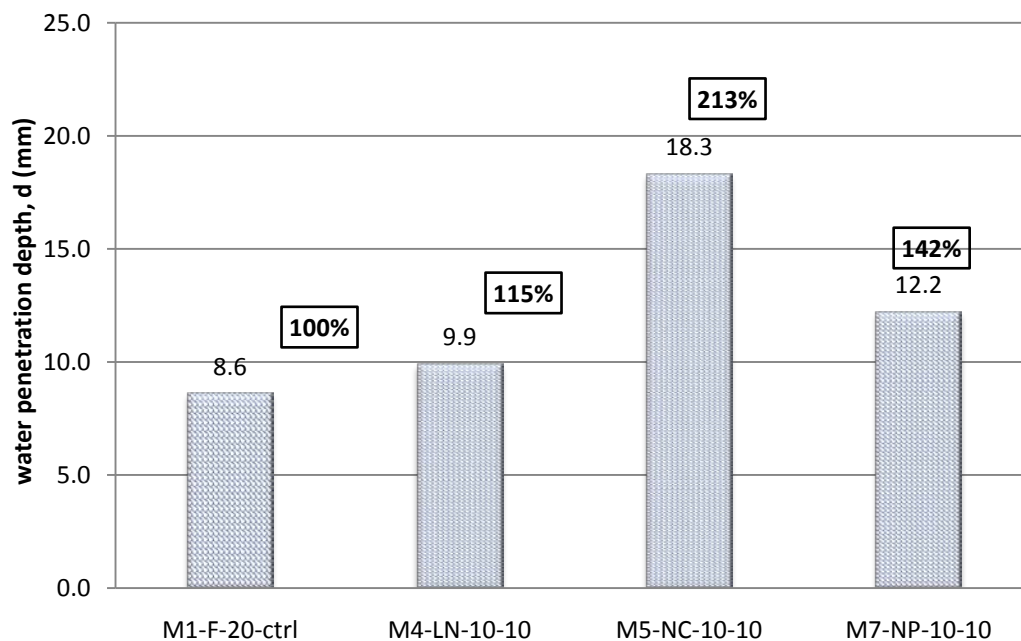


**Figure 5.29:** Water penetration depth of SCC mixtures with NP.

### 5.5.3 Mixes containing MK

Figure 5.30 shows the water penetration depth of SCC specimens for mixes containing MK. Going by the arguments presented in section 5.5.1 on the durability improvement properties of LSP and MK, the low penetration depth of LSP-MK blend will be as expected. The explanations offered in discussion on the NP-CKD blend in the last section regarding the poor durability behavior of CKD [88, 89], will also explain the observed higher penetration depth of the MK-CKD blend (M10).

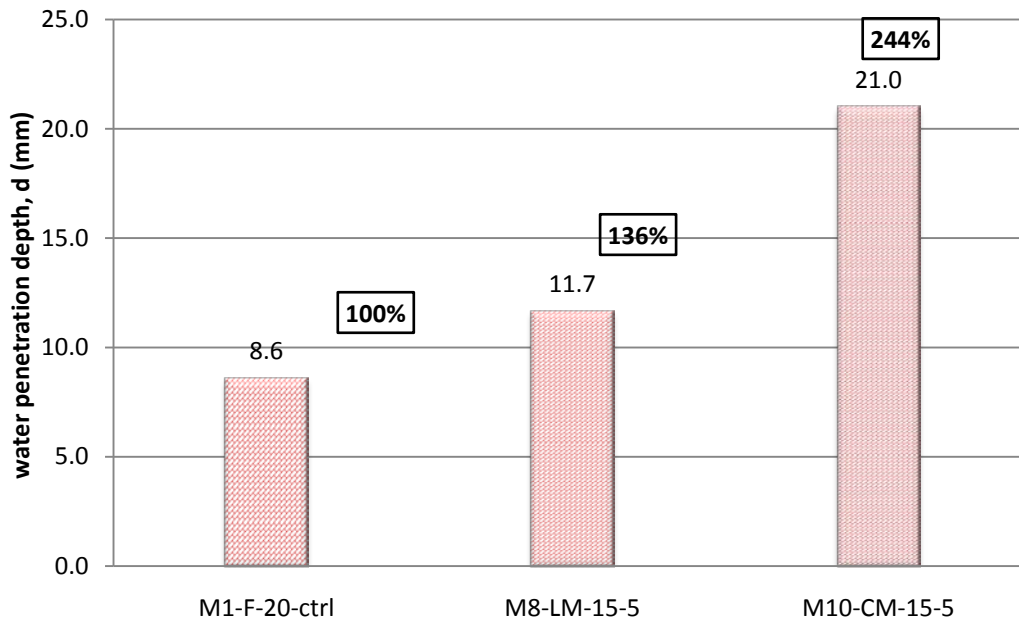


**Figure 5.30:** Water penetration depth of SCC mixtures with MK.

#### 5.5.4 Mixes containing CKD

Figure 5.31 shows the water penetration depth of SCC specimens for mixes containing CKD. The discussions of the poor durability behavior of CKD incorporating mixtures have been largely explored in the two previous sections. Nevertheless the penetration depth of these mixtures incorporating it are still in the low class, and given the cheap availability of CKD and its good behavior observed in the rheological study, it may still be used as long as its quantity is limited to around 5% [88, 89], or other durability enhancing fillers are used to boost the overall durability behavior.

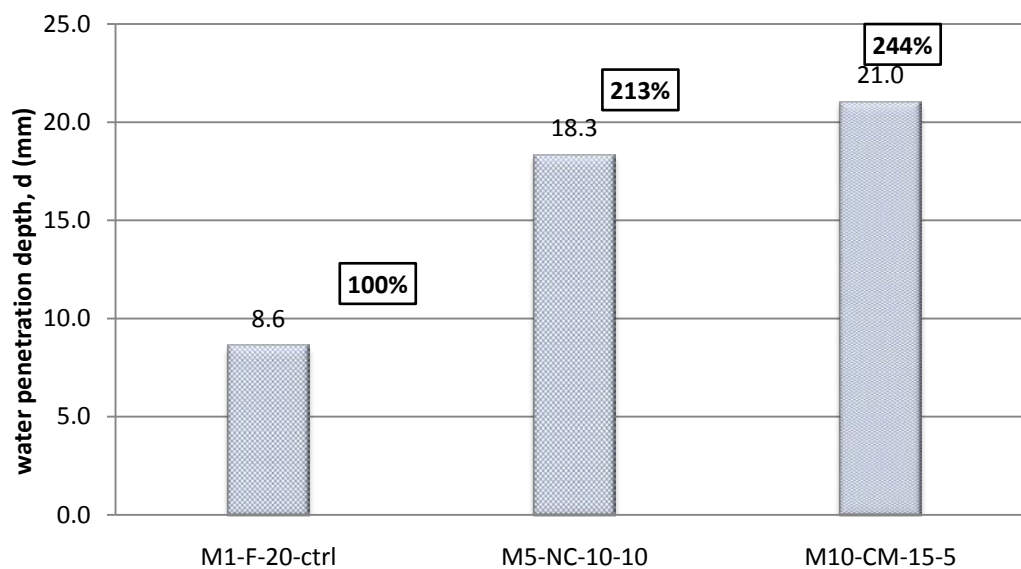


**Figure 5.31:** Water penetration depth of SCC mixtures with CKD.

Table 5.6 shows the 28-day water permeability results for the 10 SCC mixes. The reported values are averages water penetration depth (according to DIN 1048) in mm of three specimens prepared from each mix.

**Table 5.6:** Water penetration depth of SCC specimens.

MIX ID	d (mm)
M1-F-20-ctrl	8.6
M2-L-20	7.2
M3-SL-10-10	6.6
M4-LN-10-10	9.9
M5-NC-10-10	18.3
M7-NP-10-10	12.2
M8-LM-15-5	11.7
M10-CM-15-5	21.0

Looking at the results of water penetration test for the SCC mixes shown in Figure 5.6, it can be seen that all mixes belong to the low penetration classes (Table 5.5 [98]), meaning they all belong to the high durability grade of concrete with regards to the resistance to penetration of aggressive species.

## 5.6 CHLORIDE PERMEABILITY

Because of long testing time of the traditional chloride penetration test, rapid testing methods have been formulated over time. The most commonly used of them is the Rapid Chloride Penetration Test (RCPT) method of ASTM C1202 [103]. Although it's been criticized over time [104], as being misleading in some cases, it's still very popularly used and a strong correlation between the RCPT results and the 90-day ponding test have been established for many scenarios [85, 105]. Table 5.7 shows ASTM C1202-97 classification of concrete penetrability by chloride ions.

**Table 5.7:** Chloride ion penetrability based on charge passed [106].

<b>Charge passed, Coulombs</b>	<b>Chloride Permeability Class</b>
>4,000	High
2,000 – 4,000	Moderate
1,000 – 2,000	low
100 – 1,000	Very low
< 100	Negligible

### 5.6.1 Mixes containing LSP

Figure 5.32 shows the rapid chloride permeability of SCC specimens for mixes containing LSP. The values on each bar represent the charges passed, in *Coulombs*, while those in boxes are their corresponding percentages of the control mix.

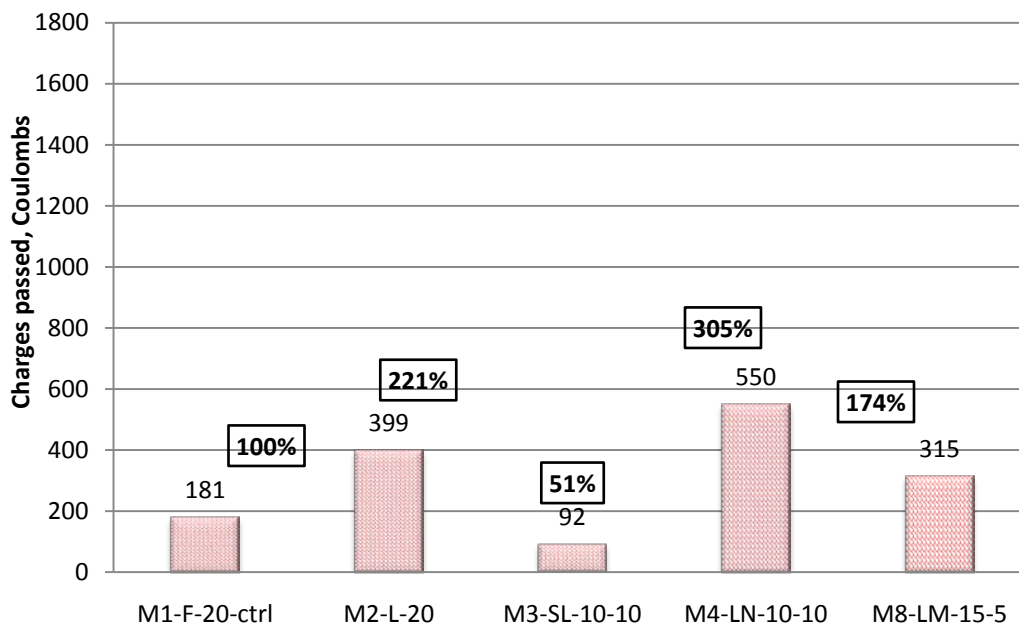


**Figure 5.32:** Rapid chloride permeability of SCC mixtures with LSP.

From the figure, it can be seen that only the LSP-SF blend (M3) show the charged passed below that of the control, while other blends that showed better resistance to chloride penetration than the control on the basis of water penetration depth cannot show exactly the same trend. These anomalies can easily be attributed to the fact that the chemistry of concrete pore solution of these mixtures varies drastically, and such anomalies as noticed here are inevitable since the result of this type of chloride permeability is highly dependent on the pore solution chemistry [104]. Therefore, the important observation here is that all

the mixes in this category are highly durable (in terms of resistance to chloride penetration), as they belong to very low (and for M3, negligible) chloride permeability class.

### 5.6.2 Mixes containing NP

Figure 5.33 shows the rapid chloride permeability of SCC specimens for mixes containing NP. Going by the same explanation of variable concrete pore solution chemistry offered in the last section, the observed anomalies here could also be understood. All, except M6, belong to low chloride permeability class and so highly durable, which is in line with the results of water penetration depths discussed in Section 5.5. For the case of M6, the observed delayed setting at the time of casting and demolding (as discussed in Section 5.1) had a lot of impact on the hardened behavior. Its compressive strength was the least at all ages up to 28 days. Therefore the observed relatively large quantity of charge passed will be expected.

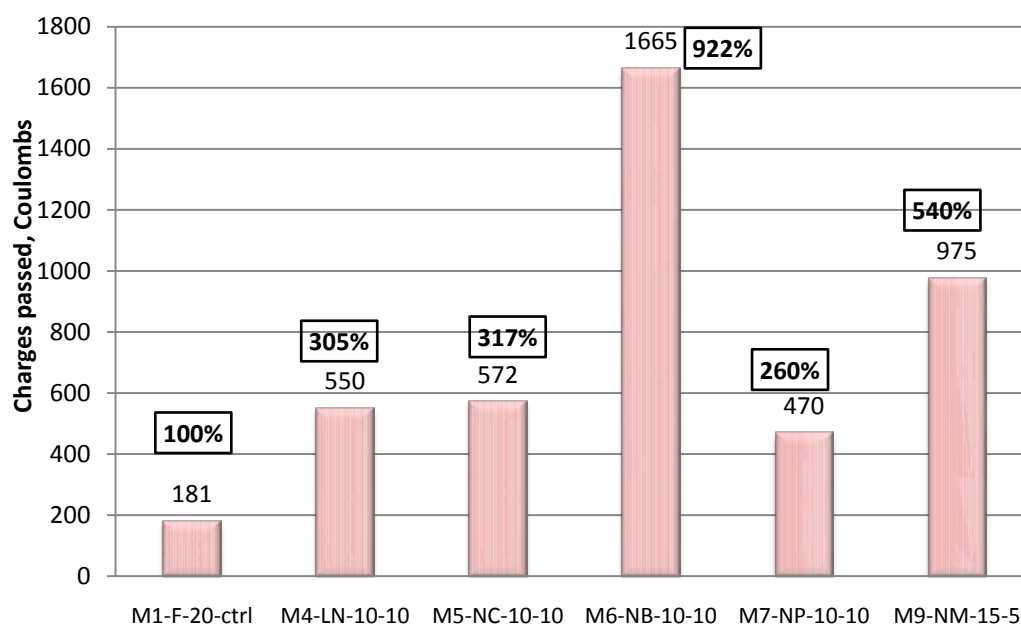


**Figure 5.33:** Rapid chloride permeability of SCC mixtures with NP.

### 5.6.3 Mixes containing MK

Figure 5.34 shows the rapid chloride permeability of SCC specimens for mixes containing MK. In line with the ongoing previous argument on the impact of variable concrete pore solution chemistry on the quantity of charges passed [104], the low chloride permeability results of these mixtures is the most important observation that can be dwelled upon.

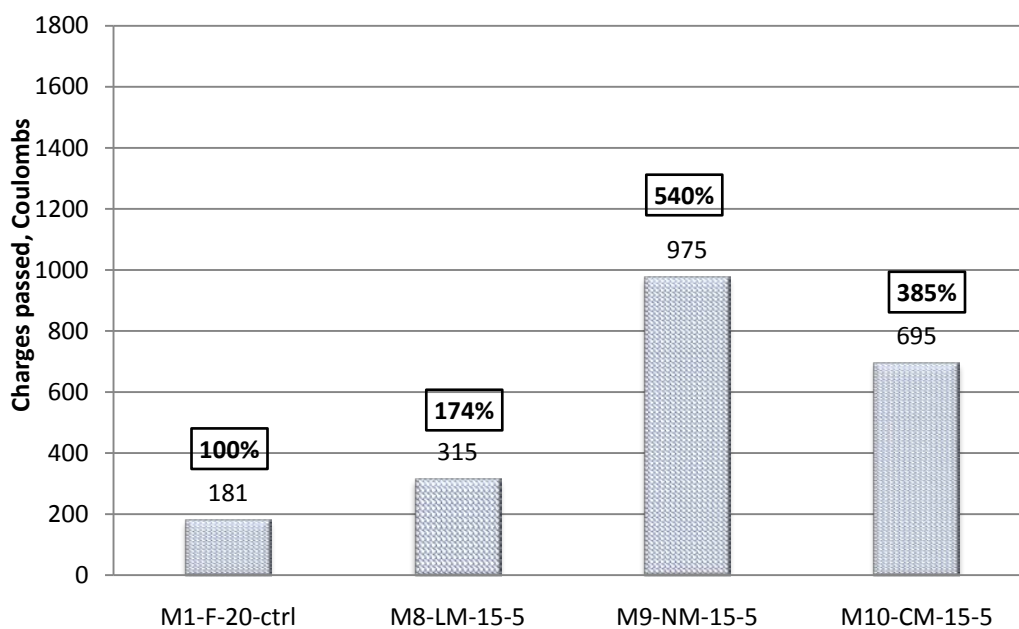


**Figure 5.34:** Rapid chloride permeability of SCC mixtures with MK.

### 5.6.4 Mixes containing CKD

Figure 5.35 shows the rapid chloride permeability of SCC specimens for mixes containing CKD. From the results in the figure it can be noticed that these mixes too belong to high durability class with respect to their resistance to chloride permeability, not minding the actual figures of the charges passed.

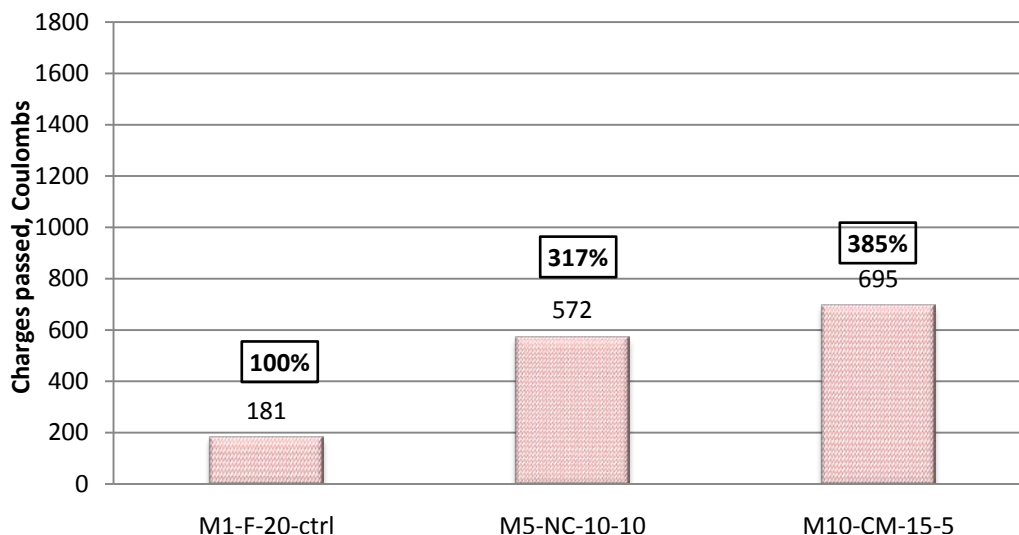


**Figure 5.35:** Rapid chloride permeability of SCC mixtures with CKD.

Table 5.8 shows the 28-day rapid chloride permeability (RCP), measured in terms of the total amount of charges in coulombs passing through a 51 mm concrete disk in a 6 hrs period under the influence of 60 V potential difference [106]. The reported values are averages of three specimens prepared from each mix.

**Table 5.8:** Rapid chloride permeability of SCC specimens.

Mix ID	Charge passed,
M1-F-20-ctrl	181
M2-L-20	399
M3-SL-10-10	92
M4-LN-10-10	550
M5-NC-10-10	572
M6-NB-10-10	1665
M7-NP-10-10	470
M8-LM-15-5	315
M9-NM-15-5	975
M10-CM-15-5	695



As can be seen from the classification [106] of Table 5.7, all the mixtures fall in the ‘very low’ chloride permeability class, except the SF-LSP (M3) and NP-BHD (M6) blends that fall in the ‘negligible’ and ‘low’ classes, respectively.

## 5.7 CORROSION POTENTIALS

Corrosion potential measurement is one of the popular methods for monitoring reinforcement corrosion in concrete [107] in accordance with the provisions of ASTM C876 [108]. Figures 5.36 through 5.39 show the variation of corrosion potentials ( $E_{\text{corr}}$ ) with exposure time to 5% NaCl solution for each group of SCC specimens. The plot covers only 95 days so far up to the time of this reporting. The red dashed lines in the graphs represent the corrosion activity threshold level of  $E_{\text{corr}}$  measured on a rebar at which corrosion is assumed to be active, according to ASTM C876. This threshold value of  $E_{\text{corr}}$  is  $-270$  mV SCE for the standard Calomel electrode [108] used for this monitoring process.

### 5.7.1 *Mixes containing LSP*

Figure 5.36 shows the variation of corrosion potentials with exposure time of SCC specimens representing the mixes containing LSP. From the figure, it is clear that none of these mixtures has the embedded steel in the active state of corrosion yet. These mixtures have showed a high durability in the previous sections on the basis of water penetration depth and RCPT results. Also, the potentials are not in an uptrend, which is an indication that the time to initiation of corrosion may be very long. This observed high durability qualities are attributable to the excellent filling effect of LSP and other pozzolans in these blends.

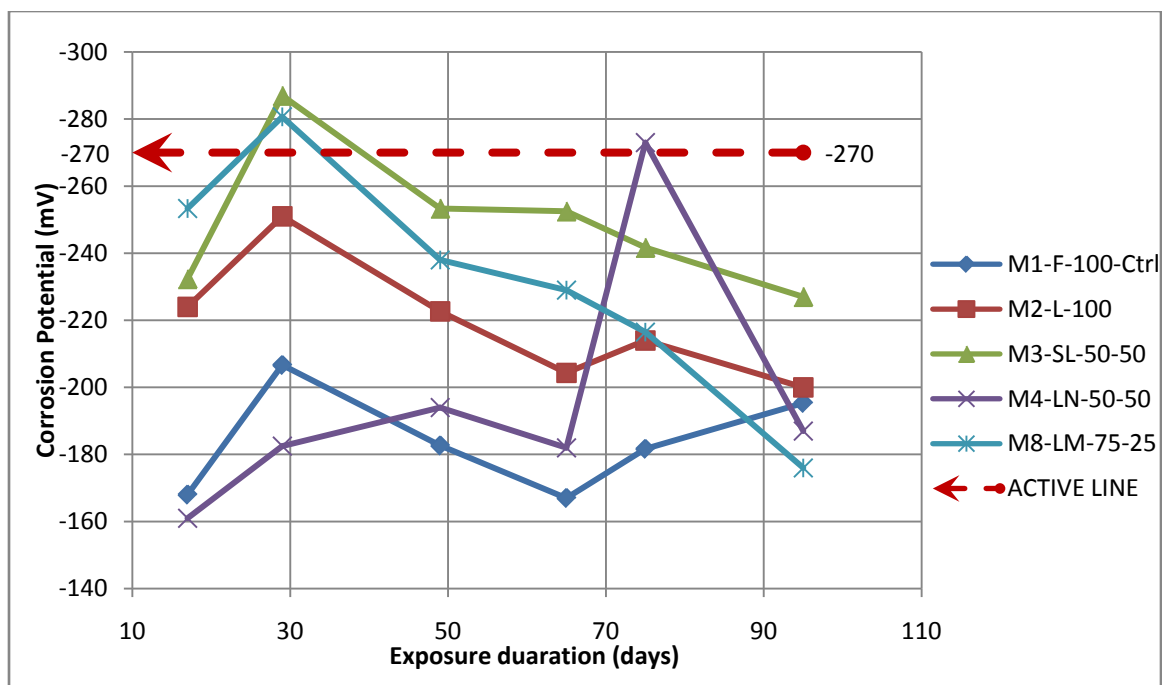


**Figure 5.36:** LSP mixes – variation of corrosion potential with exposure time.

### 5.7.2 Mixes containing NP

Figure 5.37 shows the variation of corrosion potentials with exposure time of SCC specimens representing the mixes containing NP. Looking at Figure 5.37, the NP-BHD blend can be seen to display an active state of corrosion at around 95 days of exposure. This poor durability can also be traced back to the delayed setting problem it encountered, making it the weakest of all mixtures studied in this research. Also the NP-CKD blend can be seen to be close to corrosion initiation, which is still in line with the observations of previous researchers [88, 89], who have reported the poor durability performance of CKD. The case of the NP-MK blend (M9) cannot easily be judged until after a longer duration of exposure, as the corrosion potential stayed ‘high up in the sky’, right from the time of exposure. Also, looking at its potential-time curve, it’s somewhat in a downtrend. As for

other blends (M4 and M7), they're as resistant as the control mixture to corrosion. This is in line with their observed low water and chloride permeability results.

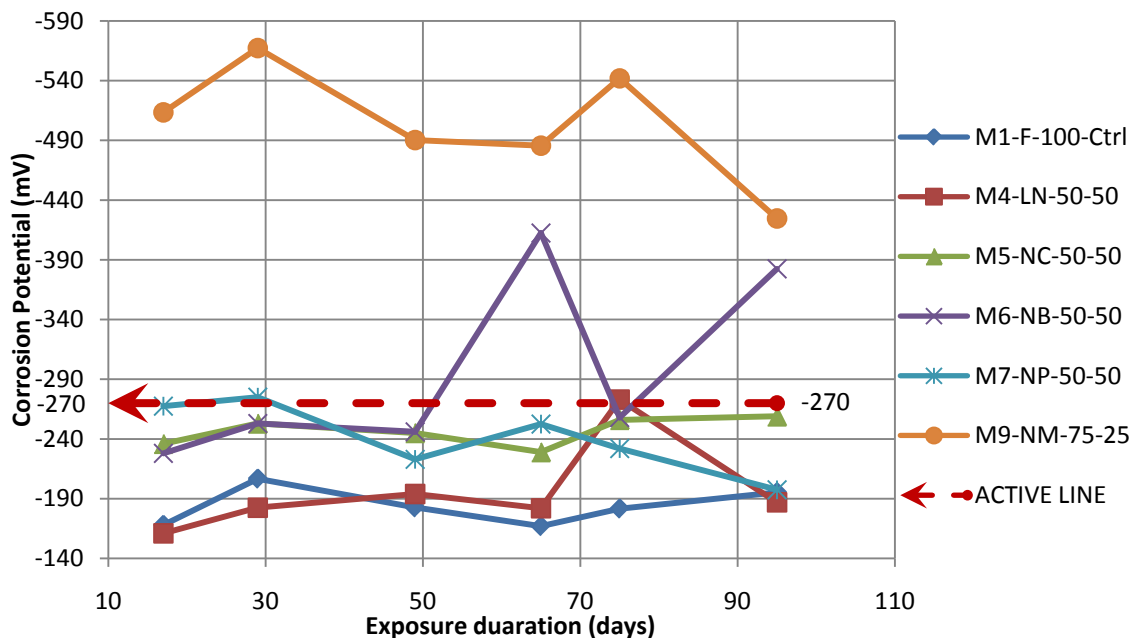


**Figure 5.37:** NP mixes – variation of corrosion potential with exposure time.

### 5.7.3 Mixes containing MK

Figure 5.38 shows the variation of corrosion potentials with exposure time of SCC specimens representing the mixes containing MK. The observed corrosion resistance of the LSP blend (M8) as can be seen from Figure 5.38 had been explained in Section 5.7.1, which was attributed to the LSP filling effect. MK had been reported by several researchers as being good in durability improvement [85, 86, 101, 102]. Hence the high potentials shown here for M9 and M10 may need to be watched further in the course of time.

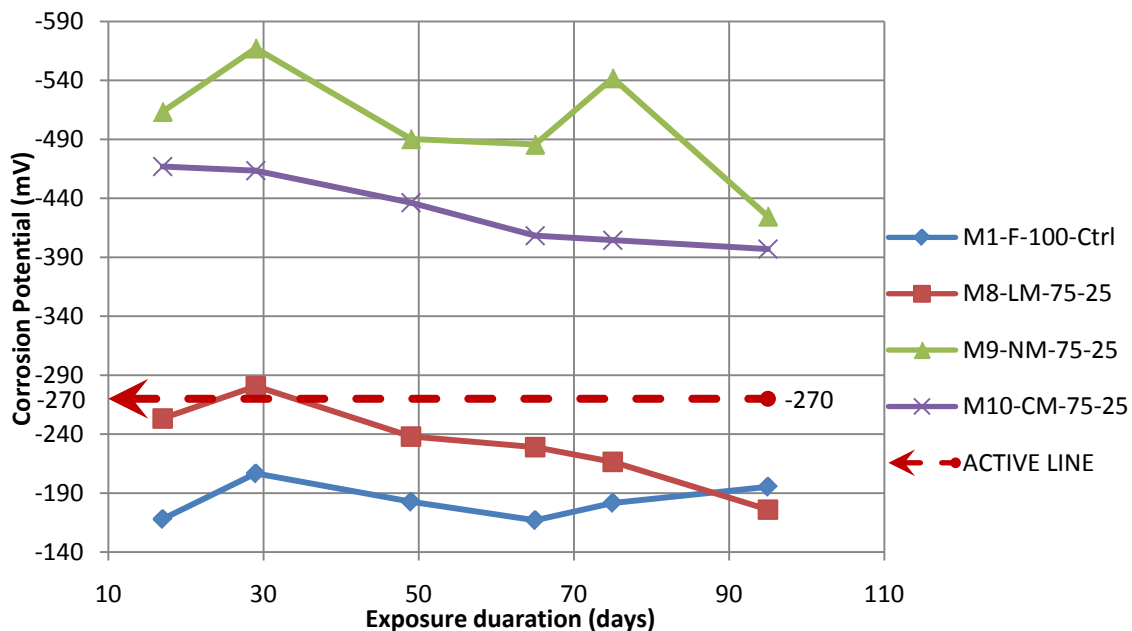


Figure 5.38: MK mixes – variation of corrosion potential with exposure time.

#### 5.7.4 Mixes containing CKD

Figure 5.39 shows the variation of corrosion potentials with exposure time of SCC specimens representing the mixes containing CKD. Again the inclusion of CKD seems to be responsible for the low corrosion resistance exhibited by these mixtures. It was said earlier that CKD's durability behavior is poor, particularly at a dosage more than 5% of cement [88, 89] .

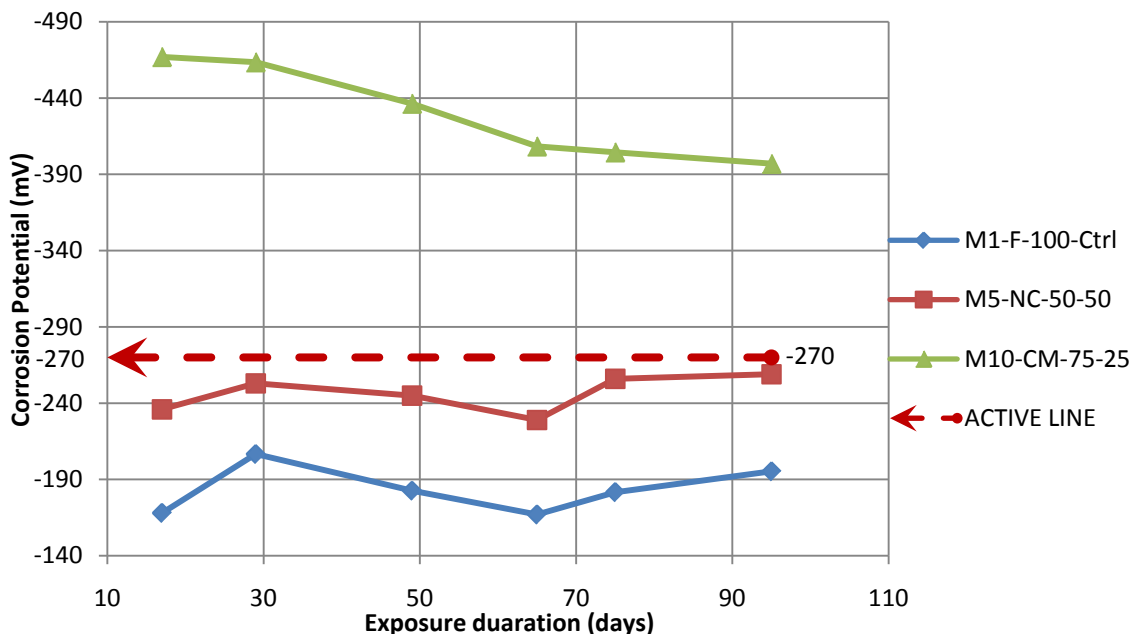


Figure 5.39: CKD mixes – variation of corrosion potential with exposure time.

## 5.8 CORROSION CURRENT DENSITY

Figures 5.40 through 5.43 show the variation of corrosion current density,  $I_{\text{corr}}$ , with exposure time to 5% NaCl solution for each group of SCC specimens. From the figures, it can be seen that many of the observations noticed in each group of specimens in the discussion of corrosion potentials were supported by the corresponding  $I_{\text{corr}}$  values, as mixtures with  $E_{\text{corr}}$  values in the vicinity of the threshold value ( $-270$  mV SCE) also displayed similar patterns of  $I_{\text{corr}}$  values close or above the threshold value of  $0.3 \mu\text{A}/\text{cm}^2$  as at 90 days of exposure. The  $I_{\text{corr}}$  generally increased with exposure time for all the SCC mixtures.

### 5.8.1 Mixes containing LSP

Figure 5.40 shows the variation of corrosion current density of SCC specimens for mixes containing LSP. From the figure, the excellent filling ability of LSP [85, 86, 101, 102] is obvious, as all the LSP blends maintained  $I_{\text{corr}}$  values below  $0.1 \mu\text{A}/\text{cm}^2$ , far from the threshold value of  $0.3 \mu\text{A}/\text{cm}^2$ , at which the probability of corrosion initiation becomes very high. All of these blends perform close enough to the control mixture.

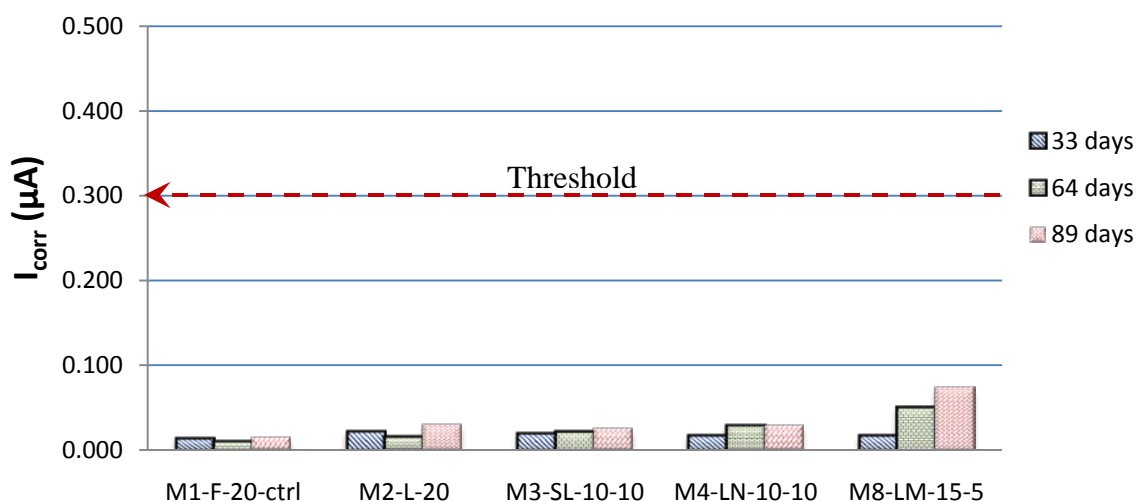


**Figure 5.40:** LSP mixes – variation of corrosion current density with exposure time.

### 5.8.2 Mixes containing NP

Figure 5.41 shows the variation of corrosion current density of SCC specimens for mixes containing NP. It can be seen from the figure that the BHD and MK blends with NP have crossed the threshold value of  $0.3 \mu\text{A}/\text{cm}^2$ , which is in good agreement with the observations made in Section 5.7.2 on corrosion potential measurements.

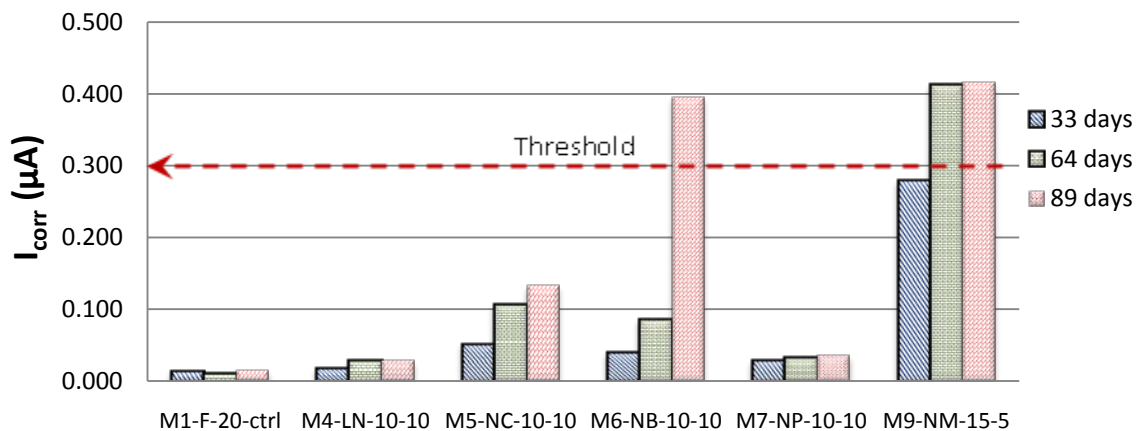


Figure 5.41: NP mixes – variation of corrosion current density with exposure time.

### 5.8.3 Mixes containing MK

Figure 5.42 shows the variation of corrosion current density of SCC specimens for mixes containing MK. Like it was observed in the corrosion potential measurements for this group (Section 5.7.3), the MK blends show signs of early corrosion initiation. The same can also be noticed here with their  $I_{corr}$  values being in the vicinity of the threshold value of  $0.3 \mu A/cm^2$ .

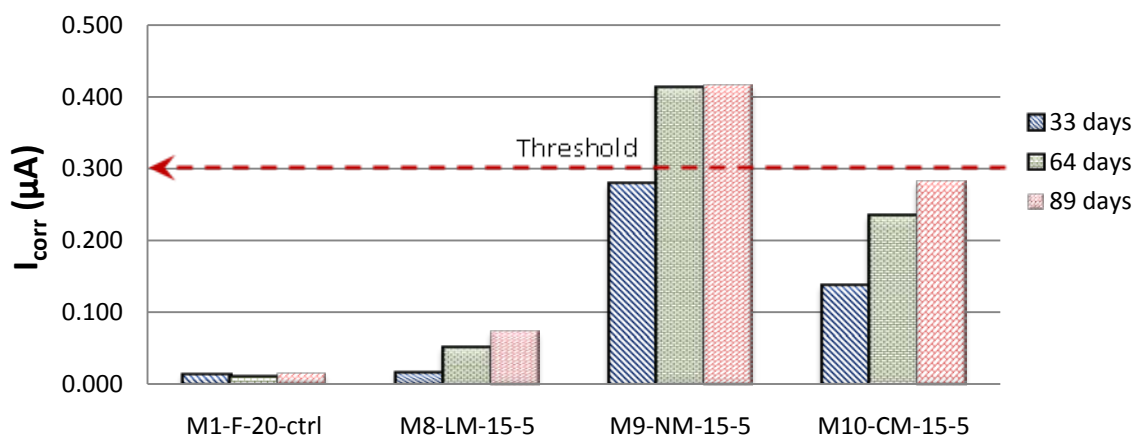
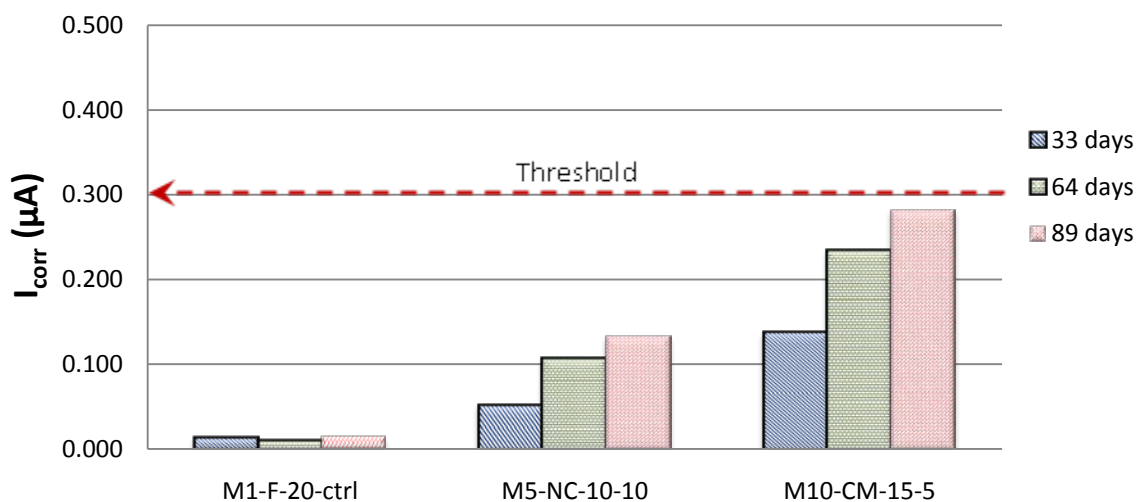


Figure 5.42: MK mixes – variation of corrosion current density with exposure time.

#### 5.8.4 Mixes containing CKD

The variation of corrosion current density of SCC specimens for mixes containing CKD is shown in Figure 5.43. Again, like it was noticed from the corrosion potential measurements (Section 5.7.4) it can also be seen here that SCC blends with CKD have lower corrosion resistance, owing to their high  $I_{\text{corr}}$  values. Further, with the  $I_{\text{corr}}$  in M10 (15% CKD) specimens being higher than in M5 (10 % CKD) for the same duration and condition of exposure, it follows that the corrosion resistance reduces with increasing CKD content. Therefore, it is important to limit the CKD content in mixtures intended for corrosion-critical applications. This agrees with the conclusions drawn in previous studies on the use of CKD in CVC [88, 89].



**Figure 5.43:** CKD mixes – variation of corrosion current density with exposure time.



## 5.9 ELECTRICAL RESISTIVITY

Since corrosion is an electro-chemical process, the flow rate of the ions through concrete between the anodic and cathodic areas of a depassivated rebar embedded in concrete determines the rate at which corrosion can occur in that rebar. This flow rate of ions is affected by the resistivity of the concrete [109]. Therefore, measuring the electrical resistivity of concrete could give some clues as to the likelihood of corrosion taking place[107]. Table 5.9 shows the empirical indication of likelihood of corrosion of a depassivated rebar for various resistivity ranges of covercrete.

The electrical resistivity was measured at 7 different moisture contents for each of the 10 SCC mixes using the two-electrode method. Figures 5.44 through 5.47 show the electrical resistivity for each group of SCC mixtures. From the figures, it can be seen that the relative differences in resistivity values are somewhat close to the trends observed for the varying levels of corrosion resistance of the various SCC mixtures.

**Table 5.9:** Empirical resistivity thresholds for depassivated steel [109, 110].

Resistivity range	Likelihood of corrosion
$\rho < 5.0 \text{ K}\Omega\text{-cm}$	Very high
$\rho = 5.0 - 10.0 \text{ K}\Omega\text{-cm}$	High
$\rho = 10.0 - 20.0 \text{ K}\Omega\text{-cm}$	Low to moderate
$\rho > 20.0 \text{ K}\Omega\text{-cm}$	Low to negligible

### 5.9.1 Mixes containing LSP

Figure 5.44 shows the electrical resistivity of SCC specimens for mixes containing LSP at 3% moisture content. Going by the criteria [109, 110] in Table 5.9, all the blends in this group have ‘low to negligible’ probability of corrosion initiation on a depassivated steel at 3% concrete moisture content. This complies with the previous observations made on the performance of LSP blends.

Looking at the figure, the obviously highest resistivity mixture (M3-SL-10-10) is expected to lead the race in this category, as it was noticed in all other durability indices. However, the higher resistivity of M8 than all others is conspicuously contradictory to the trends noticeable from previous data in this group. This discrepancy will not be surprising given the fact that the values of electrical parameters like resistivity is affected the chemistry of the concrete pore solution [104], and since the other fillers apart from LSP are not the same in each mixture, the resulting concrete pore solution are bound to be chemically different from each other, and consequently, anomalies like this cannot be ruled out.

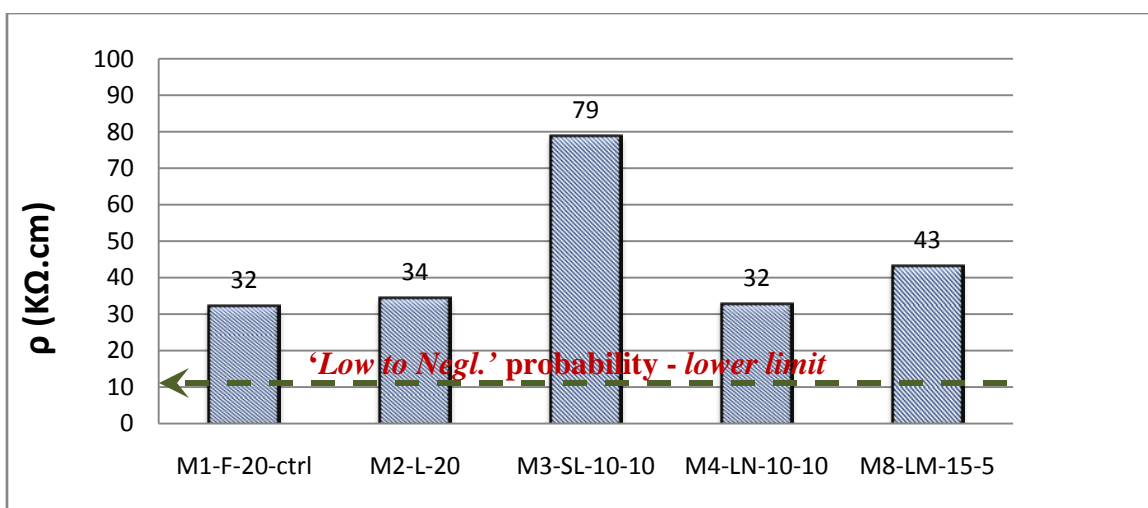
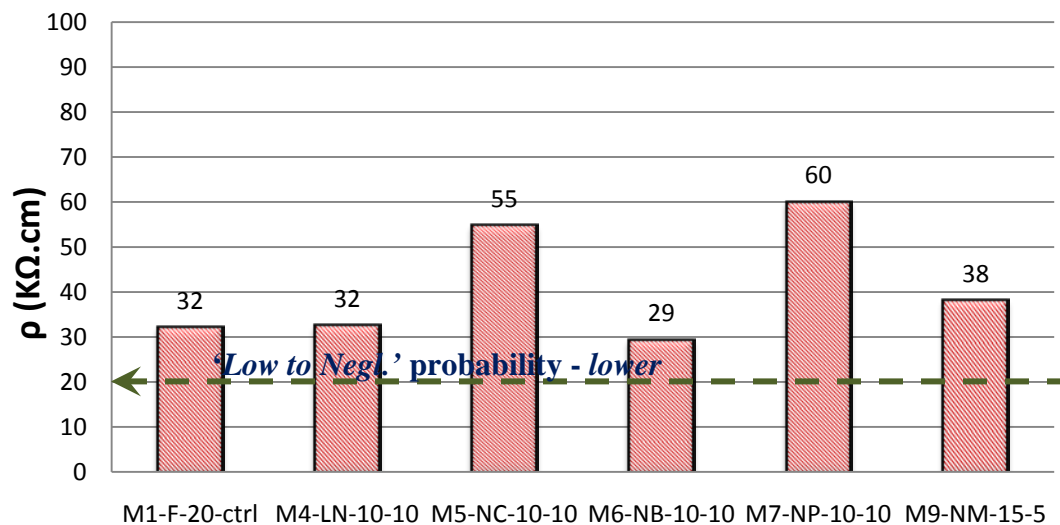


Figure 5.44: Electrical resistivity of SCC mixtures with LSP.

### 5.9.2 Mixes containing NP

Figure 5.45 shows the electrical resistivity of SCC specimens for mixes containing NP at 3 % moisture content. The case here is also full of several anomalies, ranging from M6 (which has been seen as the least resistant mixture to corrosion) showing similar value of electrical resistivity to that of the control mixture, to CKD blend (the next lower resistant mixture to corrosion) having far higher resistivity than almost all the blends. The explanation offered in the previous section will also be relevant here to understand these anomalies.



**Figure 5.45:** Electrical resistivity of SCC mixtures with NP.

### 5.9.3 Mixes containing MK

Figure 5.46 shows the electrical resistivity of SCC specimens for mixes containing MK at 3 % moisture content. The observation here is similar to what was noticed in the last two sections in terms of unexpected high resistivity of SCC mixtures that has previously been

shown to be less resistant to corrosion. So, the same line of reasoning will also suffice to understand the anomalies.

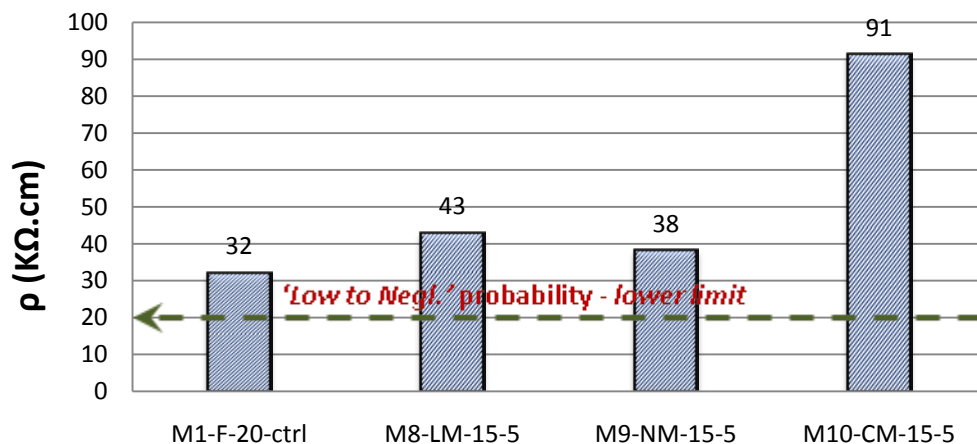


**Figure 5.46:** Electrical resistivity of SCC mixtures with MK.

#### 5.9.4 Mixes containing CKD

Figure 5.47 shows the electrical resistivity of SCC specimens for mixes containing CKD at 3 % moisture content. The interesting fact obtainable from this figure is that a reader looking at the figure could erroneously think that CKD is an excellent admixture for increasing concrete's corrosion resistance, since the electrical resistivity steadily increases with the CKD content (0% in the control mixture, and 10% and 15% in the next 2 mixtures). The reverse is, however, the case. Therefore, the effect of the chemical makeup of the concrete pore solution on the electrical resistivity of the mixtures is so heavy that it reverses the fact established from other more consistent durability indices.

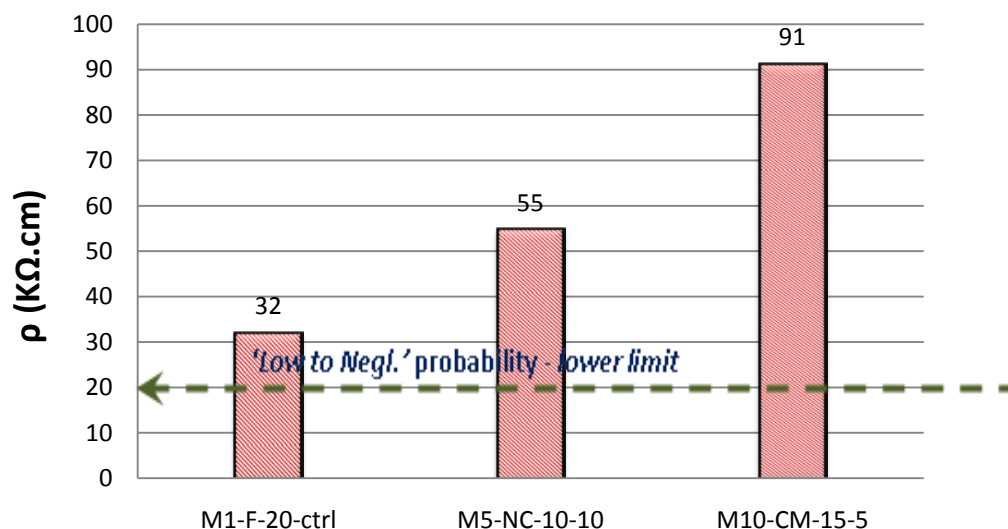


**Figure 5.47:** Electrical resistivity of SCC mixtures with CKD.

Attempts at correlating the measured resistivity to the corresponding moisture content proved successful for all the mixes. An exponential relationship of the form:  $\rho(m) = Ce^{km}$  was found to give the best correlation. An example of the electrical resistivity – moisture content curve is shown in Figure 5.48 for the SCC mixture M5-NC-10-10.  $C$  and  $k$  are constant for each mixture, and  $m$  is the moisture content. Table 5.10 shows the summary of the obtained correlation parameters and corresponding electrical resistivity in  $k\Omega.cm$  at a moisture content of 3%.

From the values of electrical resistivity shown in Table 5.10 for the SCC mixtures, the criteria set forth in Table 5.9 will indicate that the chance of corrosion is very remote even when the steel bars embedded in such concrete mixtures get depassivated, as the mixture with the least electrical resistivity (M6) has a value higher than  $20\Omega.cm$ . This, however, is

subject to skepticism, since the previous free potentials values showed that some of the concrete mixtures are at, or close to corrosion initiation as at 90 days of exposure.

**Table 5.10:** Correlation parameters and electrical resistivity of SCC specimens

MIX ID	C	k	R <sup>2</sup>	$\rho(m) = Ce^{km}$ , k $\Omega$ .cm
M1-F-20-ctrl	10812	-1.941	0.9874	32
M2-L-20	9593	-1.88	0.9843	34
M3-SL-10-10	7253.5	-1.508	0.9855	79
M4-LN-10-10	22004	-2.173	0.9780	32
M5-NC-10-10	3773.1	-1.411	0.9945	55
M6-NB-10-10	5159.2	-1.724	0.9667	29
M7-NP-10-10	12609	-1.783	0.9795	60
M8-LM-15-5	21246	-2.069	0.9982	43
M9-NM-15-5	7757.1	-1.773	0.9623	38
M10-CM-15-5	4853.2	-1.325	0.9661	91

This discrepancy is normal as the moisture content at which these values are computed (3%) is far lower than that of the specimens in chloride exposure, where they were submerged permanently in 5% NaCl solution. Consequently, the values will just give indications of relative corrosion resistance of each SCC mixture, rather than agreeing with the previous corrosion monitoring parameters.

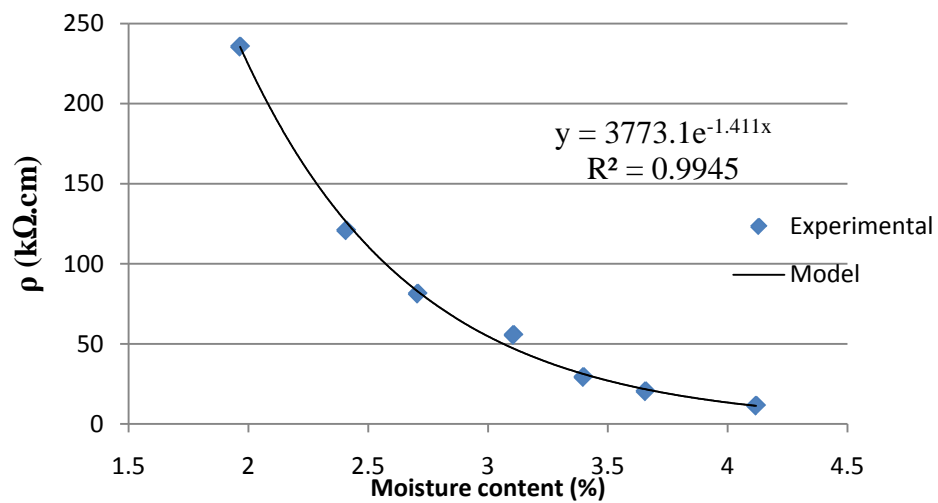


**Figure 5.48:** Electrical resistivity – moisture content curve for M5-NC-10-10.

## CHAPTER SIX

### CONCLUSIONS AND RECOMMENDATIONS

#### 6.1. CONCLUSIONS

Based on the experimental data obtained in this study, the following conclusions can be drawn:

##### *6.1.1. Waste Materials*

- 1 All the waste materials performed satisfactorily, though some waste materials such as BHD (EAFD), PSS and NP demanded high dosages of SP and consequently of VMA.
- 2 These high demands for chemical admixtures may impact on the overall cost, but given the observed high strength and durability shown by most of the mixtures, and the abundant availability of the materials at low cost and mostly free of cost, their use in SCC is feasible and highly promising.
- 3 Most of the waste materials are very promising in strength and durability (pertaining to corrosion resistance). The only exceptions, as could be seen in the discussion, were BHD and MK.
- 4 The BHD-NP blend suffered delayed setting causing it to exhibit low strength and durability.



- 5 The CKD and MK blends were mostly very good in strength, but produced low durability materials.
- 6 PSS also showed good contribution to mechanical and durability property of SCC.

### ***6.1.2. Mechanical Properties of SCC mixtures developed***

- 1 All the SCC blends produced (except the one with BHD) with these waste materials were high compressive strength concrete, with an average 3-day strength of around 40 MPa, and 28-day strengths in the range of 64 to 79 MPa.
- 2 The average elastic moduli of the SCC mixtures ranged from 38 – 43 GPa, while the tensile and bond strengths ranged between 5.4 – 6.4 MPa and 27 – 37 MPa respectively.
- 3 Given the fact that all the mixtures (except the BHD-NP blend) exhibited very good mechanical properties, the developed SCC mixtures utilizing the indigenous waste materials are not only economical advantageous, but also structurally competitive.

### ***6.1.3. Durability Properties of SCC mixtures developed Related to Reinforcement Corrosion Resistance.***

- 1 The water penetration depths for all mixtures studied were far below 30 mm on the average.
- 2 The RCPT indicated that all the mixtures were 'very low' chloride permeability SCC materials, while for all mixtures studied, the electrical resistivities indicated 'low to

negligible' probability of corrosion taking place on a depassivated steel embedded in these mixtures at 3% moisture content of the concrete material.

- 3 All LSP and NP (except with MK, BHD) blends have not been active in corrosion at 90 days of exposure to 5% chloride solution.
- 4 All CKD (except with NP) and MK (except with LSP) were active within 90 days of exposure to 5% chloride solution.
- 5 Given the challenging marine environment we have to work with in the Kingdom, particularly in the eastern province, the high corrosion resistance exhibited by most of the developed mixtures are a pointer to the fact that suitable SCC mixtures for our environment can be made with these by-products.

## **6.2. RECOMMENDATIONS**

- 1 Waste materials such as BHD (EAFD), PSS and NP should be limited in SCC because of their high demand for SP and VMA.
- 2 CKD should be limited to < 10% of the total powder to guarantee a durable SCC mixture with it. If it has to be up to 10% (but should not be more, proven durability enhancing fillers, such as LSP has to be used with it to boost the overall durability.
- 3 In order to get the full strength and durability benefit from NP blends, it is important to cure them further than 28 days, if the construction and service schedule can accommodate longer curing time.

- 4 SCC produced with CKD and MK (Qatif) can be used in high strength applications where reinforcement corrosion is not critical.
- 5 SCC made with LSP, SF and NP is recommended for use in high strength applications even where reinforcement corrosion is critical.

### **6.3. RECOMMENDATIONS FOR FUTURE WORKS**

- 1 Given the problems shown by the BHD mixtures, further research needs to be carried out to investigate into the probable solution to make it work in SCC. This may involve trying some other chemical admixtures of different chemical makeup from those used in this study.
- 2 Different other combinations of these waste materials should be tried and also at different proportions to obtain the best combinations of these waste materials in producing SCC of competitive mechanical and durability properties.
- 3 Each waste material needs to be used at varying dosages and varying mix parameters in order to obtain optimized dosages and mix parameters for each of the waste materials.
- 4 Investigate other durability parameters of SCC produced with these waste materials such as under heat-cool and wet-dry cycles, and resistance to carbonation.

## REFERENCES

1. Su, N., K.-C. Hsu, and H.-W. Chai, *A Simple Mix Design Method for Self-Compacting Concrete*. Cement and Concrete Research, 2001. **31**(12): p. 1799-1807.
2. Dehn, F., K. Holschemacher, and D. Weibe, *Self-Compacting Concrete Time Development of the Material Properties and the Bond Behavior*, in *LACER*. 2000. p. 115-124.
3. Khayat, K.H., J. Assaad, and J. Daczko, *Comparison of Field-Oriented Test Methods to Assess Dynamic Stability of Self-Consolidated Concrete*. ACI Materials Journal, 2004. **101**(2): p. 168-176.
4. Ouchi, M., et al., *A Quantitative Evaluation Method for the Effect of Superplasticizer in Self-Compacting Concrete*. Transactions of JCI, 2001: p. 15-20.
5. Kapoor, Y.P., C. Munn, and K. Charif, *Self-Compacting Concrete - an Economic Approach*, in *7th International Conference on Concrete in Hot & Aggressive Environments*. 2003: Manama, Kingdom of Bahrain. p. 509-520.
6. Zhu, W. and P.J.M. Bartos, *Permeation Properties of Self-Compacting Concrete*. Cement and Concrete Research, 2003. **33**(6): p. 921-926.
7. Ramsburg, P., et al., *Durability of Self Consolidating Concrete in Precast Applications*. 2003, ISHPC ([www.oldcastle-precast.com](http://www.oldcastle-precast.com)). p. 1-7.
8. Patel, R., et al., *Development of Statistical Models for Mixture Design of High-Volume Fly Ash Self-Consolidating Concrete*. ACI Materials Journal, 2004. **101**(4): p. 294-302.
9. Nehdi, M., M. Pardhan, and S. Koshowski, *Durability of Self-Consolidating Concrete Incorporating High-Volume Replacement Composite Cements*. Cement and Concrete Research, 2004. **34**(11): p. 2103-2112.
10. Persson, B., *Chloride Migration Coefficient of Self-Compacting Concrete*. Materials and Structures, 2004. **37**(2): p. 82-91.
11. Assie, S., et al., *Durability Properties of Low-Resistance Self-Compacting Concrete*. Magazine of Concrete Research, 2006. **58**(1): p. 1-7.
12. Assié, S., G. Escadeillas, and V. Waller, *Estimates of Self-Compacting Concrete 'Potential' Durability*. Construction and Building Materials, 2007. **21**(10): p. 1909-1917.
13. Holschemacher, K. and Y. Klug, *A Database for the Evaluation of Hardened Properties of Scc*, in *Leipzig Annual Civil Engineering Report No. 7*. 2002. p. 123-134.

14. LEEMANN, A. and C. HOFFMANN, *Properties of Self-Compacting and Conventional Concrete : Differences and Similarities*. Vol. 57. 2005, London, ROYAUME-UNI: Telford. 5.
15. Mata, L.A., *Implementation of Self-Consolidating Concrete (Scc) for Prestressed Concrete Girders*. 2004, North Carolina State University.
16. Krieg, W., *Self-Compacting Concrete: Definition, Development, and Applications*, in *A Technical Paper presented in the Meeting of the ACI, Saudi Arabia Chapter, Eastern Province*. 2003.
17. EFNARC, *Specifications and Guidelines for Self-Compacting Concrete*, in *Specifications and Guidelines for Self-Compacting Concrete*. 2002, EFNARC, UK ([www.efnarc.org](http://www.efnarc.org)). p. 1-32.
18. Magyar, Z., *An Attempt to Establish a History of Concrete*. Kísérlet a beton történetének megfogalmazásához, 2011. **39**(3-4): p. 353-410.
19. Kenai, S. and R. Bahar, *Evaluation and Repair of Algiers New Airport Building*. Cement and Concrete Composites, 2003. **25**(6): p. 633-641.
20. Hover, K.C., *Concrete Mixture Proportioning with Water-Reducing Admixtures to Enhance Durability: A Quantitative Model*. Cement and Concrete Composites, 1998. **20**(2-3): p. 113-119.
21. Kenneth C, H., *The Influence of Water on the Performance of Concrete*. Construction and Building Materials, 2011. **25**(7): p. 3003-3013.
22. Okamura, H. and M. Ouchi, *Self-Compacting High Performance Concrete*. Progress in Structural Engineering and Materials, 1998. **1**(4): p. 378-383.
23. Ouchi, M., et al., *Applications of Self-Compacting Concrete in Japan, Europe and the United States*, in *ISHPC*. 2003. p. 1-20.
24. Bouzoubaâ, N. and M. Lachemi, *Self-Compacting Concrete Incorporating High Volumes of Class F Fly Ash: Preliminary Results*. Cement and Concrete Research, 2001. **31**(3): p. 413-420.
25. Khayat, K.H. and J. Assaad, *Air-Void Stability in Self-Consolidating Concrete*. ACI Materials Journal, 2002. **99**(4): p. 408-416.
26. Chan, Y.W., Y.S. Chen, and Y.S. Liu, *Development of Bond Strength of Reinforcement Steel in Self-Consolidating Concrete*. ACI Materials Journal, 2003. **100**(4): p. 490-498.
27. Sonebi, M., M. Rooney, and P.J.M. Bartos. *Assessment of the Segregation Resistance of Fresh Self-Compacting Concrete*. in *6th CANMET/ACI International Conference in Recent Advances on Concrete Technology*. 2003. Bucharest.
28. Jacobs, F. and F. Hunkeler, *Design of Self-Compacting Concrete for Durable Concrete Structures*. 1th International RILEM-Symposium on self-compacting concrete, 1999: p. 397-407.

29. Edamatsu, Y., N. Nishida, and M. Ouchi, *A Rational Mix-Design Method for Self-Compacting Concrete Considering Interaction between Coarse Aggregate and Mortar Particles*. Proc., 1st RILEM Symposium on Self-Compacting Concrete, 1999: p. 309-320.
30. Melo, K.A. and A.M.P. Carneiro, *Effect of Metakaolin's Finenesses and Content in Self-Consolidating Concrete*. Construction and Building Materials, 2010. **24**(8): p. 1529-1535.
31. Saak, A.W., H.M. Jennings, and S.P. Shah, *New Methodology for Designing Self-Compacting Concrete*. ACI Materials Journal, 2001. **98**(6): p. 429-439.
32. Brouwers, H.J.H. and H.J. Radix, *Self-Compacting Concrete: Theoretical and Experimental Study*. Cement and Concrete Research, 2005. **35**(11): p. 2116-2136.
33. Sedran, T. and F. De Larrard, *Optimization of Self-Compacting Concrete Thanks to Packing Model*. Proceedings of the 1st RILEM Symposium on Self-Compacting Concrete, 1999: p. 321-332.
34. Okamura, H. and K. Ozawa, *Mix Design for Self-Compacting Concrete*. Concrete Library, JSCE, 1995(25): p. 107-120.
35. Sonebi, M., *Applications of Statistical Models in Proportioning Medium-Strength Self-Consolidating Concrete*. ACI Materials Journal, 2004. **101**(5): p. 339-346.
36. Assaad, J. and K.H. Khayat, *Assessment of Thixotropy of Self-Consolidating Concrete and Concrete-Equivalent-Mortar - Effect of Binder Composition and Content*. ACI Materials Journal, 2004. **101**(5): p. 400-408.
37. Assaad, J., K.H. Khayat, and H. Mesbah, *Assessment of Thixotropy of Flowable and Self-Consolidating Concrete*. ACI Materials Journal, 2003. **100**(2): p. 99-107.
38. Assaad, J., K.H. Khayat, and H. Mesbah, *Variation of Formwork Pressure with Thixotropy of Self-Consolidating Concrete*. ACI Materials Journal, 2003. **100**(1): p. 29-37.
39. Khayat, K.H. and J.J. Assaad, *Use of Thixotropy-Enhancing Agent to Reduce Formwork Pressure Exerted by Self-Consolidating Concrete*. ACI Materials Journal, 2008. **105**(1): p. 88-96.
40. Bui, V.K., et al., *Rapid Testing Method for Segregation Resistance of Self-Compacting Concrete*. Cement and Concrete Research, 2002. **32**(9): p. 1489-1496.
41. Rashad, M.M., et al., *Transformation of Silica Fume into Chemical Mechanical Polishing (Cmp) Nano-Slurries for Advanced Semiconductor Manufacturing*. Powder Technology, 2011. **205**(1-3): p. 149-154.
42. Xian Linyuan Micro-Silica Fume Co. Ltd. *Micro-Silica Fume*. 2008; Available from: <http://www.xalinyuan.com>.
43. Meyer, C., *The Greening of the Concrete Industry*. Cement and Concrete Composites, 2009. **31**(8): p. 601-605.

44. Gencil, O., et al., *Mechanical Properties of Self-Compacting Concrete Reinforced with Polypropylene Fibres*. Materials Research Innovations, 2011. **15**(3): p. 216-225.
45. Turk, K. and M. Karatas, *Abrasion Resistance and Mechanical Properties of Self-Compacting Concrete with Different Dosages of Fly Ash/Silica Fume*. Indian Journal of Engineering and Materials Sciences, 2011. **18**(1): p. 49-60.
46. Iyer, R.S. and J.A. Scott, *Power Station Fly Ash — a Review of Value-Added Utilization Outside of the Construction Industry*. Resources, Conservation and Recycling, 2001. **31**(3): p. 217-228.
47. Goodarzi, F., *Characteristics and Composition of Fly Ash from Canadian Coal-Fired Power Plants*. Fuel, 2006. **85**(10–11): p. 1418-1427.
48. Al-Amoudi, O.S.B., M. Maslehuddin, and I.M. Asi, *Performance and Correlation of the Properties of Fly Ash Cement Concrete*. Cement, Concrete and Aggregates, 1996. **18**(2): p. 71-77.
49. Sidney, M., *Acoustic Emission*, in *Handbook on Nondestructive Testing of Concrete Second Edition*. 2003, CRC Press.
50. Khatib, J.M., *Performance of Self-Compacting Concrete Containing Fly Ash*. Construction and Building Materials, 2008. **22**(9): p. 1963-1971.
51. Hameed, M.S. and A.S.S. Sekar, *Self Compaction High Performance Green Concrete for Sustainable Development*. Journal of Industrial Pollution Control, 2010. **26**(1): p. 49-55.
52. Kim, Y.J., Y.W. Choi, and M. Lachemi, *Characteristics of Self-Consolidating Concrete Using Two Types of Lightweight Coarse Aggregates*. Construction and Building Materials, 2010. **24**(1): p. 11-16.
53. Kou, S.C. and C.S. Poon, *Properties of Self-Compacting Concrete Prepared with Recycled Glass Aggregate*. Cement and Concrete Composites, 2009. **31**(2): p. 107-113.
54. Kumar, P., H.M. Ajazul, and S.K. Kaushik, *Early Age Strength of Scc with Large Volumes of Fly Ash*. Indian Concrete Journal, 2004. **78**(6): p. 25-29.
55. Mohammed, S., *Medium Strength Self-Compacting Concrete Containing Fly Ash: Modelling Using Factorial Experimental Plans*. Cement and Concrete Research, 2004. **34**(7): p. 1199-1208.
56. Pathak, N. and R. Siddique, *Properties of Self-Compacting-Concrete Containing Fly Ash Subjected to Elevated Temperatures*. Construction and Building Materials, 2012. **30**(7): p. 274-280.
57. Siddique, R., *Properties of Self-Compacting Concrete Containing Class F Fly Ash*. Materials and Design, 2011. **32**(3): p. 1501-1507.

58. Topçu, I.B. and T. Uygunođ lu, *Effect of Aggregate Type on Properties of Hardened Self-Consolidating Lightweight Concrete (Scl)*. Construction and Building Materials, 2010. **24**(7): p. 1286-1295.
59. Türkel, S. and A. Kandemir, *Fresh and Hardened Properties of Scc Made with Different Aggregate and Mineral Admixtures*. Journal of Materials in Civil Engineering, 2010. **22**(10): p. 1025-1032.
60. Xie, Y., et al., *Optimum Mix Parameters of High-Strength Self-Compacting Concrete with Ultrapulverized Fly Ash*. Cement and Concrete Research, 2002. **32**(3): p. 477-480.
61. Bonavetti, V., et al., *Limestone Filler Cement in Low W/C Concrete: A Rational Use of Energy*. Cement and Concrete Research, 2003. **33**(6): p. 865-871.
62. Bosiljkov, V.B., *Scc Mixes with Poorly Graded Aggregate and High Volume of Limestone Filler*. Cement and Concrete Research, 2003. **33**(9): p. 1279-1286.
63. Hallal, A., et al., *Combined Effect of Mineral Admixtures with Superplasticizers on the Fluidity of the Blended Cement Paste*. Construction and Building Materials, 2010. **24**(8): p. 1418-1423.
64. Liu, S. and P. Yan, *Effect of Limestone Powder on Microstructure of Concrete*. Journal Wuhan University of Technology, Materials Science Edition, 2010. **25**(2): p. 328-331.
65. Liu, S., Z. Gao, and M. Rao, *Study on the Ultra High Performance Concrete Containing Limestone Powder*. 2011. p. 686-689.
66. Valcuende, M., et al., *Influence of Limestone Filler and Viscosity-Modifying Admixture on the Shrinkage of Self-Compacting Concrete*. Cement and Concrete Research, 2012. **42**(4): p. 583-592.
67. Okamura, H. and M. Ouchi, *Self-Compacting Concrete*. Journal of Advanced Concrete Technology, 2003. **1**(1): p. 5-15.
68. Memon, S.A., M.A. Shaikh, and H. Akbar, *Utilization of Rice Husk Ash as Viscosity Modifying Agent in Self Compacting Concrete*. Construction and Building Materials, 2011. **25**(2): p. 1044-1048.
69. Rols, S., J. Ambroise, and J. Péra, *Effects of Different Viscosity Agents on the Properties of Self-Leveling Concrete*. Cement and Concrete Research, 1999. **29**(2): p. 261-266.
70. Domone, P.L., *A Review of the Hardened Mechanical Properties of Self-Compacting Concrete*. Cement and Concrete Composites, 2007. **29**(1): p. 1-12.
71. Khayat, K.H., K. Manai, and A. Trudel, *In Situ Mechanical Properties of Wall Elements Cast Using Self-Consolidating Concrete*. ACI Materials Journal, 1997. **94**(6): p. 491-500.
72. Soylev, T.A. and R. François, *Quality of Steel-Concrete Interface and Corrosion of Reinforcing Steel*. Cement and Concrete Research, 2003. **33**(9): p. 1407-1415.



73. Hossain, K.M.A. and M. Lachemi, *Bond Behavior of Self-Consolidating Concrete with Mineral and Chemical Admixtures*. Journal of Materials in Civil Engineering, 2008. **20**(9): p. 608-616.
74. Valcuende, M. and C. Parra, *Bond Behaviour of Reinforcement in Self-Compacting Concretes*. Construction and Building Materials, 2009. **23**(1): p. 162-170.
75. Brameshuber, W. and S. Uebachs, *Self-Compacting Concrete - Application in Germany*, in *6th International Symposium on High Strength/High Performance Concrete*. 2002: Leipzig p. 1503-1514.
76. Corinaldesi, V. and G. Moriconi, *Durable Fiber Reinforced Self-Compacting Concrete*. Cement and Concrete Research, 2004. **34**(2): p. 249-254.
77. Yu, H., et al., *Laboratory Investigation of Reinforcement Corrosion Initiation and Chloride Threshold Content for Self-Compacting Concrete*. Cement and Concrete Research, 2010. **40**(10): p. 1507-1516.
78. Hassan, A.A.A., K.M.A. Hossain, and M. Lachemi, *Corrosion Resistance of Self-Consolidating Concrete in Full-Scale Reinforced Beams*. Cement and Concrete Composites, 2009. **31**(1): p. 29-38.
79. Akram, T., S.A. Memon, and H. Obaid, *Production of Low Cost Self Compacting Concrete Using Bagasse Ash*. Construction and Building Materials, 2009. **23**(2): p. 703-712.
80. Uzal, B. and L. Turanli, *Studies on Blended Cements Containing a High Volume of Natural Pozzolans*. Cement and Concrete Research, 2003. **33**(11): p. 1777-1781.
81. Andrade, C., et al., *Determination of the Corrosion Rate of Steel Embedded in Concrete*. ASTM Special Technical Publication STP 906, Philadelphia, 1986: p. 43.
82. Lambert, P., C.L. Page, and P.R.W. Vassie, *Investigations of Reinforcement Corrosion: Electrochemical Monitoring of Steel in Chloride-Contaminated Concrete*. Materials and Structures, 1991. **24**: p. 351-358.
83. Shannag, M.J., *High Strength Concrete Containing Natural Pozzolan and Silica Fume*. Cement and Concrete Composites, 2000. **22**(6): p. 399-406.
84. Shannag, M.J. and A. Yeginobali, *Properties of Pastes, Mortars and Concretes Containing Natural Pozzolan*. Cement and Concrete Research, 1995. **25**(3): p. 647-657.
85. Ramezaniapour, A.A. and H. Bahrami Jovein, *Influence of Metakaolin as Supplementary Cementing Material on Strength and Durability of Concretes*. Construction and Building Materials, 2012. **30**: p. 470-479.
86. Sabir, B.B., S. Wild, and J. Bai, *Metakaolin and Calcined Clays as Pozzolans for Concrete: A Review*. Cement and Concrete Composites, 2001. **23**(6): p. 441-454.

87. Syed, K.N., *Production of Medium to Low Strength Concrete Utilizing Indigenous Waste Products in Civil Engineering*. 2011, King Fahd University of Petroleum and Minerals: Dhahran.
88. Al-Harthy, A.S., R. Taha, and F. Al-Maamary, *Effect of Cement Kiln Dust (Ckd) on Mortar and Concrete Mixtures*. *Construction and Building Materials*, 2003. **17**(5): p. 353-360.
89. Maslehuddin, M., et al., *Properties of Cement Kiln Dust Concrete*. *Construction and Building Materials*, 2009. **23**(6): p. 2357-2361.
90. Wang, M.L. and V. Ramakrishnan, *Evaluation of Blended Cement, Mortar and Concrete Made from Type Iii Cement and Kiln Dust*. *Construction and Building Materials*, 1990. **4**(2): p. 78-85.
91. Chaunsali, P. and S. Peethamparan, *Evolution of Strength, Microstructure and Mineralogical Composition of a Ckd-Ggbfs Binder*. *Cement and Concrete Research*, 2011. **41**(2): p. 197-208.
92. Konsta-Gdoutos, M.S. and S.P. Shah, *Hydration and Properties of Novel Blended Cements Based on Cement Kiln Dust and Blast Furnace Slag*. *Cement and Concrete Research*, 2003. **33**(8): p. 1269-1276.
93. Wang, C.K., C.G. Salmon, and J.A. Pincheira, *Reinforced Concrete Design*. 2006: John Wiley & Sons.
94. Felekoğlu, B., S. Türkel, and B. Baradan, *Effect of Water/Cement Ratio on the Fresh and Hardened Properties of Self-Compacting Concrete*. *Building and Environment*, 2007. **42**(4): p. 1795-1802.
95. Chapman, R.A. and S.P. Shah, *Early-Age Bond Strength in Reinforced Concrete*. *ACI Materials Journal*, 1987. **84**: p. 501-510.
96. Shoaib, M.M., M.M. Balaha, and A.G. Abdel-Rahman, *Influence of Cement Kiln Dust Substitution on the Mechanical Properties of Concrete*. *Cement and Concrete Research*, 2000. **30**(3): p. 371-377.
97. Orangun, C.O., J.O. Jirsa, and J.E. Breen, *A Reevaluation of Test Data on Development Length and Splices*. *ACI Journal*, 1977. **74**(3): p. 114-122.
98. The Concrete Society, *Permeability Testing of Site Concrete - a Review of Methods and Experience*, in *Technical Report No. 31*. 1987. p. 75.
99. Fajardo, G., P. Valdez, and J. Pacheco, *Corrosion of Steel Rebar Embedded in Natural Pozzolan Based Mortars Exposed to Chlorides*. *Construction and Building Materials*, 2009. **23**(2): p. 768-774.

100. Kaid, N., et al., *Durability of Concrete Containing a Natural Pozzolan as Defined by a Performance-Based Approach*. Construction and Building Materials, 2009. **23**(12): p. 3457-3467.
101. Bai, J., S. Wild, and B.B. Sabir, *Chloride Ingress and Strength Loss in Concrete with Different Pc-Pfa-Mk Binder Compositions Exposed to Synthetic Seawater*. Cement and Concrete Research, 2003. **33**(3): p. 353-362.
102. Güneyisi, E., et al., *Strength, Permeability and Shrinkage Cracking of Silica Fume and Metakaolin Concretes*. Construction and Building Materials, 2012. **34**(0): p. 120-130.
103. Ramezaniapour, A.A., et al., *Practical Evaluation of Relationship between Concrete Resistivity, Water Penetration, Rapid Chloride Penetration and Compressive Strength*. Construction and Building Materials, 2011. **25**(5): p. 2472-2479.
104. Shi, C., *Effect of Mixing Proportions of Concrete on Its Electrical Conductivity and the Rapid Chloride Permeability Test (Astm C1202 or Asshto T277) Results*. Cement and Concrete Research, 2004. **34**(3): p. 537-545.
105. American Society for Testing and Materials, *Standard Test Method for Electrical Indication of Concrete's Ability to Resist Chloride Ion Penetration*, in *ASTM C 1202, Annual Book of ASTM Standards, Vol. 4.02*. 1994: Philadelphia.
106. American Society for Testing and Materials, *Standard Test Method for Electrical Indication of Concrete's Ability to Resist Chloride Ion Penetration*, in *ASTM C 426, Annual Book of ASTM Standards, Vol. 4.01*. 1997.
107. Ahmad, S., *Reinforcement Corrosion in Concrete Structures, Its Monitoring and Service Life Prediction—a Review*. Cement and Concrete Composites, 2003. **25**(4–5): p. 459-471.
108. American Society for Testing and Materials, *Standard Test Method for Corrosion Potentials of Uncoated Reinforcing Steel in Concrete*, in *ASTM C 876, Annual Book of ASTM Standards, Vol. 4.02*. 1994: Philadelphia.
109. Broomfield, J.P., *Corrosion of Steel in Concrete: Understanding, Investigation and Repair*. 2003: Spoon Press.
110. Bungey, J.H., *The Testing of Concrete in Structures*. 1989, London: Surrey University Press, London.

## **VITA**

**Name:** Saheed Kolawole Adekunle.

**Nationality:** Nigerian.

**Permanent Address:** GBK 45, Gbedemuke zone, Atolu Lay-out, Oremeji-Agugu,  
Ibadan, Oyo State.

**Email:** saeedade@yahoo.com

**Institutions Attended:** University of Ilorin, Ilorin – BEng.(Civil), 2003.